UNIVERSITÀ
DEGLI STUDI
DI PADOVA

Universitá degli Studi di Padova
Dipartimento di Fisica ed Astronomia
Galileo Galilei

SCUOLA DI DOTTORATO DI RICERCA IN ASTRONOMIA
INDIRIZZO: EXTRAGALATTICO
CICLO: XXIV

GROUPS OF GALAXIES:

A KEY ENVIRONMENT FOR GALAXY EVOLUTION

Direttore della scuola: Ch.mo Prof. Gianpaolo Piotto
Supervisore: Dr.ssa Bianca Maria Poggianti

Dottoranda: Rosa Calvi

Contents

List of Figures

List of Tables

Riassunto

I gruppi di galassie sono le strutture più comuni nell'universo e, poiché abbracciano una vasta gamma di densità locali mostrando proprietà che si estendono da quelle tipiche degli ammassi a quelle tipiche del campo, rappresentano il luogo ideale per indagare l'evoluzione delle galassie. In particolare, i pre-processi responsabili delle trasformazioni delle galassie possono avvenire su queste scale; per tale motivo, essi possono avere un profondo effetto sulla popolazione complessiva di galassie in quanto più del 50 per cento di tutte le galassie dell'universo oggi sono in gruppi. Lo scopo della tesi è stato quindi quello di esplorare le proprietà delle galassie nei gruppi e capire se e come esse variano in funzione dell'ambiente in cui risiedono.

In questa tesi presento innanzitutto la costruzione e le caratteristiche di un nuovo catalogo di gruppi e di galassie rappresentativo della popalazione di campo a basso redshift, il Padova Millennium Galaxy and Group Catalog (PM2GC). Il metodo utilizzato per identificare i gruppi di galassie si basa sull'algoritmo "Friends-of-Friends" che sfrutta due quantità disponibili nei cataloghi osservativi delle galassie: la separazione proiettata nel cielo e la differenza di velocità nello spazio dei redshift. Le galassie che non risultano essere membri dei gruppi sono state suddivise in galssie appartenenti a sistemi "binari" costituiti da due oggetti vicini molto luminosi e galassie "singole" senza alcun compagno, al fine di identificare diversi ambienti utili per l'analisi scientifica.

Ho confrontato le proprietà delle galassie nei gruppi con quelle di galassie più isolate appartenenti ad altri ambienti nel catalogo PM2GC e con galassie di ammasso prese dalla WIde-field Nearby Galaxy cluster Survey (WINGS). Ho quindi eseguito un'analisi mor-

fologica studiando la relazione tra morfologia e massa tra le galassie singole, binarie, di gruppo e di ammasso. Ho trovato un andamento molto regolare in funzione dell'ambiente per tutti i tipi morfologici fatta eccezione per le galassie S0 negli ammassi. Inoltre, ho mostrato che la frazione morfologica dipende fortemente dalla massa delle galassie soprattutto per masse molto grandi.

Infine, ho esaminato la funzione di massa stellare delle galassie (MF) per capire se le variazioni che abbiamo osservato nelle proprietà morfologiche delle galassie possono essere spiegate dalla dipendenza della massa stessa della galassia dall'ambiente. Ho scoperto che a basso redshift, contrariamente alle aspettative, la funzione di massa delle galassie di campo è indistinguibile da quella degli ammassi di galassie e tale differenza diventa evidente solo considerando aloni con masse più basse, vale a dire le galassie singole. Ho anche trovato indicazione che vi è una dipendenza del limite di massa superiore dei diversi campioni di galassie dall'ambiente con le galassie più massicce che sono ospitate dagli aloni più massicci.

Tutti questi risultati ci danno importanti indicazioni che non solo la massa stellare ma anche l'ambiente in cui esse risiedono gioca un ruolo nell'evoluzione delle galassie. Inoltre, essi evidenziano che esiste un effetto specifico degli ammassi di galassie che agisce esclusivamente sulle classi di galassie S0 e spirali poiché un numero significativo di galassie S0 negli ammassi ha un'origine diversa rispetto alle S0 in altri ambienti. Questo significa che probabilmente la popolazione di galassie S0 negli ammassi è strettamente collegata a quella delle spirali.

Abstract

Galaxy groups are the most common structure in the universe and, as they span a wide range in local density, showing properties which range from cluster-like to field-like represent the ideal place to investigate galaxy evolution. In particular, on these scales can be active fundamental pre-processes responsible of galaxy transformations; thus, they can have a profound effect on the overall galaxy population since $\geq 50\%$ of all galaxies are in groups by $\mathrm{z} \sim 0$. The aim of the thesis has been to explore the properties of galaxies in groups and to understand whether and how they vary as function of global environment in which they reside.

In this thesis I first present the construction and the characteristics of a new catalog of groups and galaxies representative of the general field population at low redshift, the Padova Millennium Galaxy and Group Catalogue (PM2GC). The group building method used to identify galaxy groups is based on a Friends-of-Friends algorithm which takes advantage of two available quantities in observational galaxy catalogs: the projected separation in the sky and the velocity difference in the redshift space. Non-group galaxies were subdivided into "binary" systems of two bright close companions, and "single" galaxies with no companion, in order to identify different environments useful scientific analysis.

I compared galaxy groups properties with those of more isolated galaxies in other environments in PM2GC and with cluster galaxies from the WIde-field Nearby Galaxy cluster Survey (WINGS). I performed a morphological analysis studying the relation between morphology and mass among single, binaries, group and cluster galaxies. I found a very smooth trend of all morphological types with environment except for S0 galaxies in clus-

ters. Moreover, I shown that the morphological fraction depends strongly on galaxy stellar mass at very high masses.

Finally, I investigated the galaxy stellar mass function (MF) to understand if the observed variations in the galaxy morphology can be explained by the dependence of the galaxy mass itself on environment. I found that at low redshift, contrary to expectations, the mass function of general field is indistinguishable from that of galaxy clusters while the difference becomes evident only considering lowest mass haloes, i.e. single galaxies. I also found indication that there is a dependence of the upper mass limit of samples on environment with the most massive galaxies only hosted by the most massive haloes.

All these results represent a very important indications that not only stellar mass but also the environment in which a galaxy resides play a role in galaxy evolution. Moreover, they highlight that exist a cluster specific effect which acts on the classes of spirals and S0s galaxies since a significant number of S0s in clusters has a different origin with respect to S0s in other environments. This means that S0 population in clusters probably are closely related to spiral one.

Chapter 1

Environment: implications for galaxy formation and evolution

1.1 Introduction: the Hierarchical universe

As we direct a telescope at the sky in a bright night it is quite clear that galaxies are not uniformly distributed through space. Only on very large scale, of order 100s of Mpc, the universe display a coherent structure and can be reasonably approximated as homogeneous and isotropic. Instead on smaller scales - from galaxies to superclusters and voids - it exhibits a great deal of structures.

Understanding the origin and evolution of the cosmic structures of the universe is the major goal in modern cosmology and currently the working hypothesis about this topic is described through the dissipationless gravitational collapse in a universe dominated by Dark Matter. In the last year, the most accreditated cosmological model to describe the distribution of the large scale universe is the Cold Dark Matter (CDM) model plus a dark energy field (indicated by Λ). These two "dark" components account for $\sim 95\%$ of the total energy of the Universe Komatsu et al. (2009) and although their nature is still a debated question they nicely integrate cosmological theories (Big Bang and Inflation) and many important observational constraints, such as the anisotropies of cosmic microwave background, the observations of the present acceleration of cosmic expansion as inferred from supernovae explosions (Perlmutter et al., 1999), the structure seen in the z = 3 Lyα

forest (Mandelbaum et al., 2003) and the power spectrum of low redshift galaxies (Percival et al., 2007).

According to the ΛCDM model, the dominant force that drives structure formation is gravity. A full mathematical treatment of the model requires General Theory of Relativity and proceeds with the description of how the density perturbation field evolves and it is beyond the scope of this introduction. More general is nowdays accepted that quasi-equilibrium dark matter clumps or "haloes" grow by the collapse and *hierarchical* aggregation of ever more massive systems, a process well described by the phenomenological model of Press and Schechter and its extensions (Press& Schechter, 1974; Lacey& Cole, 1993). Galaxies form at the centres of these dark haloes when gas condenses into stars once it becomes sufficiently warm and dense. Groups and clusters of galaxies form as haloes aggregate into larger systems and represent the high density nodes of the cosmic network.

Over the past decades, different methods have been developed to study galaxy formation and evolution in a cosmological context. The strongest evidence in favour of the hierarchical scenario comes from the development of numerical simulations. Simulations with semi-analytic models (SAMs) provide a flexible and widely used tool to test theories of cosmic structures formation and to efficiently predict the observations, linking these to the properties of dark matter haloes where galaxies reside. A SAM is a collection of simplified physical recipes that describe gas condensation, how stars are formed within galaxies and evolve and how black holes grow (Cole, 1991; White& Frenk, 1991; Lacey& Silk, 1991; Kang et al., 2005; Baugh, 2006; De Lucia& Blaizot, 2007). SAMs can also easily include different feedback effects as stellar winds, active galactic nuclei (AGN) or supernovae (SNe) feedbacks (Croton et al., 2006; Somerville et al., 2008; Ricciardelli& Franceschini, 2010), and can be used to explore ideas of galaxy formation and evolution and to understand what physical processes are the most important in the life of a galaxy by changing the recipes describing the physics.

Often the evolution of dark matter haloes described by SAMs are parameterized with dark matter halo merger trees (Figure1.1) that allow the hierarchical nature of gravitational instabilities to be explicitly taken into account (Baugh et al., 1998). Even though merger trees are directly derived from simulations, they can be derived also by using Monte Carlo techniques. In such case the extended Press-Schechter (EPS) theory (Lacey& Cole, 1993;

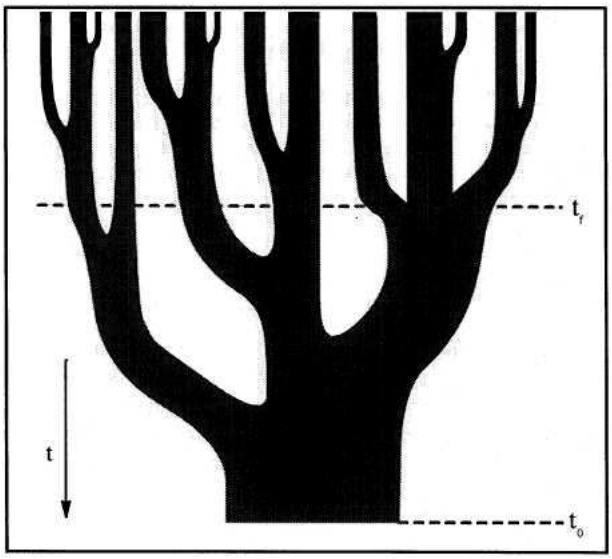

Figure 1.1: A representation of a merger tree depicting the growth of a halo as the result of a series of mergers. Time increases from top to bottom and the widths of the branches of the tree represent the masses of the single parent haloes. The horizontal lines are the the present time t_0 and the formation time t_1, respectively. (Lacey& Cole, 1993)

Bond et al., 1991) is often used.

Using simulations, it becomes possible to construct realistic mock catalogs that contain not only physical information about model galaxies such as masses, star formation rates, luminosities, etc. but also dynamically consistent redshift and spatial information, like in real redshift surveys. The mock catalogs make possible to carry-out detailed comparisons with observational data at different cosmic epochs providing useful information on the relative importance of different physical processes in establishing a certain observational trend, and on the physics which is eventually missing in these models.

1.2 Galaxies: an overview

Known as ”nebulae” in the old astronomical terminology for the appearance of a cloud of gas and dust, galaxies are now considered a vast conglomerates of hundreds of millions or billions of stars thanks in large part to the work of Edwin Hubble. In the following I present a brief overview of the different features of a galaxy which make it different from

the others.

1.2.1 Galaxy morphology

Galaxies have a wide range of inexplicable forms and until the advent of the massive surveys was possible to analyze the properties of only relatively nearby galaxies by meticulous visual morphological studies. The pioneering studies of Hubble further elaborated by de Vaucouleurs, Kormendy, Sandage, van den Bergh and others have led to morphological classification schemes which contain a vast amount of detail but, the size of the new galaxy samples, which encompass a much greater number of objects (about 200,000 galaxies), has provided new classification schemes based upon parameters derived from computer analysis of the galaxy images and spectra and which make in relationship the morphology with the physical content of stars and gas. This new approach loses in detail but this loss is compensated by the huge statistics involved and less subjective nature of the classification.

The most widely used classification scheme is the Hubble's "tuning-fork" diagram and galaxies typically fall into two main classes: the early-type galaxies (ellipticals and S0s), that lie towards the left-hand end of the sequence and the late-type galaxies (spiral) that lie towards the right-hand.

Elliptical galaxies The elliptical galaxies are smooth systems with a continuously declining brightness distribution (Figure1.2). They have no disk, no spiral structure and only small amounts of the gas and dust. They are dominated by old stars and are found mostly in the denser regions of the universe, from rich clusters to small groups. They are subclassificated according to apparent ellipticity $\mathrm{E_n}$, where $\mathrm{n} = 10(1 - \mathrm{b/a})$, b/a being the apparent flattening between 0 (for apparently round galaxies) and 7 (for the most elongated galaxies). The n value in the $\mathrm{E_n}$ classification is simply the projected ellipticity then it is not a physical classification (Kormendy et al., 1989). Luminous ellipticals are thought to be triaxial in structure with an anisotropic velocity dispersion tensor, while lower luminosity ellipticals are more isotropic oblate rotators (Davies et al., 1983). Studies of rotational to random kinetic energy (V/σ) versus apparent flattening (ρ) show that massive ellipticals are slow anisotropic rotators. Ellipticals follow a "fundamental plane" relationship between

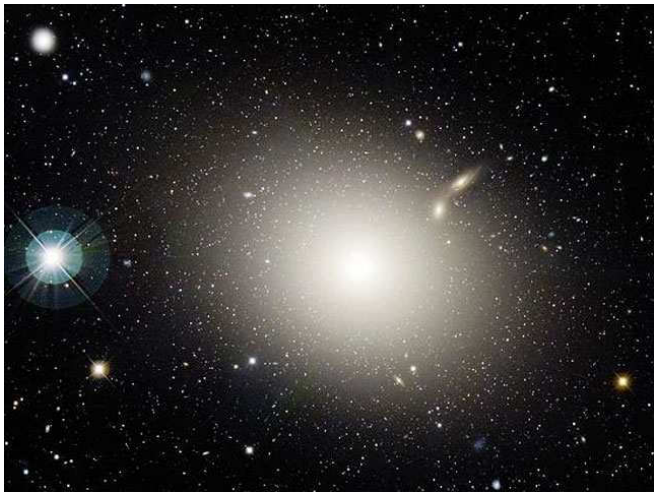

Figure 1.2: M87 is an elliptical galaxy at the center of a cluster of galaxies known as the Virgo Cluster, and shows an unusually high number of globular clusters. The image was taken by the Canada-France-Hawaii Telescope on top of the dormant volcano Mauna Kea in Hawaii, USA.

the effective radius $\mathrm{r_e}$ of the light distribution, the central velocity dispersion σ_0, and mean effective surface brightness $< \mathrm{I_e} >$ (see review by Kormendy et al. (1989)). Dwarf elliptical galaxies may not follow the same relation as massive ellipticals; this is discussed by Ferguson& Binggeli (1994).

S0 galaxies S0 galaxies are introduced by Hubble as a morphological transition between ellipticals and early-type spirals. Indeed they are characterized by the presence of a disk, a bulge and no spiral arms and are designated as S0 or SB0 according to whether they have a bar or not (Figure1.3). The central brightness concentration, similar to an elliptical, represents the bulge or spheroidal component surrounded by a disk, which has a different brightness profile with respect to the spheroidal component, being characterized by an intensity which decreases more rapidly with radius. Typically the disk component is characterized by the presence of a dust lane and the family of S0s is subdivided into three classes, $\mathrm{S0_1}$, $\mathrm{S0_2}$, $\mathrm{S0_3}$, according to the growing strength of dust absorption. Also the barred lenticulars are divided into three classes: $\mathrm{SB0_1}$, $\mathrm{SB0_2}$ and $\mathrm{SB0_3}$ and the division is made according to the prominence of the bar rather than to the dust strength.

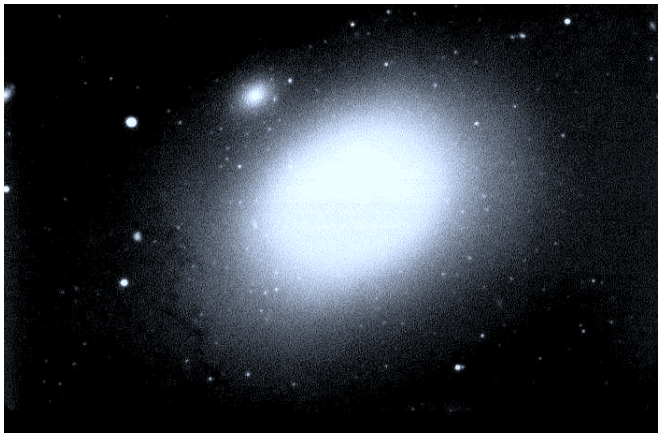

Figure 1.3: Lenticular galaxy M86 in the Virgo cluster as photographed by the KPNO 4-meter Mayall telescope in 1975.

Spiral galaxies Spiral galaxies have a disk structure formed by a central bulge and large sweeping arms that spiral outward from the center (Figure1.4). They are morphologically divided into normal (S) and barred (SB) and each of these can be further separated into a finer classification: Sa, Sab, Sb, Sbc, Sc (and SBa, SBab, SBb, SBbc, SBc) according to three criteria: i) the prominence of the central luminous bulge; ii) openess of spiral pattern; iii) the distribution of stars in the arms. Sa and SBa have luminous bulges ($\mathrm{L_{bulge}}/\mathrm{L_{disc}} \sim 0.3$), spiral arms tightly wound and an uniform distribution of stars towards the arms. Passing from a to c the bulge become less prominent ($\mathrm{L_{bulge}}/\mathrm{L_{disc}} \sim 0.05$), the spiral arms widen out and the stars more clumpily distributed.

Galaxies with no apparent structure have been classified in:

Irregular galaxies The class of irregular galaxies included every galaxy disorganised and amorphous which could not be incorporated into the standard Hubble sequence (Figure1.5). Many of these were similar to the companion galaxies of our own Galaxy, the Magellanic Clouds, and these were designated Irr I or Magellanic irregulars, and may show bar-like structures and incipient spiral structure. A small class of irregulars that consists of galaxies where there was no evidence of resolution into stars and of any regular structure were classified Irr II galaxies (such as M82 , NGC 520 and NGC 3077). Galaxies like the LMC can be considered to belong to stages in the Hubble

Figure 1.4: Classified as an Sc galaxy, the grand design of M74's graceful spiral arms are traced by bright blue star clusters and dark cosmic dust lanes.The above image was obtained using 19 hours of exposure on the 1.23-meter telescope at Calar Alto Observatory in the Sierra de Los Filabres mountain range in Spain.

sequence later than Sd and are denoted Sm. The Irr II systems find no natural place in the revised sequence and are designated I0 by de Vaucouleurs. The characteristics of the I0 irregular galaxies are that they are very rich in interstellar matter and contain young stars and active regions of star formation; a number of these would be classified as starburst galaxies.

Peculiar and interacting galaxies Galaxies with very strange appearances (Figure.1.6) are referred to as peculiar galaxies (Arp, 1966), to indicate that they cannot be associated with any standard galaxy type. A few galaxies are known, for example, in which the stellar component is in the form of a ring rather than a disc or spheroid, the Cartwheel being a beautiful example of this type of galaxy, known as ring galaxies. Most of these remarkable structures are due to strong gravitational interactions, or collisions, between galaxies. In the early 70's, Toomre and Toomre, by performing a numerical integration of the restricted three body problem, carried out pioneering computer simulations of close encounters between galaxies which showed how such events could modify the structure of the galaxies involved in the process, giving rise

Figure 1.5: Colour composite image of NGC 1427A, based on observations collected with FORS1 in Service mode.

to remarkable asymmetric structures (Toomre, A. & Toomre, J., 1972). Collisions between galaxies have a central role in models of galaxy formation because strong gravitational encounters between galaxies are essential in forming the structures we observe today.

1.2.2 Star Formation

Through the measurements of spectral lines and continuum emission the galaxy spectra provide the best insight of the galaxy stellar content which represents the most important feature of the Hubble classification itself (Hubble, 1926) and is fundamental to understand galaxy evolution.

In order to reveal the presence of stars of different ages and obtain a comprehensive analysis of the global SFRs of galaxies have been carried out surveys focused on the H_α (Kennicutt, 1983a; Gallagher et al., 1984; Caldwell et al., 1991; Kennicutt et al., 1994; Young et al., 1996), UV continuum (Donas et al., 1987; Deharveng et al., 1994), FIR data (Sauvage& Thuan, 1992; Walterbos& Greenawalt, 1996; Tomita et al., 1996; Devereux&

Figure 1.6: Cataloged as Arp 273 (also as UGC 1810), the galaxies are an example of interacting galaxies.

Hameed, 1997), and multiwavelength observations (Gavazzi& Scodeggio, 1996; Gavazzi et al., 1996). The absolute SFRs in galaxies, expressed in terms of the total mass of stars formed per year, show an enormous range, from virtually zero in gas-poor elliptical, S0, and dwarf galaxies to $\gg 20\mathrm{M}_{\odot}\mathrm{yr}^{-1}$ in gas-rich spirals. Larger global SFRs are associated almost uniquely with strong tidal interactions and mergers; up to $\gg 100\mathrm{M}_{\odot}\mathrm{yr}^{-1}$ can be found in optically selected starburst galaxies while values as high as $1000\mathrm{M}_{\odot}\mathrm{yr}^{-1}$ may be reached in the most luminous IR starburst galaxies. In Figure 1.7 is shows the distribution of $\mathrm{H}_{\alpha} + [\mathrm{NII}]$ equivalent widths (EWs) in a sample of 227 nearby bright galaxies ($\mathrm{BT} < 13$), subdivided by Hubble type, taken from the photometric surveys of (Kennicutt& Kent, 1983; Romanishin, 1990). The EW is defined as the emission-line luminosity normalized to the adjacent continuum flux, and hence it is a measure of the SFR per unit (red) luminosity. The EWs show a strong dependence on Hubble type. It increases from zero in E/S0 galaxies (within the observational errors) to 20-150 Åin late type spiral and irregular galaxies. In terms of absolute SFRs, this corresponds to a range of $0 - 10\mathrm{M}_{\odot}\mathrm{yr}^{-1}$ for an $\mathrm{L}^{\star}$ galaxy (roughly comparable in luminosity to the Milky Way). The SFR measured in this way increases by approximately a factor of 20 between types Sa and Sc (Caldwell et

al., 1991; Kennicutt et al., 1994) and that derived from the UV continuum and broadband visible colors show comparable behavior (Larson& Tinsley, 1978; Donas et al., 1987; Deharveng et al., 1994; Buat et al., 1989). A factor of 10 is present in SFRs among galaxies of the same type. Different factors can contribute to the SFR variations: variations in gas content, nuclear emission, interactions. Although the absolute SFR varies considerably among spirals (types Sa and later), some level of massive star formation is always observed in deep H_α images (Caldwell et al., 1991). However, many of the earliest disk galaxies (S0-S0/a) show no detectable star formation at all.

Nowdays, the spectral synthesis instead of observed stellar libraries is the standard technique to derive the salient properties of the stellar populations in galaxies and to investigate the whole range of stellar parameters. The single stellar population (SSP) spectra at medium and high resolution, together with the availability of more and more details in both observed stellar atmospheres and stellar evolution models makes it much easier to reproduce an observed galactic spectrum as a combination of simple stellar population spectra.

An excellent example of the new generation of data is given by the Sloan Digital Sky Survey (SDSS) (Gunn et al. 1998, York et al. 2000, Strauss et al. 2002) at low redshift and DEEP2survey (Davies et al. 2003) at higher redshift. From the analysis of the SDSS local sample (Heavens et al. 2004) has been found that exist a very clear evidence for "downsizing" - the process by which star formation at low redshift takes place predominantly in low-mass galaxies while massive galaxies have the bulk of their star formation activity at high redshift. In addition has been determined the star formation history (SFH) of the Universe showing that the stellar birthrate peaked at $z \simeq 1$ and then declined by a factor of around ten to its present value in according with the results derived from high redshift galaxies elsewhere in the Universe.

1.2.3 Galaxy bimodality: the red and blue sequences

As seen above galaxies were first classified on their single-color morphological properties. With the advent of color measurement, morphology-color relations were established. The

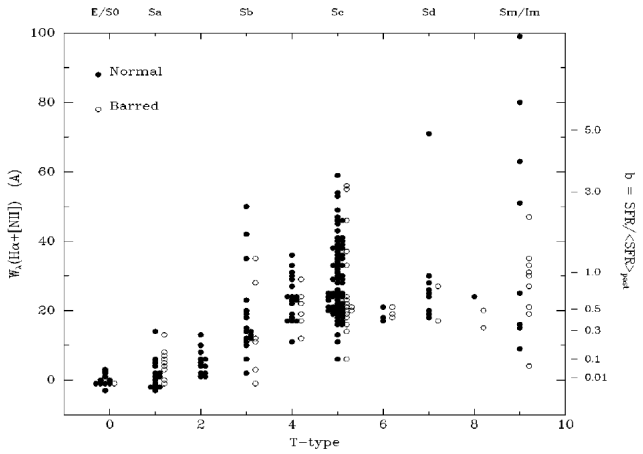

Figure 1.7: Distribution of integrated $H_\alpha + [NII]$ emission-line equivalent widths for a large sample of nearby spiral galaxies, subdivided by Hubble type and bar morphology. The right axis scale shows corresponding values of the stellar birthrate parameter b, which is the ratio of the present SFR to that averaged over the past (Kennicutt& Kent, 1983).

color of a galaxy is the ratio of the fluxes observed in two different filters A and B:

$$C = m_A - m_B = -2.5log(\frac{f_A}{f_B}) \tag{1.1}$$

where $\mathrm{f_A}$ and $\mathrm{f_B}$ are the fluxes into the two bands, and $\mathrm{m_A}$ and $\mathrm{m_B}$ are the corresponding magnitudes (defined as $\mathrm{m_A} = -2.5\mathrm{log}\mathrm{L_A}/4\pi\mathrm{d}^2 + \mathrm{k}$, d is the distance of the objects expressed in pc and $\mathrm{L_A}$ is total energy output of the galaxy in the waveband A, i.e. the luminosity). According to the definition, the colour index is larger for galaxies that emit more light at longer wavelengths and can give a quantitative measure of star formation activity. In particular late type galaxies, which consist of both a stellar disk and a cold gas disk, have an ongoing star formation activity that gives them the blue colors typical of massive, and therefore young, stars. Early type galaxies have a very little star formation and consist of an old, red stellar population with gas generally hot and diffuse.

In a plane color-absolute magnitude (CMD) a relation between these variables has been noted because galaxies populate two distinct areas showing a well precise bimodal distri-

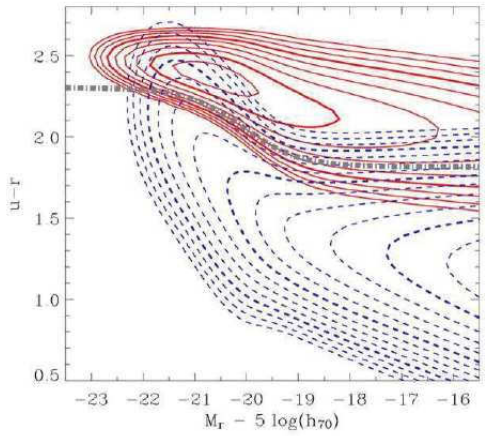

Figure 1.8: The colour-magnitude diagram of SDSS galaxies. The solid contours represent the red distribution, while the dashed contours represent the blue distribution (Baldry et al., 2004).

bution. These areas are defined as *red sequence* and *blue cloud*:

- The *red sequence* consists of non-starforming, high mass spheroidal galaxies or, more colloquially "old, red and dead" galaxies.
- The *blue cloud* consists of star-forming, low mass galaxies which are disc-dominated.

Figure1.8 shows a CMD in the SDSS (Baldry et al., 2004). The red sequence is defined roughly by early-type galaxies (Baldry et al., 2004; Driver et al., 2006), and integrated colors become progressively redder at bright magnitudes. Late-type galaxies, instead, populate the wider and more dispersed blue cloud at fainter magnitudes. The evidence of these double sequences is also confirmed looking at the colour distribution of galaxies that can be approximated by a bimodal function made by the sum of two Gaussian functions (Figure1.9) and this trend is evident across seven magnitudes (Kauffmann et al., 2003).
Bimodality is also present in the structural properties of the galaxies. An indication of whether a galaxy is better represented as a disk or a bulge is provided by the Sérsic index n, which is a measure of a galaxy's light profile. In Figure1.10, the Sérsic index n can be used to divide galaxies into spheroidal-dominated and disc-dominated galaxies (Driver et al. 2006). The spheroid-dominated systems are most commonly found with Sérsic pa-

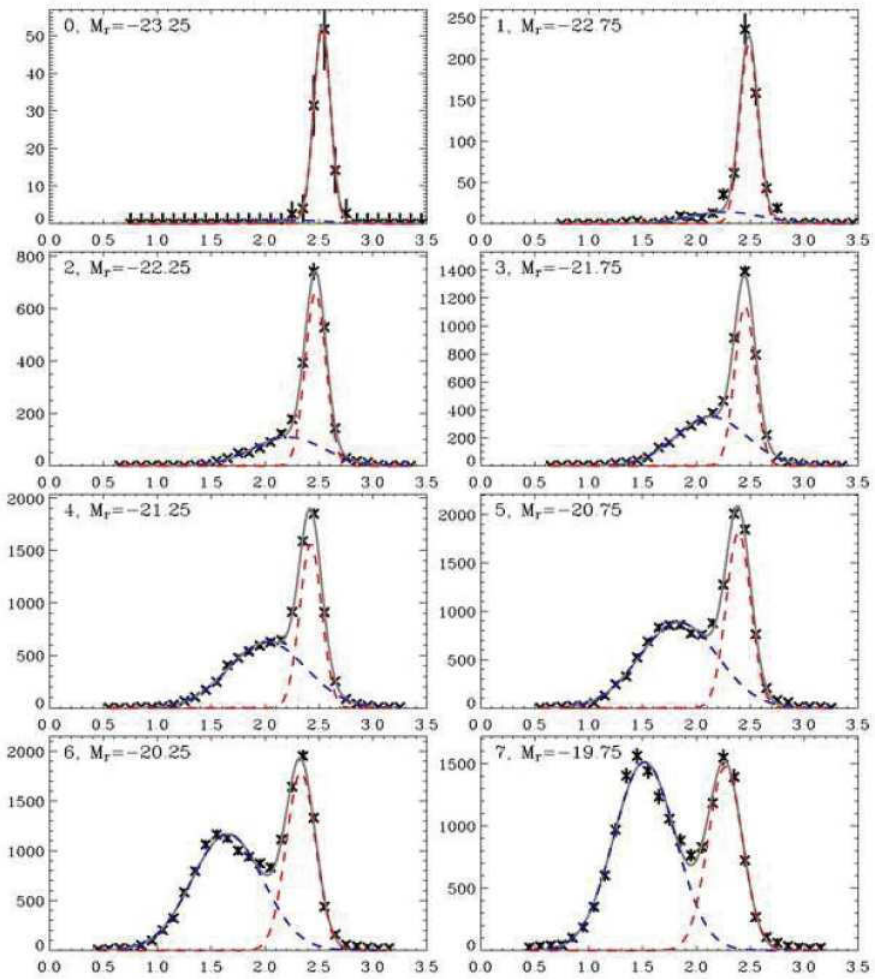

Figure 1.9: Colour distributions in absolute magnitude bins of width 0.5. Each plot shows galaxy number counts vs. rest-frame $u - r$ colour. The solid lines represent double-Gaussian fits, while the dashed lines represent the single Gaussians of the blue and red distributions (Baldry et al., 2004).

rameter n = 4, whereas the disc-dominated systems typically have n = 1. There is a clear separation between these systems in Figure1.10 and the dividing line between the two sequences occurs about n = 2.

One of the most important result concerning the bimodal behaviour of the galaxy population is that it is strongly dependent on galaxy stellar mass. Using a sample of 122,808 galaxies from the SDSS, Kauffmann and her colleagues measured the age of the stellar populations and the degree of concentration of the light towards their centres analysing (i) the amplitude of the Balmer break, or discontinuity, at 400 nm, Dn(4000), and (ii) the Balmer absorption line index $\mathrm{H}_{\delta\mathrm{A}}$[1] [47]. They have shown that these indices provide good measures of star formation activity over the last 10^9 and $(1.10) \times 10^9$ years respectively. The concentration index C is defined to be the ratio C = (R90/R50), where R90 and R50 are the radii enclosing 90% and 50% of the Petrosian r-band luminosity of the galaxy and is strongly correlated with Hubble type, thus with morphology and the value C = 2.6 separates early from late-type galaxies. Those galaxies with concentration indices $\mathrm{C} \geq 2.6$ are early-type galaxies, reflecting the fact that the light is more concentrated towards their centres.

In Figure1.11 Dn(4000) and $\mathrm{H}_{\delta\mathrm{A}}$ are plotted against the concentration index C and the mean stellar mass density within the half light radius $\mu^{\star}$. The panels show that the galaxy populations are divided into two distinct sequences and the dividing line between the two sequences occurs at a stellar mass $\mathrm{M} \approx 3 \times 10^{10}\mathrm{M}_{\odot}$. Lower mass galaxies have young stellar populations, low surface mass densities and the low concentration indices typical of disks. For stellar masses $\mathrm{M} \geq 3 \times 10^{10}\mathrm{M}_{\odot}$, the fraction of galaxies with old stellar populations increases rapidly. These also have the high surface mass densities and high concentration indices typical of spheroids or bulges.

[1]The $\mathrm{H}_{\delta\mathrm{A}}$ measures the strengths of the Balmer absorption line which are particularly strong in galaxies which have undergone a recent burst of star formation.

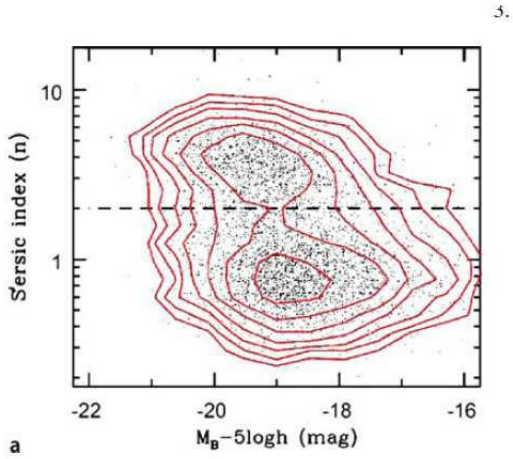

Figure 1.10: A plot of the observed value of the Sérsic index n as a function of the absolute blue magnitude in a sample of 10,095 galaxies from the Millennium Galaxy catalog.

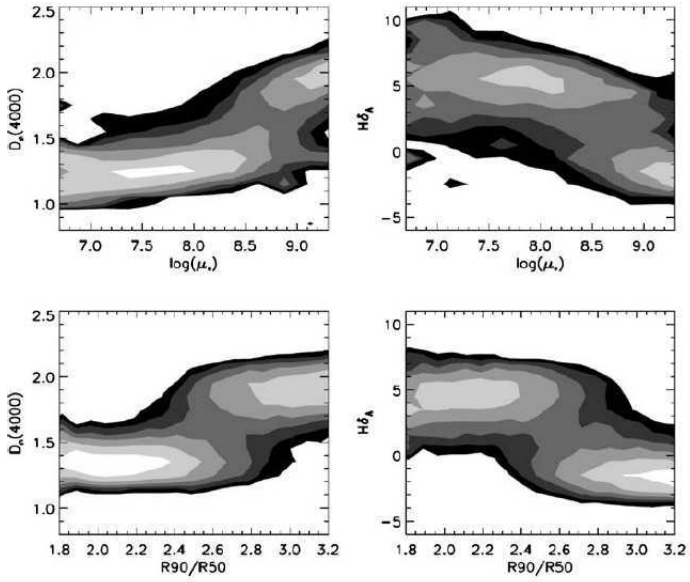

Figure 1.11: Density distributions in the Sloan showing the trends of the stellar age indicators Dn(4000) and $\mathrm{H}_{\delta\mathrm{A}}$ with concentration index C = (R90/R50) and surface mass density $\mu^{\star}$ (Kauffmann et al., 2003).

1.2.4 Luminosity function and Mass function

The frequency with which galaxies of different intrinsic luminosities are found in space is described by the luminosity function (LF), $\Phi(\mathrm{M})$ conventionally normalized by setting

$$\int_{-\infty}^{\infty} \Phi(M) dM = \nu \tag{1.2}$$

where ν is the total number of galaxies per unit of volume, so that $\Phi(\mathrm{M})\mathrm{dM}$ specifies the number density of galaxies in the magnitude range(M, M+dM).

An efficient parametrisation of the LF was proposed by Schechter (Schechter et al., 1976):

$$\Phi(M) = (0.4 \ln 10)\Phi^{\star} 10^{0.4(\alpha+1)(M^{\star}-M)} \exp(-10^{0.4(M^{\star}-M)}) \tag{1.3}$$

where $\Phi^{\star}, \mathrm{M}^{\star}, \alpha$ are chose to fit the observations. Passing in luminosities and defining $\Phi(\mathrm{L})\mathrm{dL}$ the number density of galaxies with luminosities in the range (L,L+dL) the corrisponding function is

$$\Phi(L) = (\Phi^{\star}/L^{\star})(L/L^{\star})^{\alpha} \exp(-L/L^{\star}) \tag{1.4}$$

where $\mathrm{L}^{\star}$ is the luminosity corresponding to an absolute magnitude of $\mathrm{M}^{\star}$. Thus, α sets the slope of the luminosity function at the faint end, $\mathrm{L}^{\star}$ or $\mathrm{M}^{\star}$ gives the characteristic luminosity above which the number of galaxies falls sharply and $\Phi^{\star}$ sets the over-all normalization of galaxy density.

In general, the Schechter function provides a reasonable fit to the LFs derived from a number of galaxy redshift surveys and has been found that the optical data are reasonably representative of the galaxies' over-all stellar population. Dividing galaxies into different types it became clear that they can have significantly different LFs. Figure**??** shows the luminosity functions of some 19000 galaxies in the Las Campanas Redshift Survey. It is found that emission and non-emission galaxies have very different luminosity functions: the emission galaxies dominate the faint end and non-emission galaxies prevail in the bright end. In particular, emission galaxies constitute about 15% of the total at M = -22, rising to about 80% at M = -17 while the number densities near the full-sample $\mathrm{M}^{\star}$ are quite similar. This result is not unexpected because the two populations are the mirror of the

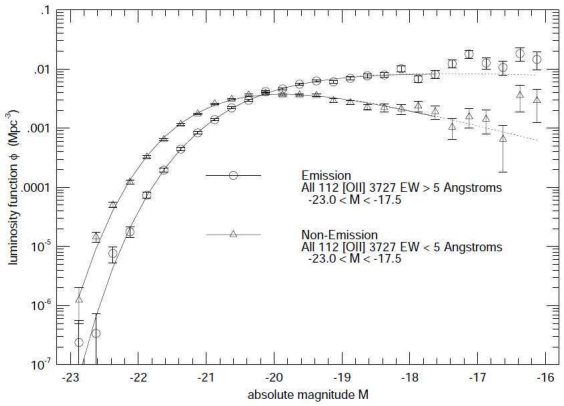

Figure 1.12: Luminosity functions for the combined LCRS sample, divided by [OII] 3727 equivalent width (Lin et al., 1996).

morphological division in late-type, blue galaxies (with emission line) and early-type, red galaxies (without emission line).

The galaxy luminosity in optical and NIR bands are directly related to the stellar mass and until a few years ago, the LFs were the most used diagnostic tool to estimate galaxy stellar masses and to study galaxy properties. However, the development of stellar population synthesis models and deep multi-wavelength surveys have greatly improved the ability to estimate the stellar mass. The distribution in stellar mass (galaxy stellar mass function, MF), its behavior and how it evolves over cosmic time is a more powerful parameter because it takes into account for both the hierarchical mass assembly by dark matter halos and the transformation processes that galaxies experience during their lifetimes and change the path of their evolution.

Brinchmann & Ellis (Brinchmann & Ellis, 2000) using a novel technique that utilizes K-band photometry to estimate the stellar masses of galaxies were able to probe the mass assembly of morphological populations, demonstrating how the global mass density of late-type galaxies has declined since $z \sim 1$, while that of spheroidals has grown (Figure1.13) - a process suggestive of a transformation between the two populations. A deep analysis on the MFs will be addressed in Chapter 4.

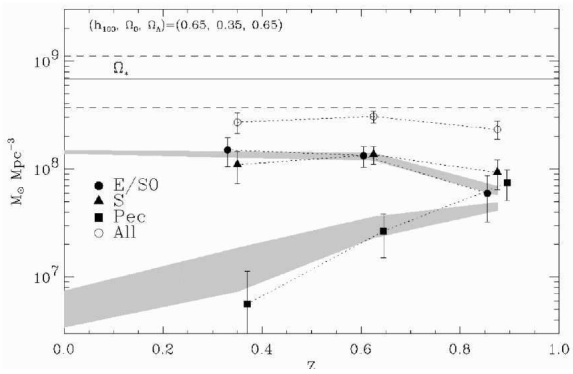

Figure 1.13: The evolution in the global stellar mass density of E/S0's, spirals, and peculiars defined by visual HST morphology (from Brinchmann & Ellis (2000)). The shaded regions show predictions from simple merger models.

1.3 Galaxy mass assembly history

In the hierarchical clustering scenario the cosmic structures form by a process of continuous mass aggregation, the mass aggregation history (MAH), which alternates some smooth phases with others more violent due to major mergers. By using the ΛCDM model, several studies showed that most of the mass of the present-day haloes has been aggregated by accretion while major major merging was more frequent in the past.

The major merging is important for several reason: it explains, for example, the formation of massive galaxy spheroids and the phenomena related to this process like QSOs, supermassive black hole growth, obscured star formation bursts, etc. Numerical simulations (Di Matteo et al. 2005) have shown that major mergers of two gas-rich disk galaxies can produce elliptical galaxies (see §1.2.1). In this encounters the stellar disks are detroyed, a nuclear starbursts triggers and feeds the growth of the internal black hole. The starburst consumes a great part of the gas while the remaining part is expelled through galactic winds and black hole's feedbacks (Mihos & Hernquist 1994, 1996). However, it is necessary a major merger with masses ratio below $\sim 3:1$ in order to induce the tidal torques and such a strong central inflow of gas able to modify the morphology. The most frequent mergers are those of higher mass-ratio (e.g. 10:1). In these cases a central component like a spheroid surrounded by a surviving disk structure is formed. Other processes such as harassment may be able to produce spheroid component, but the analysis of these structures show that

the kinematics and properties are different from those observed for elliptical galaxies. In this scenario galaxy disks are envisioned to form as the result of gas accreted smoothly from the intergalactic medium (Katz& Gunn, 1991).

Both the mass aggregation rate and major merging rate histories depend strongly on environment: the denser is the environment, the higher is the merging rate in the past. However, in the dense environments (group and clusters) form typically structures more massive than in the less dense regions (field and voids). Once a large structure virializes, the smaller galaxy-sized haloes become subhaloes with high velocity dispersions: the mass growth of the subhaloes is truncated, or even reversed due to tidal stripping, and the merging probability strongly decreases.

The environments can be deeply different for density, shape, photometric and dynamic properties and range from the enormous *voids* in which the number density of galaxies is greatly depleted, the *field* where galaxies are relatively isolated, the *binary systems* with two galaxies bound gravitationally to each other, the *groups* of a few close galaxies and *clusters* where 100-1000 galaxies are bound together by gravitational forces. If we now assume that galaxies form and reside in dark matter haloes, it becomes obvious that the properties of the galaxy population are related to the structures to which they belong.

1.4 Effects of environment on galaxy properties

Historically to assess the role of environment in galaxy evolution, the attention has been focused mainly on galaxy clusters. Rich clusters of galaxies are the largest gravitationally bound systems we know of in the Universe and are characterized by deep gravitational potential wells which can be observed through the bremsstrahlung X-ray emission of hot gas which forms an atmosphere within the cluster. The hot gas can also be detected through the decrements which it causes in the CMB adiation as a result of the Sunyaev-Zeldovich effect. Clusters, therefore, provide laboratories for studying many different aspects of galactic evolution. The first reason for this is the practical advantage of having many galaxies in a relatively small region of the sky and all approximately at the same redshift. They allow to study interactions among galaxies and with the intergalactic medium and the distribution and nature of the dark matter, which dominates their dynamics. From the perspective of

the formation of large-scale structure, the mass distribution of clusters provides constraints on the development of structure on large scales and on cosmological parameters.

An impressive number of spectroscopic and photometric results reveal that properties of galaxies such as the colours, morphologies and star-formation histories show some clear trends in these environments significantly different from those in field. In the next sections I will summarize some findings from the observations.

1.4.1 Morphological variations

One of the major property of a galaxy is its morphology. In a typical environment spiral and irregular galaxies account for $\sim 70\%$ of all galaxies with the rest being elliptical and SO galaxies. In the past decades it was recognized that galaxies in clusters are much more likely to be ellipticals or SOs than are those in the field (Hubble& Humason 1931, Zwicky 1936). Clusters are very dense systems and the core volume is usually permeated by extremely hot plasma with a pressure much higher than that of a galaxy's interstellar gas. At such densities, interactions with the plasma and direct encounters with other cluster members are likely to be important events in the life of a galaxy.

In 1951, Walter Baade and Lyman Spitzer suggested that SO galaxies are the final product of spiral galaxies that crossing in the dense environment of a cluster have their interstellar gas stripped losing their ability to form new stars. To be effective, this process requires a relatively rapid encounter (common in a rich cluster) because a low-speed collision would probably result in the merging or disruption of the original spirals. However, mergers are less likely than more elastic encounters because in dense clusters the speeds are $\sim 1000\mathrm{kms}^{-1}$, much greater than the orbital speeds of stars in the galaxies. Thus, if mergers were responsible for forming cluster ellipticals, they occurred relatively early, when the rich cluster was a collection of poorer, less-dense groups, each with a lower characteristic speed of member galaxies. Furthermore, the stellar density at the center of an elliptical galaxy is typically much higher than in a spiral suggesting that a significant amount of dissipation must have occurred and probably galaxies were more gaseous. Both of these arguments suggest that if mergers were important in forming elliptical and perhaps SO galaxies, they might have occurred so early as to be considered part of the formation process.

However, not all clusters are the same. Oemler (Oemler, 1974) found that $\sim 40\%$ of the galaxies in some clusters are elliptical while in others the proportion of ellipticals is more like $\sim 15\%$. The elliptical fraction was found to correlate with the morphology of the cluster: a large value of the elliptcal fraction tends to have a regular, symmetric appearance, often with a giant cD galaxy[2] at its center, while a small values of this fraction is generally associated to a cluster with a ratty appearance. Oemler's observations are also consistent with the fact that the fraction of spirals increases with the radius of the clusters. These discoveries provided the existence of a morphology-radius relation in clusters.

The first largescale study of morphological segregation was made by Dressler (Dressler, 1980) who obtained the morphological types of ~ 6000 galaxies in 55 clusters. Dressler's analysis confirmed that the fraction of spiral galaxies increases with the radius R (see left panel of Figure1.14) with the fraction of S0s that falls near the center but he concluded that correlations involving R are not fundamental ones and that galaxy type is really dictated by the local density[3] of galaxies inferring the existence of a morphology-density relations in clusters (see right panel of Figure1.14).

1.4.2 Star Formation variations

The star-formation properties of galaxies in rich clusters differ significantly from those of field galaxies (Osterbrock 1960, Dressler, Thompson & Shectman 1985, Balogh et al. 1997, Koopmann & Kenney 2004) . In the field, the star formation of galaxies is higher than in systems of similar luminosity in the core of clusters and this is due in part to the morphology-density relation because elliptical and S0 galaxies, principally passive systems, are more abundant in clusters.

However, there is evidence that also later type galaxies in clusters form stars at lower rates than in the field (Balogh, Navarro & Morris 2000). Balogh et al. (1999) shown that the [O II] equivalent widths, on average, are much larger for field galaxies then their counter-

[2]cD galaxies which are surrounded by extensive stellar envelopes. Many of these have extraordinary luminosities and masses, well above those found for galaxies in low-density environments. The view is commonly held (and supported by some admittedly disputed evidence) that cD galaxies have cannibalized neighboring galaxies, accreting by nondissipative mergers unfortunate companions that stray into their domain

[3]The local density of a galaxy is defined as the number of companion galaxies divided by the volume of the sphere enclosing them.

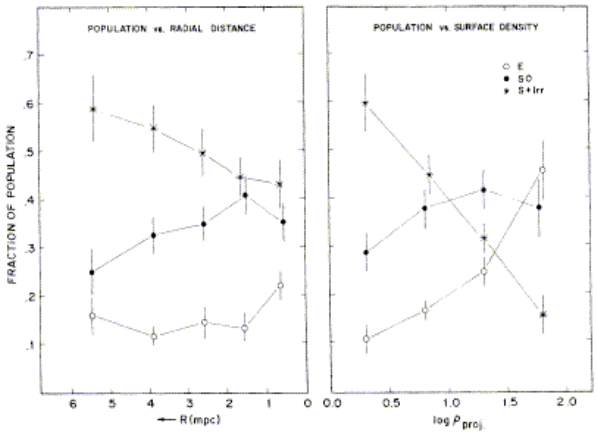

Figure 1.14: Fraction of galaxies for different morphological type as a function of distance from the centre R (left panel), and of density (right panel) (Galactic Astronomy, Binney & Merrifield).

parts in rich cluster with the same bulge-to-disk ratios and luminosities. The star-formation rate from [O II] can be influenced by dust (Smail et al. 1999, Poggianti & Wu 2000) but this limit can be overcome using the H_α index, which is less sensitive to dust effects (Kennicutt, 1998). From the analysis of an $\sim \mathrm{H}_\alpha$ survey of galaxies in three clusters at $\mathrm{z} \sim 0.3$, it has been found that in general only 10% of galaxies show H_α emission, with an overall star-formation rate of $\sim 4\mathrm{M}_\odot\mathrm{yr}^{-1}$ (Couch et al. (2001), Balogh & Morris (2001)) indicating a strongly suppression of the star formation.

1.4.3 Colour/Luminosity variations

The distribution in colour depends strongly on the galaxy density on $\sim 1\mathrm{Mpc}$ scales (Dekel & Birnboim 2006). blue and red galaxies tend to populate the low- and high-density environments respectively (Blanton et al. 2005a, Hogg et al. 2003, Balogh et al. 1997, Blanton et al. 2006, Kauffmann 2004).

Analysing the distribution of $\mathrm{g} - \mathrm{r}$ colour, mean surface brightness, Sérsic index and luminosity of ~ 114000 galaxies in the SDSS Blanton et al (2006) found that galaxy colour is the most predictive property of local environment as shown by the dominant horizontal contours in the lower-right panel of (Figure1.15). However, the basic result is that *at fixed luminosity and color, there is not a strong relationship between density and either Sersic*

index or surface brightness implying that the morphology-density relation is driven by the more fundamental colour-density relation. Balogh et al. (2004) studying the $\mathrm{u}-\mathrm{r}$ and luminosity dependence on density for a sample of ~ 25000 SDSS reached slightly different results. They observed that fixing the luminosity, the mean colour of the blue distribution is roughly independent on environment; in contrast, the fraction of galaxies in red distribution as function of density changes drammatically with environment passing from 10-30% in the low density regions up to $\sim 70\%$ in the high density regions (see Figure1.16) (Balogh et al., 2004).

Figure1.17 shows the luminosity functions (LFs) for galaxies in different environments, from rich clusters to the field, subdivided by morphological type. It is important to note that the peculiar characteristics observed in the total LFs for each environment are the product of thevariation in the relative proportions of each galaxy type between cluster and field regions. The studies of the LF have shown that the bright end is mostly populated by red galaxies and, on the contrary, the faint end is principally dominated by blue systems: the luminosity value at which this sharp transition occurs is slightly below $\mathrm{L}_\star$ which corresponds to a stellar mass $\sim 2\mathrm{M}_{\mathrm{crit}}$[4] (Dekel & Woo 2003).

1.5 Physical processes in high density environments

Galaxy transformations within dense environment are driven by a wide variety of physical processes. In the following, I will make an overview of these processes and their relative importance at different masses, times, and environments.

- Mergers : Galaxy mergers are generally strong galaxy-galaxy interactions and are commonly rare in massive clusters because of the large velocity dispersion of these systems. They are more efficient in the infalling group environment and may therefore represent an important "preprocessing" step in the evolution of cluster galaxies. Mergers are intrinsically included in standard semi-analytic models of galaxy formation and represent the main channel for the formation of bulges. In the hierarchical galaxy formation scenario, more massive galaxies form through the mergers of smaller objects and larger systems are expected to be made up by a larger number

[4] $\mathrm{M}_{\mathrm{crit}} \simeq 3 \times 10^{10}\mathrm{M}_\odot$

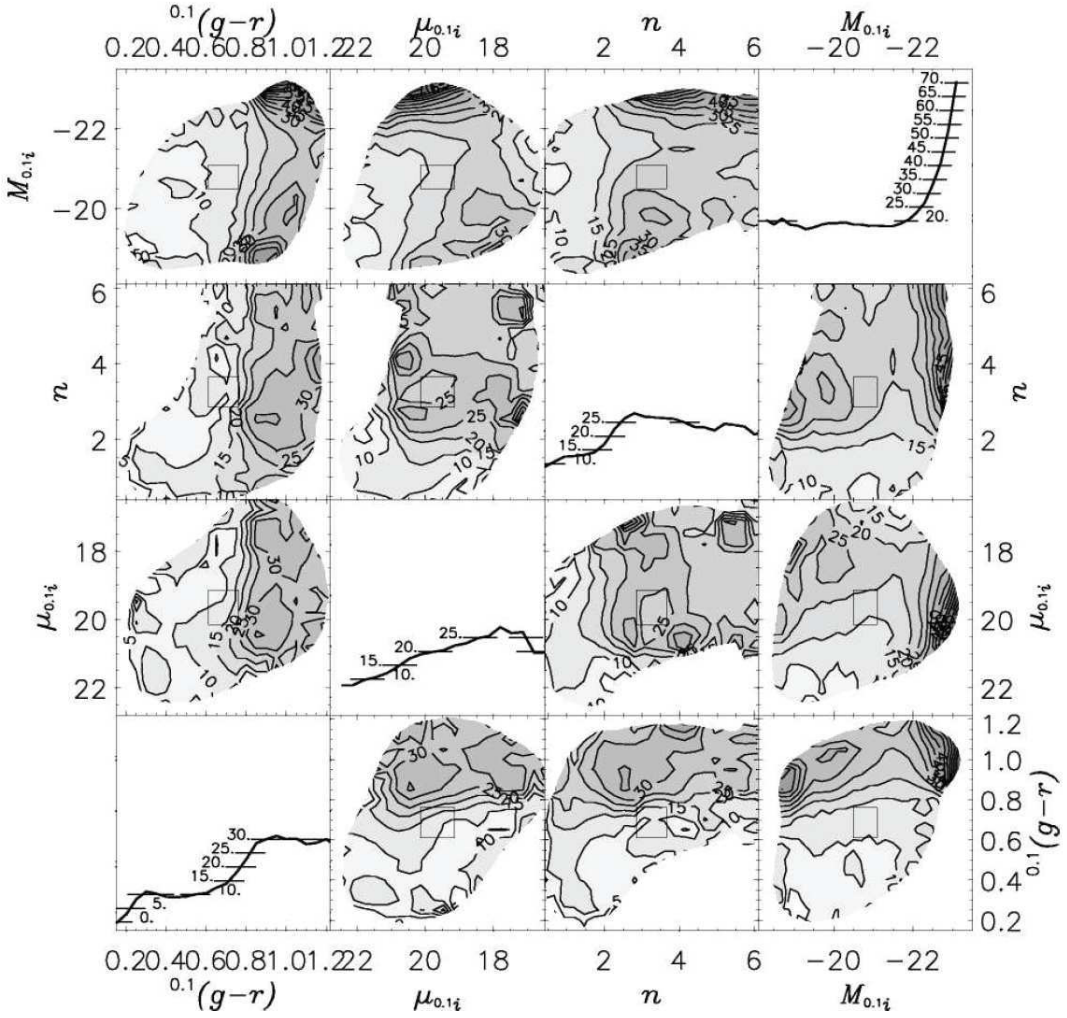

Figure 1.15: Mean local overdensity on 1Mpc scales as a function of pairs of galaxy properties. Off-diagonals show the mean overdensity as a colour-coded contour plot in which darker areas indicate galaxies in denser environments (The contours on the greyscale indicate the areas containing 97%, 84% and 52% of the distribution, from the outer to the inner). For example, in the lower-right corner, the blue, low-luminosity galaxies are on average in the least dense environments and the red, high-luminosity galaxies are on average in the most dense environments. Plots along the diagonal show the mean overdensity as a function of colour, surface brightness, Sersic index and magnitude on a linear scale. The mean is calculated in a sliding box with widths 0.15, 1.0, 0.8, and 0.6 in colour, surface brightness, Sersic index and absolute magnitude respectively (Blanton et al. 2006).

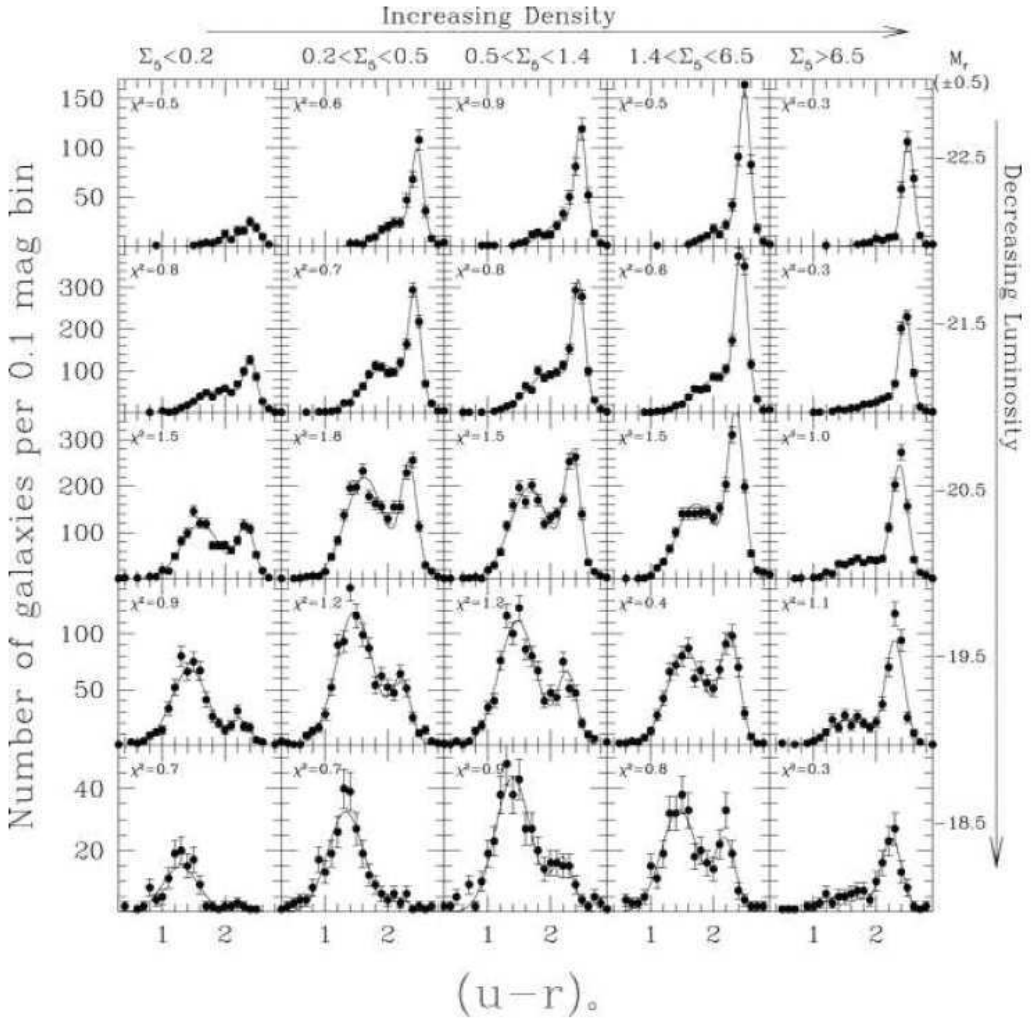

Figure 1.16: The solid points in each panel show the $\mathrm{u}-\mathrm{r}$ color distribution of galaxies in bins of local density and luminosity. The population is divided into five density bins with the three middle bins having an equal number of galaxies and the least and most dense having half as many, to sample the extremes of the distribution. The solid line is the double Gaussian fit. The reduced χ^2 of the fit is reported in each panel ().

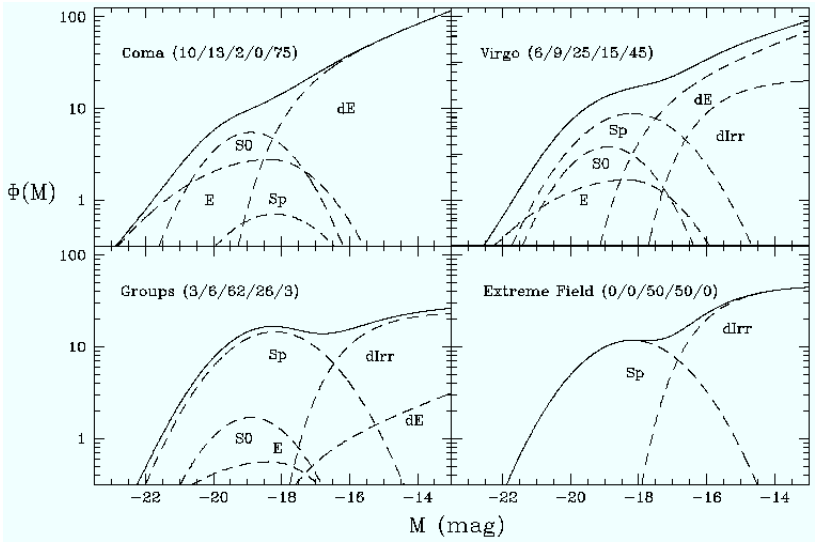

Figure 1.17: The luminosity function for different morphological types computed in different environments. The solid curves represent the total LF. The number in each panel represent the number of E, S0, Sp, dIrr, dE galaxies respectively from left to right.

of progenitor galaxies. De Lucia et al. 2006 have investigated how the number of progenitors varies as a function of galaxy mass and the result is that more massive galaxies are made up of more pieces. However, the number of effective progenitors is less than 2 up to stellar masses of $10^{11}\mathrm{M}_{\odot}$, indicating that the formation of these systems typically involves only a small number of major mergers and only more massive galaxies are built through a larger number of mergers.

- Harassment : Galaxy harassment is a process that is not usually included in semi-analytic models of galaxy formation and consists of repeated fast encounters coupled with the effects of the global tidal field of the cluster (Moore et al. 2006). Numerical simulations (Farouli& Shapiro 1981) indicate that the efficiency of this process is largely limited to low-luminosity hosts, due to their slowly rising rotation curves and their low-density cores. For this reason, it is believed that harassment might have an important role in the formation of dwarf ellipticals or in the destruction of low-surface brightness galaxies in clusters, but it is less able to explain the evolution of luminous cluster galaxies.

- Ram pressure stripping : Galaxies in groups and clusters that travel through a dense intra-cluster medium (ICM) suffer a strong ram-pressure stripping that sweeps cold gas out of the stellar disc (Gunn & Gott 1972). The ICM will either be forced to flow around the galaxy or will blow through it removing some of the diffuse interstellar medium (ISM) depending on the binding energy of the ISM itself. Related mechanisms are thermal evaporation (Cowie & Songaila 1977) and viscous stripping of galaxy discs (Nulsen 1982), that occur when ram-pressure is not effective. In this case, turbulence in the gas flowing around the galaxy entrains the interstellar medium resulting in its depletion. Unlike the physical mechanism discussed before, gas stripping does not affect galaxy morphology directly even if once star formation is halted in a disc, this can fade significantly and the bulge-to-disc relative importance can change. The effect of ram-pressure stripping has been discussed only in a couple of studies using semianalytic techniques (Okamoto & Nagashima 2003; Lanzoni et al. 2005): the inclusion of this additional physical process, infact, causes only mild variations in galaxy colours and star formation rates because the stripping of the hot gas from galactic haloes (see below) suppresses the star formation so efficiently that the effect of ram-pressure is only marginal.

- Strangulation : Current theories of galaxy formation suggest that when a galaxy is accreted onto a larger structure, the gas supply can no longer be replenished by cooling that is suppressed (Larson, Tinsley, & Caldwell 1980). This process has been given the quite violent name of ”strangulation” (or starvation or suffocation) and it represents one important element of semi-analytic models of galaxy formation. Generally strangulation is expected to affect a galaxy star formation history on a quite long timescale and therefore to cause a slow declining activity. This is not what happens in practice. If this process is combined with a relatively efficient supernovae feedback (and this is the case in many recent models), galaxies that fall into a larger system consume their cold gas very rapidly, moving onto the red-sequence on quite short time-scales.

1.6 The role of lower mass systems

As discussed in §1.4 the major discoveries concerning the impact of hierarchical assembly and thus environment on galaxy evolution come from the studies conducted on clusters. The Butcher-Oemler effect, the morphology vs. density relation and the star formation vs. density relation have shown that the properties of galaxies within clusters are strongly correlated with the local environment and evolve with redshift (see, e.g., Dressler 1980; Butcher & Oemler 1984; Dressler et al. 1997; Poggianti et al. 1999; Balogh & Bower 2003). In agreement with the observed trends a presumable scenario is that the clustering process itself would drive the evolution of the galaxy properties and the typical increase of the early-type fraction with decreasing redshift would be due to gas-rich, star-forming disk galaxies which fall into clusters at higher redshift (z$\sim$0.5-1) and have their gas reservoir depleted by some mechanism that transforms them into red, bulge-dominated and quiescent galaxies at z$\sim$0. Among the numerous mechanisms I described in §1.5 the most accreditated to deplete the reservoir of gas in late-type galaxies are ram-pressure and/or tidal stripping (Gunn & Gott, 1972), interaction with the cluster potential (Byrd & Valtonen, 1984) and repeated high-velocity encounters ("harassment") (Moore et al., 1996). But, clusters are rare and biased systems. Only about 10% of the cosmic galaxy population resides today in clusters, and this fraction decreases with increasing redshift. Then, although they play a crucial role in the morphological transformation of galaxies, they cannot have a large effect on the properties of galaxies to explain, for example, the decline of the star formation density of the Universe as a whole.

Recent results (Zabludoff & Mulchaey, 1998; Mulchaey et al., 2003) have focused on the hypothesis that the anomalous fraction of early-type galaxies in clusters is the consequence of some pre-process which takes place in *groups* before galaxies are accreted into the cluster. This hypothesis is supported by the observations of a decline in star formation rate (SFR) in the outskirts of clusters, well outside the virial radius (Balogh et al., 1999; Lewis et al., 2002). Even if the pre-processes in the group environment seem not to produce a large effect (Berrier et al., 2009), it is nevertheless true that the mechanisms like galaxy mergers and strangulation that efficiently act also in groups could play a very important role in the formation of the galaxy populations, as it has been shown by combining high-resolution N-body simulations with semi-analytic models for galaxy evolution (Springel

et al., 2001; Kang et al., 2005; Mihos, 2004; Toomre, A. & Toomre, J., 1972; Barnes & Hernquist, 1996; Cox et al., 2008; Murante et al., 2007; Somerville et al., 2008; Guo et al., 2011; Wang, Kauffman & De Lucia, 2007; Font et al., 2008; Weinmann et al., 2010).

Compared to clusters, galaxy groups are more difficult to detect because they have a lower density with respect to the background galaxy population. But, understanding the physical processes in action in galaxy groups and their effects on the properties of galaxy population is important for two reasons: 1) they are the most common structures in local universe and over 60% of galaxies are in these systems 2) the transition between galaxy properties typical of field and clusters happens just at the characteristic densities of groups (Zabludoff& Mulchaey 1998). Thus, groups are thought to be the ideal place to investigate galaxy evolution and to provide a clear framework on the nature of the physical galaxy transformation mechanisms.

1.7 Outlines and goals of the thesis

The goal of the thesis is to analyze the main galaxy properties in groups and to investigate how they evolve in relation to different environments.

In Chapter 2, I describe the Friends-of-Friends algorithm used to build a catalog of groups and galaxies representative of the general field population at low redshifts with high quality data, the Padova Millennium Galaxy andd Group catalog (PM2GC). Following this method I also identify other environments: the isolated sample and the binary systems sample. Then, I describe how the galaxy stellar masses have been derived.

In Chapters 3, I make a direct comparison of the morphology of group galaxies with those of other environments in my catalog and with cluster galaxies from the WIde-field Nearby Galaxy cluster Survey (WINGS). I describe the MORPHOT tool used to morphologically classify galaxies. Finally, I show how the distribution of morphological mix and the morphology-mass relation vary in the different environments considered.

In Chapter 4, I completed the work starded with the morphological analysis using the galaxy mass function (MF) and investigate its variation with global environment. Comparing the stellar masses in a consistent manner I found important indication on how the effect of mass and environment are related and whether environment can influence the stellar

mass distribution.

Chapter 2

Galaxy Groups

2.1 A global picture

A galaxy group is a concentration of galaxies physically bound together due to their mutual gravitational attraction and the presence of the dark matter halo. However, not all observed groupings of galaxies are real physical and gravitationally bound systems. Often, they are systems gravitationally unbound (called pseudo-groups) that can be a result of superpositions of galaxies at different distances or galaxies within filaments that are viewed edge-on (Hernquist et al., 1995, Ramella et al., 1997). A group of galaxies typically contain fewer than ~ 50 members, is $\sim 1-2$ Mpc in a diameter and has a total mass $\mathrm{M_{DM}} \sim 10^{12.5-14.0}\mathrm{h^{-1}M_{\odot}}$ (Huchra & Geller, 1982), while typical clusters contain more than 300 galaxies, are about one order of magnitude more massive and a few times larger (Einasto et al., 2003a, 2005, Koester et al., 2007).

The study of galaxy groups (and clusters) can be dated back to 1933 and since then several authors conclude that the majority of galaxies in the Universe lie in groups (Huchra & Geller 1982, Holmberg 1950, Humason et al. 1956, Geller & Huchra 1983, Nolthenius & White, 1987, Ramella et al., 1989, Karachentsev 2005). Large astronomical redshift surveys such as the 2dFGRS (2dF Galaxy Redshift Survey) and SDSS (Sloan Digital Sky Survey) have also produced large group catalogs (Eke et al. 2004a,b, MerchÃ¡n & Zandivarez, 2005, Tago et al. 2006, Berlind et al., 2006, Yang et al., 2007, Knobel et al., 2009) with up to ten thousand groups (Balogh et al., 2004). To identify groups using the redshift-space

information a vast number of grouping algorithm exist but the most frequently applied is the Friends-of-Friends one (in the subsection §2.3.2 I will give a description of the FoF algorithm used).

Groups algorithms produce catalogs of galaxy systems with a vast amount of different properties that can be classified as loose (Ramella et al. 1995, Tucker et al. 2000, Einasto et al. 2003b), poor (Zabludoff &Mulchaey 1998, Mahdavi et al. 1999), compact (Shakhbazyan 1973, Hickson 1982, Hickson et al. 1989, Diaferio et al. 1994, Barton et al. 1996, Tovmassian et al. 2006) and fossil groups (Ponman et al. 1994, Jones et al. 2003, von Benda-Beckmann et al. 2008) according to the diversity of evolutionary stages within which they can be found. For example, compact groups are assumed to be observed briefly before they are about to merge, while fossil groups are the end product of such a merging.

The first basic property of groups is the velocity dispersion σ_v that usually ranges up to a few hundred $\mathrm{km\,s^{-1}}$ (while clusters show dispersions up to about a thousand $\mathrm{km\,s^{-1}}$) and is often measured in radial direction due to the difficulties in measuring the true 3-dimensional motions of galaxies. In general the velocity dispersion is only a meaningful quantity if the group is a gravitationally bound system, otherwise some of the members in the pure Hubble flow and their radial velocities are biased (Baryshev et al. 2001, Macció et al. 2005, Chernin et al. 2009). For this reason there is no guarantee that the FoF algorithm identifies only groups that are bound structures.

As said at the end of chapter 1 groups span a wide range of galaxy populations and, even so the physical processes operating in groups of galaxies are still poorly understood, they are known to be important for several reasons. For example, dark matter haloes and even galaxies merge together (§1.3) and mergers are only effective in systems with a velocity dispersion smaller than or comparable to the internal velocities of galaxies. Hence galaxy mergers are assumed to take place effectively in groups of galaxies. Before groups can be used to study the evolution of galaxies or even before any group properties can robustly be measured, groups of galaxies must be correctly identified and discriminated from other forms of structures like binary galaxy pairs, large clusters of galaxies and most importantly from chance alignments.

2.2 Evolution in groups

Our understanding of how galaxies evolve in relation to the large-scale structure in which they live is based on a well defined result: the early-type galaxies (ellipticals and S0s) inhabit dense regions of the universe such as clusters while late-type galaxies are more common in the field (e.g Abell 1965, Oemler 1974, Bahcall 1977). Being galaxy groups a transient environment in the context of the hierarchical formation scenario in which most of the evolution of a galaxy takes place is fundamental to investigate the evolutionary history even on these scales.

It is known that the increasing fraction of early-type galaxies since $\mathrm{z} \sim 0.5$ in clusters corresponds mainly an increasing of lenticular galaxies (S0) with a constant elliptical fraction (Dressler 1997, Fasano et al. 2000). At higher redshift there is no evidence for any further evolution of the S0 fraction in clusters to $\mathrm{z} \sim 1$ (Smith et al. 2005, Postman et al. 2005, Desai et al. 2007). The morphology-density relation found by Dressler (1980) can be interpreted as evidence that local processes played a crucial role in determining galaxy type. Postman& Geller (1984) found that this relation extends smoothly to galaxy groups but vary strongly from group to group. At $\mathrm{z} \sim 0$ elliptical/passive galaxy dominate the members of optically selected groups (Wilman et al. 2005a) while spiral/star-forming galaxy dominate the more massive X-ray selected groups (Jeltema et al. 2007). This result is evident also at intermediate redshift but seems not be correlated with velocity dispersion or local density as in low-redshift groups (Postman& geller 1984, Zabludoff& Mulchaey 1998, Poggianti et al. 2006). Recently, Wilman et al. 2009 analyzing a sample of groups at $\mathrm{z} \sim 0.4$ selected from the Canadian Network for Observational Cosmology (CNOC2) redshift survey observed that in groups there is a much higher fraction of S0s than in the lower density field at fixed luminosity similar to that in clusters at same redshift and this fraction is less common in the inner region than at larger distances. On the contrary, the fraction of late-type galaxyes is mostly suppressed in groups compared to the field. They conclude that the low mass groups *are likely the dominant environment for the formation of S0s* and the evolving fraction of S0s in clusters might be due to an accreted galaxy population that infall from groups and the field.

In group-scale environments is also well established the suppression of star formation rate (Balogh et al. 2004). The first studies of star formation focused on optical indicators

emission lines (H_α or [OII]$\lambda 3727$) or ultraviolet continuum indicated a significant lower level of star formation activity in groups than in the field (Wilman et al. 2005a, Gerke et al. 2007, Iovino et al. 2010, Peng et al. 2010). Tyler et al (2011) investigating IR luminosities of a sample of groups at intermediate redshift found that although groups and field galaxies not differ significantly in term of their SFRs there is a large fraction of early-type spirals that are still forming stars at a significant level and this may explain why the LFs of the groups and field are nearly identical despite the overall decrease in star forming activity in the groups.

Moreover, study at optically wavelengths have shown that at both locally and intermediate redshift the ratio between dynamical mass and optical light (M_{200}/L_{opt}) increases strongly with mass. Using NIR data, more sensitive to stellar masses regardless of the star formation, from the William Herschel Telescope and from the Spitzer telescope Infrared Array Camera (IRAC) data archive Balogh et al. (2007) found that galaxies in groups are predominantly old, passively evolving systems even at $z \sim 0.4$.

All these studies point to the role of groups as the locations in which crucial transformations occur. In the following sections and in the chapter 3 and 4 I investigated the main properties of a new sample of galaxy groups and for the first time I compared them in a consistent manner with those of galaxies in the widest range of environments at low redshift.

2.3 The Padova-Millennium Galaxy and Group catalog (PM2GC): the FoF method and the catalogs of group, binary and single field galaxies

Until recently, the difficulties in obtaining large, unbiased samples of groups have forced most of the studies to use small samples selected, for example, from the Hickson compact group catalog (Hickson, Kindl & Auman, 1989), from the CfA redshift survey (Geller & Huchra, 1983; Moore, Frenk & White, 1993), and from X-ray surveys (Henry et al., 1995; Mulchaey et al., 2003). Only with the advent of large galaxy redshift surveys, such as the Two degree Field Galaxy Redshift Survey (2dFGRS), the Sloan Digital Sky Survey (SDSS)

and the Canadian Network for Observational Cosmology Redshift Survey (CNOC2), has it become possible to generate large group catalogs in the local Universe (e.g. Huchra & Geller 1982; Ramella, Geller & Huchra 1989; Ramella, Pisani & Geller 1997; Ramella et al. 1999; Hashimoto et al. 1998; Tucker et al. 2000; Martínez et al. 2002; Eke et al. 2004; Balogh et al. 2004), and at intermediate redshift (Carlberg et al., 2001; Wilman et al., 2005). The 2PIGG (2dFGRS Percolation-Inferred Galaxy Group) catalog (Eke et al., 2004) and the SDSS group catalog (Berlind et al., 2006) are two of the largest available samples of galaxy groups which use "realistic" mock catalogs to calibrate the parameters associated with the group-finder algorithm.

The motivation for another group catalog and for our work is to provide a new dataset characterized by both high spectroscopic completeness, to define galaxy environment well, with high quality imaging, to investigate galaxy properties such as galaxy morphologies which could not explored in detail in other catalogs.

In the following I present the construction and describe the properties of the Padova-Millennium Galaxy and Group catalog (PM2GC), a galaxy catalog representative of the general field population in the local Universe.

2.3.1 The Datasets

To build a catalog that satisfies the requirements of spectroscopic and photometric completeness, I used a set of galaxies derived from the Millennium Galaxy catalog (MGC) (Liske et al., 2003; Cross et al., 2004; Driver et al., 2005), a B-band imaging survey, both deep and wide, which provides a high quality, complete representation of the nearby galaxy populations.

A detailed description of the survey strategy, the photometric and astrometric calibration and the object detection and classification can be found in Liske et al. (2003). In brief, the survey extends along an equatorial strip covering an area of $\sim$37.5 deg^2 and consists of 144 overlapping fields taken with the WFC four-CCD mosaic on the Isaac Newton Telescope, with a uniform isophotal detection limit of 26.0 mag arcsec^{-2}. The catalog contains about one million of objects reduced by the Cambridge Astronomy Survey Unit (CASU) (Irwin & Lewis, 2001) and classified using Source Extractor (SExtractor, Bertin & Arnouts (1996)). The entire set of objects, spanning the range $16 \leq B_{MGC} < 24$,

ENVIRONMENT	NUMBER OF GALAXIES	
	$0.04 \lesssim z \lesssim 0.1$	$0.03 \leq z \leq 0.11$
Groups	1057	–
field-single	846	1141
field-binary	367	490
Mix sample	208	522
General field	2460	3210

Table 2.1: List of the number of galaxies in the different environments.

was next divided into two magnitude ranges to better address the division between stars and galaxies: the MGC-BRIGHT catalog, which contains all objects with B_{MGC} <20 mag, and the MGC-FAINT catalog which contains the others. For this analysis I selected a sample of galaxies from the MGCz catalog - a version of the total MGC database available on DVD - that is the spectroscopic extension of MGC-BRIGHT. It was built upon the redshifts provided by the 2dFGRS and the SDSS-EDR/DR1, in which the MGC survey region is fully contained, and completed with redshifts taken by the MGC team at the Anglo Australian Telescope using the 2dF facility (Driver et al., 2005), as well as redshifts from the NASA Extragalactic Database (NED), the 2dF QSO Redshift Survey (2QZ), the Paul Francis' Quasar Survey and of some low surface brightness galaxies. The total spectroscopic completeness of galaxies obtained by MGC team is greater than 96 per cent for B_{MGC} <20, so I have no need to apply a statistical completeness correction to sample[1].

At the beginning, I extracted galaxies at 0.03≤z≤0.11; I chose this redshift range to avoid galaxies too close by whose spectra only sample the central regions, while remaining at sufficiently low redshifts to retain a deep absolute magnitude completeness limit. Absolute B-band magnitudes were obtained k-correcting the observed SEXTRACTOR 'BEST' magnitudes (MAGAUTO, except in crowded region where the ISOCOR magnitude was used instead), corrected for Galactic extinction. The k-corrections were taken from Poggianti (1997) using the galaxy redshift and the Sloan galaxy color provided in the MGCz catalog (hereafter, MGC-SDSS).

To build my catalogs I used only 3210 bright galaxies with a magnitude M_B <-18.7 corresponding to the k-corrected B_{MGC} =20 magnitude at my redshift upper limit. In Fig.2.1 a plot of absolute magnitude vs. redshift for this sample is shown. The high spec-

[1]For the additional completeness test see §2.4.2

troscopic completeness to B_{MGC} <20, coupled with the photometric depth, makes it a complete absolute magnitude-limited sample for $\mathrm{M_B} \leq -18.7$.

2.3.2 Group building method

The approach I used to identify galaxy groups is similar to that adopted by McGee et al. (2008), and is based on a plain FoF algorithm. According to FoF criteria, two galaxies, *i* and *j*, are physically related and join the same group if their distances in the projected direction (D) and in the line-of-sight (V) are less than some fixed thresholds, i.e.

$$D_{ij} \leq D_L; \quad V_{ij} \leq V_L \tag{2.1}$$

D_L and V_L are called "linking lengths" and link together all galaxies within a particular linking volume. I chose these lengths to take into account the typical gravitational bounds of groups and to follow a similar approach of that used to identify groups at high redshift in the ESO Distant Cluster Survey (White et al., 2005; Halliday et al., 2004; Milvang-Jensen et al., 2008; Poggianti et al., 2006). Similarly to other studies (McGee et al., 2008; Wilman et al., 2005), we adopted for a linking volume a cylinder centred on each galaxy with radius

$$D_L = 0.5 h^{-1} Mpc \tag{2.2}$$

corresponding to a density contour $\frac{3}{4\pi D_L^3 n} = 216.6 gal^{-1}$, being n the mean observed number density of galaxies in the total sample. The line-of-sight depth V_L is equal to three times the velocity dispersion, fixed at 500 $\mathrm{km\,s^{-1}}$ rest frame, of the galaxy redshift.

For each galaxy in my sample brighter than M_B =-18.7, I obtained its first neighbours in the cylinder defined above, and added to these, by a recursive procedure, neighbors of neighbors, until no more are found. The resulting system I defined the "trial" group. Only systems with at least three galaxies were further considered as group candidates.

As a second step, I computed for each trial group its median geometric centre, median redshift and velocity dispersion using the statistical methods by Beers, Flynn & Gebhardt (1990), considering the gapper scale estimator for groups with less than ten galaxies and the biweighted scale estimator for more populous systems. A galaxy was considered member

of a group if its spectroscopic redshift lay within $\pm 3\sigma$ from the median group redshift and if it was located within a projected distance of $\pm 1.5\, R_{200}$ from the geometrical centre. R_{200} is an approximation of the virial radius - the radius which delimites a sphere with mean interior density 200 times the critical density - computed as in Finn et al. (2005) Finn et al. (2005)

$$R_{200} = \frac{1.73\sigma}{1000 km s^{-1}\sqrt{\Omega_\Lambda + \Omega_0(1+z)^3}} h^{-1} Mpc \tag{2.3}$$

where σ and z are the group's velocity dispersion and median redshift, respectively.

I iterated the second step several times, recalculating every time the group redshift, velocity dispersion and R_{200}, and moving to the next iteration only those groups with at least three members. The process stops when the last two iterations have identical output. At most, three iterations were sufficient to reach convergence. I consider members of the final groups only those galaxies that are within $1.5\, R_{200}$ from the group centre and 3σ from the group redshift.

Using this method I obtained a sample of 176 galaxy groups in the redshift range 0.04≤z≤0.1 containing in total 1057 group members with magnitude M_B <-18.7.

Groups below z∼0.04 and above z∼0.1 are disregarded in the following analysis, because, for a maximum velocity dispersion of 800 $\mathrm{km\,s^{-1}}$, and due to the redshift limits of my original sample $(0.03 - 0.11)$, they can suffer from spectroscopic incompleteness.

I have mentioned before that the total spectroscopic completeness of my sample is 96% to $B = 20$. Sky regions with the highest galaxy density, such as groups, might in principle suffer from higher incompleteness, due to the difficulty to place fibers close together. This problem is strongly mitigated in the MGC sample, because it is a combination of three different spectroscopic campaigns (SDSS, 2dF and MGCz). However, in order to double-check the completeness in groups, I performed an additional test. For each PM2GC group, within the angular radius corresponding to R_{200} from the group's centre, I counted the number of MGC galaxies with redshift and the total number of galaxies in the photometric catalog brighter than $B = 20$. The ratio of the sum of all galaxies with redshift and the sum of all galaxies in the photometric sample for all groups is r_1. Using the same R_{200} I considered for each group a random RA, DEC for the group centre within the MGC area and counted again the number of galaxies with redshift and the number in the photometric catalog brighter than $B = 20$ within the same R_{200}. For each group I repeated this 100

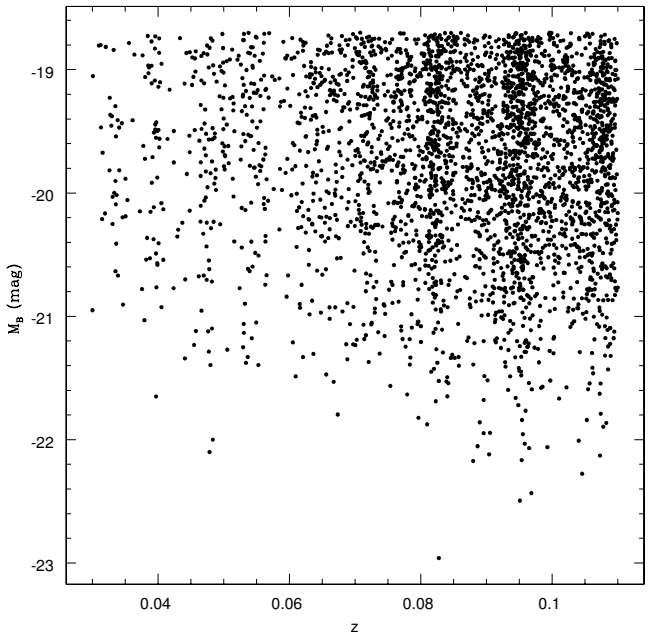

Figure 2.1: Absolute magnitude in B band vs. redshift for my data sample.

times, finding each time a value r_2. The mean value of the ratio r_1/r_2 is 0.999 confirming the high spectroscopic completeness of the galaxy redshift catalog even for galaxies preferentially clustered in groups.

Moreover, I analyzed my 176 groups to assess whether they are fully contained in the narrow strip of the MGC survey: the aim was to understand how many and which groups suffer from edge problems and therefore need to be treated with caution in the subsequent analysis. Looking at the group centre position coordinates, I flagged those 66 groups for which $RA_{centre} \pm R_{200}$ and/or $DEC_{centre} \pm R_{200}$ fall out of the ranges of the MGC strip.[2] Six of these had clear edge problems also from the comparison with the 2PIGG survey (see §2.6).

[2]The fractional area lost adopting these limits instead of $RA_{centre} \pm 1.5\, R_{200}$ and $DEC_{centre} \pm 1.5\, R_{200}$ is negligible, therefore also the difference in number of galaxies falling outside of the field is irrelevant.

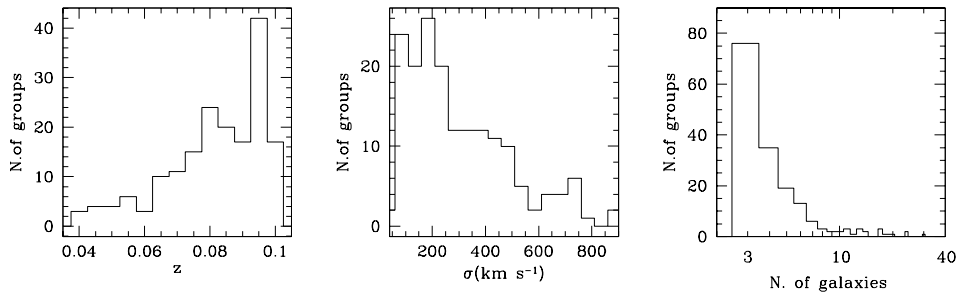

Figure 2.2: Redshift (z) distribution (left), velocity dispersion (σ) distribution (centre) and number of members distribution (right) of the 176 groups at 0.04≤z≤0.1.

2.3.3 Other environments

Galaxies that are not members of my 176 groups are treated separately, to study galaxy properties in several environments and compare the results.

I named "field-single" and "field-binary" those subsets of galaxies at 0.03≤z≤0.11 that have no friends (1141) or solely one friend (490) in their original trial cylindrical volume, respectively. The first sample, which contains isolated galaxies, is considered as pure field; the second one is composed of binary systems of galaxies, i.e. those pairs of bright galaxies that have a projected mutual separation within $0.5h^{-1}$Mpc and a redshift within $1500\mathrm{km\,s^{-1}}$.

The remaining 522 galaxies that are not in groups, field-single or field-binary environments are either those that are in groups at z<0.04 or z>0.1 (302) or those galaxies that, although located in a trial group, did not make it into the final group sample (220). These galaxies are part of the outer regions of groups (outside $1.5\,R_{200}$), therefore I prefer not to consider them as "single".

Finally, the sample of all galaxies in all environments at 0.03≤z≤0.11 is named "general field" (GF from now on), and is representative of the general field low-z galaxy population. In Table 2.1 I list the number of galaxies in different environments.

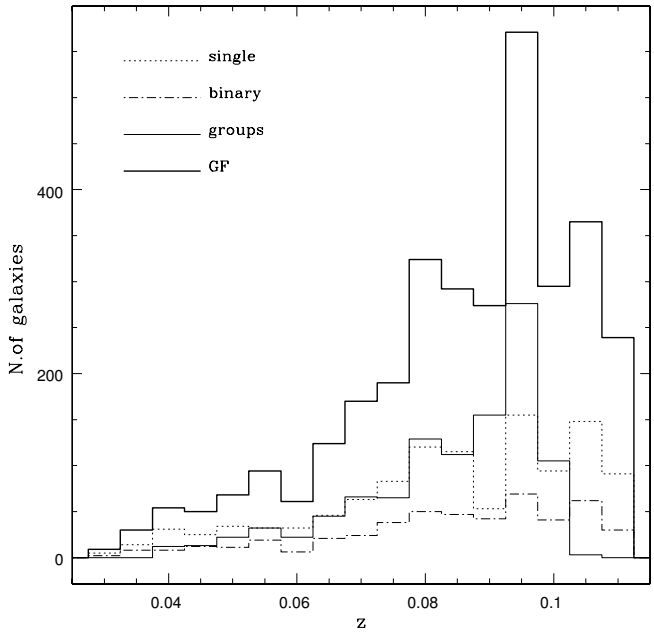

Figure 2.3: Redshift distribution for the different samples of galaxies: 1141 field-single galaxies (dotted line, 0.03≤z≤0.11), 490 field-binary galaxies (dot-short dashed line, 0.03≤z≤0.11), 1057 group galaxies (solid thin line, 0.04≤z≤0.1) and 3210 general field (GF) galaxies (solid thick line, 0.03≤z≤0.11).

2.4 Properties of groups and galaxies in the different environments

In Figure2.2 I show the general characteristics of my group sample. It is clear that, as in other catalogs, most of the groups lie in the higher redshift range, and contain fewer than 10 members. The median redshift and velocity dispersion of the sample are 0.0823 and 191.8 $\mathrm{km\,s^{-1}}$, respectively. The range of velocity dispersion is between 100 $\mathrm{km\,s^{-1}}$ and 800 $\mathrm{km\,s^{-1}}$for most groups, with 11 per cent having a velocity dispersion $<$100 $\mathrm{km\,s^{-1}}$ and 29 per cent $>$400$\mathrm{km\,s^{-1}}$. Hence, a significant fraction of the structures I identify have velocity dispersions higher than 400 $\mathrm{km\,s^{-1}}$, which is the commonly adopted limit between groups and clusters. The fraction of groups with less than five members is 63 per cent and 43 per cent have only three members.

In Figure2.3 I show a comparison of the redshift distribution of galaxies in the several

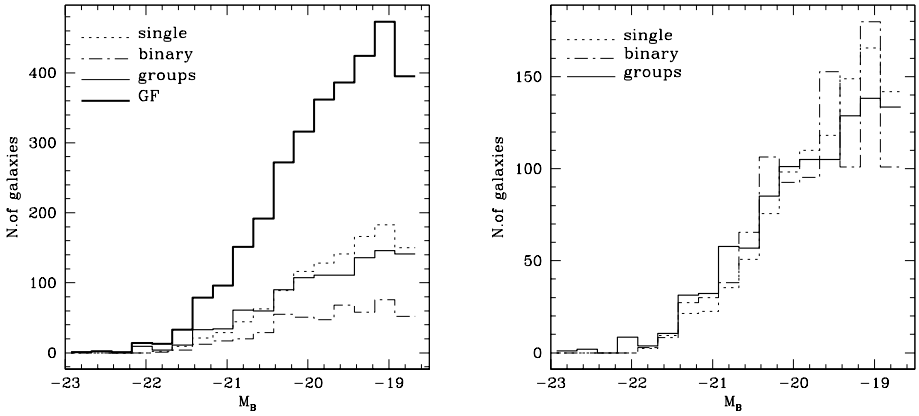

Figure 2.4: **Left.** B-band absolute magnitude distribution for the different samples of galaxies: 1141 field-single galaxies (dotted line, $0.03 \leq z \leq 0.11$), 490 field-binary galaxies (dot-short dashed line, $0.03 \leq z \leq 0.11$), 1057 group galaxies (solid thin line, $0.04 \leq z \leq 0.1$) and 3210 general field (GF) galaxies (solid thick line, $0.03 \leq z \leq 0.11$). **Right.** The absolute magnitude distributions of group, binary and field galaxies, all in the range $0.04 \leq z \leq 0.1$, normalized to the same total number of galaxies (N=1000).

environments I have identified. I note the presence of a prominent peak at $z \sim 0.095$ in the general field distribution, due to groups likely belonging to a quite populated structure at that redshift.

The magnitude distribution of galaxies in the different environments is shown in Figure2.4. Raw numbers are given in the left panel, while in the right panel the group, binary and single galaxy distributions, all in the range $0.04 \leq z \leq 0.1$, have been normalized to the same number of galaxies (N=1000) to show the differences. From this figure, the relative proportion of faint galaxies in the single and binary fields seems higher than in groups.

2.5 Dataset validation

The construction of a robust catalog of groups is essential to characterise accurately their properties. To validate my catalog, I concentrated on a direct comparison with one of the largest galaxy group sample, the 2PIGG catalog [119]. This consists of $\sim$290000

groups, with at least two members, found in the Northern and Southern Galactic Patches (NGP and SGP) in the 2dFGRS using a group finding procedure based on a FoF algorithm. They found galaxy groups using linking parameters calibrated on realistic mock catalogs identified with high-resolution N-body simulations and a semi-analytical model of galaxy formation. Their purpose was to provide overdensity regions that have velocity dispersions and projected sizes similar to those of their parent dark matter halos.

The comparison with the 2PIGG catalog is an important step to test the work assumptions I made in the FoF algorithm and validate the effectiveness of my sample. My galaxy groups are all contained in their Northern Galactic Patch.

To match my groups with the 2PIGG catalog, I checked when:

1. the geometric centres agreed within 0.1°;

2. the group redshifts differed by at most 0.0007.

81 of my groups satisfy the above criteria and match a 2PIGG group. For these, in Figure2.5 I show the comparison between my and 2PIGG redshifts (left panel) and velocity dispersions (right panel). The 2PIGG velocity dispersions used in this plot are gapper estimates, derived from their tabulated σ values using eq.(4.6) in [119]. 2PIGG adopted a fixed error on σ of 85 $\mathrm{km\,s^{-1}}$, which is displayed in Fig.4.7. For some 2PIGG groups the sigma value is 0, which means that the individual galaxy error is at least as big as their estimate of the velocity dispersion. As expected, given the large uncertainty in the σ measurements based on a few redshifts, there is a large scatter in this comparison, although 75 per cent are within the errors.

As a further step, I performed a match between the position of my group galaxies and that of 2PIGG galaxies within 3 arcsec. All of these matches agreed also in redshift. This allowed us to investigate if my group galaxies were associated with the same 2PIGG group matching in geometric centre. In this way I also found how many of my group galaxies were observed by 2PIGG.

For 23 of my groups none or fewer than 50 per cent of my galaxies have been observed by 2PIGG. Not surprisingly, these groups do not match any 2PIGG group according to criteria (1) and (2) above.

For another 20 of my groups I did not find a match in both barycentre and redshift

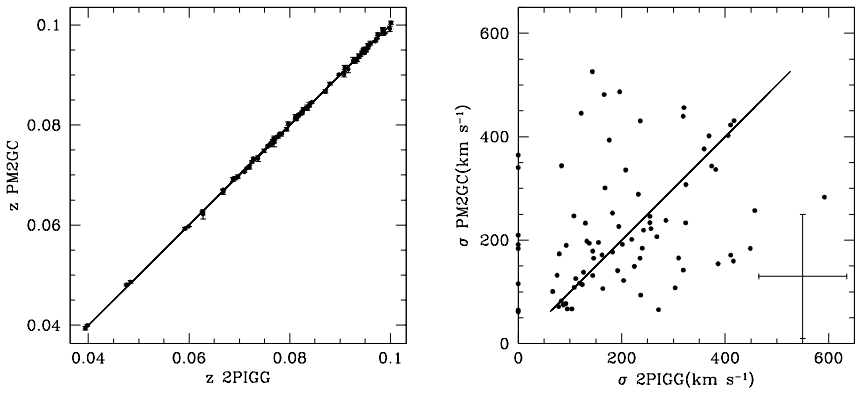

Figure 2.5: **Left.** The comparison of redshifts between the 81 groups matching a 2PIGG group. My errors are computed by propagating the error on the velocities and in many case they are as small as point size. The black line is the 1:1 relation **Right.** The comparison between the velocity dispersions. As the error bars are too large and to avoid visual confusion I plotted in the bottom right part of the panel the median error of our velocity dispersion ($\sim$120 $\mathrm{km\,s^{-1}}$) in y and the error used by 2PIGG (85 $\mathrm{km\,s^{-1}}$) in x. The black line is the 1:1 relation.

with 2PIGG although at least 50 per cent of my galaxies have been observed by 2PIGG. However, I have a higher number of redshifts than 2PIGG in most of these groups.

The remaining 52 of my 176 groups have peculiar characteristics and deviate from 2PIGG groups. 34 were associated with one group for 2PIGG but for us they were split in two or more groups; 11 groups have a high velocity dispersion for their number of galaxies; for the remaining 7 groups, the barycentre of the corresponding 2PIGG group falls out of the MGC survey strip, showing that these groups are affected by edge problems in the MGC thus they will be disregarded in my analysis.

To conclude, about half of the PM2GC groups have a correspondence in the 2PIGG catalog. In addition, I found a number of groups that 2PIGG did not identify. This is due to the higher spectroscopic completeness of the PM2GC, that contains 1074 galaxies (33 per cent of the PM2GC catalog) that were not observed by the 2dFGRS. Moreover, only 20 per cent of my field-single galaxies belong to a group according to 2PIGG, confirming the overall statistical agreement with 2PIGG.

2.6 Galaxy stellar masses

I determined the stellar masses for all galaxies in my sample using the [134] relation according to which, under the assumption of a universal IMF, the stellar mass-to-light (M/L) ratio is strongly correlated with the optical colors of the integrated stellar populations.

Using the B-band photometry, taken from MGCz, I apply the equation

$$\log_{10}(M_\star/L_B) = a_B + b_B(B-V) \tag{2.4}$$

having considered a Bruzual & Charlot model with a_B=-0.51 and b_B=1.45 for a [135] IMF (0.1-125 $M_\odot$) and solar metallicity. To compute the rest frame $(B-V)$ color I followed the filter conversions from [136], i.e.

$$(B-V)_{AB} = 0.5928 + 1.1521[(g-r) - 0.6148] \tag{2.5}$$

using the MGC-SDSS (from SDSS-EDR/DR1) $(g-r)$ color corrected for extinction. I then added 0.11 to the $(B-V)$ colors to transform them from the AB system to the Vega system, and applied the k-corrections in B and V to obtain the rest frame $(B-V)$ colors. The galaxy stellar masses found with the eq.(2.4) were subsequently scaled to a Kroupa [137] IMF to compare with the SDSS, using a conversion factor from Salpeter to Kroupa of 1/1.55 [138].

I also took into account the fact that a certain number of galaxies lie in regions where the photometry can be affected by CCD edges, satellite trails, bright stars and galaxies (B_{MGC} <12.5), diffraction spikes and so on; any object in these regions was marked by a flag in the MGCz catalog to indicate that it may have an incorrect photometry. Comparing the B_{MGC} magnitude with the $B_{MGC-SDSS}$ magnitude (determined using the MGC-SDSS color $g-r$), I have used the $B_{MGC-SDSS}$ magnitude to determine the stellar masses for those galaxies for which ΔB = |B_{MGC}-$B_{MGC-SDSS}$ | > 0.5 mag.

The histogram of the mass distribution for galaxies brighter than M_B =-18.7 in the different environments is shown in Figure2.4. The mass completeness limit was computed as the mass of the reddest M_B=-18,7 galaxy ($B-V$=0.9) at my redshift upper limit (z=0.1), and it is equal to $M_\star$=$10^{10.25}M_\odot$, so any meaningful comparison must be done above this

limit. The variation of the mass function with environment will be discussed in Chapter 4.

I also compared my mass estimates with the stellar masses computed from the Sloan collaboration from the SDSS-DR7 catalog[3] for those galaxies whose MGC and DR7 positions match within 1 arcsec. DR7 masses are computed based on the Sloan photometry, using model magnitudes, for a Kroupa IMF in the range 0.1-100 $M_{\odot}$ (J. Brinchmann 2010, private communication).

In Figure2.6 I show this comparison for the GF galaxies in common with the DR7 mass catalog. The agreement is satisfactory at masses above $\log_{10}(M_{\star}/M_{\odot}) \sim 10.3$. Here, the dispersion is similar to the typical mass error for my method that is normally taken to be 0.2-0.3 dex. At lower masses, there is a systematic effect, surely due to the different mass estimate methods, in the sense that my masses are higher than SDSS-DR7 masses by up to $\sim 0.2 - 0.3$ dex.

Finally, with the [139] method, I also computed the stellar masses using the SDSS DR7 model magnitudes corrected for extinction, obtained from the SDSS catalog Archive Server (CAS) system for 3140 of my galaxies, and verified that these masses were in very good agreement with those based on MGC-SDSS magnitudes, without any offset at low masses (plot not shown).

2.7 Summary

In this chapter I presented the construction and describe the properties of the Padova-Millennium Galaxy and Group Catalogue (PM2GC), a database of groups and galaxies at low redshift fully provided, easily upgradable and easily to be consulted. I characterized galaxy environments by identifying galaxy groups at $0.04 \leq z \leq 0.1$ with a Friends-of-Friends (FoF) algorithm using a complete sample of 3210 galaxies brighter than $M_B = -18.7$ taken from the Millennium Galaxy Catalogue (MGC, Liske et al. (2003)), a $38 \mathrm{deg}^2$ photometric and spectroscopic equatorial survey. I identified 176 groups with at least three members, comprising in total 1057 galaxies and representing $\sim$43 per cent of the general field population in that redshift range. The median redshift and velocity dispersion of groups are 0.0823 and 192 $\mathrm{km\,s^{-1}}$, respectively. 88 per cent of the groups have fewer than

[3] http://www.mpa-garching.mpg.de/SDSS/DR7/Data/stellarmass.html

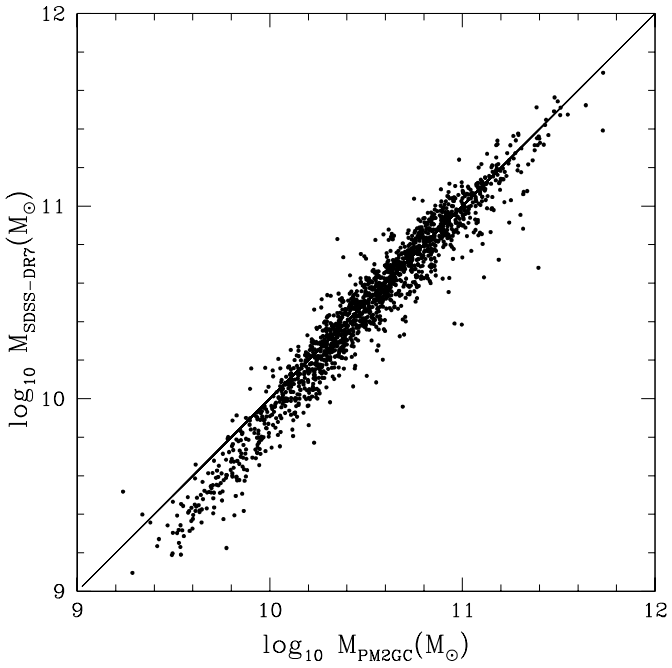

Figure 2.6: Comparison between the masses of galaxies in my total sample determined, in this thesis, using the Bell & de Jong (2001) relation and g and r MGC-SDSS magnitudes, and the masses of the same galaxies found in the SDSS-DR7 catalog. The black line is the 1:1 relation.

ten members, and 63 per cent have fewer than five members. Non-group galaxies were subdivided into "binary" systems of two bright close companions, and "single" galaxies with no companion, in order to identify different environments useful for future scientific analysis. I performed a detailed comparison with the 2PIGG catalog to validate the effectiveness of the method and the robustness of results. Galaxy stellar masses are computed for all PM2GC galaxies, and found to be in good agreement with Sloan Digital Survey Data Release 7 (SDSS-DR7) mass estimates. The catalogues of PM2GC groups, group properties and galaxy properties in all environments are publicly available on the World Wide Web.

The PM2GC redshift range ($0.03 \leq z \leq 0.11$) is similar to WINGS (WIde-field Nearby Galaxy-cluster Survey), a survey of 77 X-ray selected galaxy clusters (Fasano et al., 2006). The combined analysis of PM2GC and WINGS samples that will come in the next chapters allows the study of the properties and the evolution of galaxies in the widest possible range of environments in the local Universe and to understand the origin of the observed trends of galaxy properties versus environment.

Chapter 3

Galaxy morphologies in groups, single, binary and cluster sample at low redshift

Morphology is one of the key observables in extragalactic astronomy for understanding the formation and evolution of galaxies, and it is the consequence of all physical processes at work.

The origin of such processes can be both external (environmental) or internal (intrinsic) to the galaxy itself. The strongest evidence of a correlation between the morphological types (Hubble types) and the environment in which galaxies are located comes from studies conducted on galaxy clusters. The well-known morphology-density relation, first described by (Dressler 1980a,b) shows that ellipticals and S0s are the dominant population in high density regions while galaxies in low density regions are mainly spirals. A relation between galaxy morphologies, or structural parameters, and local density was found to exist also in galaxy groups (Postman & Geller (1984) and Tran et al. (2001)) , and in the SDSS general field (Goto et al. 2003; Kauffmann et al. 2004)..

Studies of higher redshift clusters proved the existence of a morphological evolution of galaxies (Dressler et al. 1997; Fasano et al. 2000; Postman et al. 2005) with an increase of the S0 fraction at low redshift at the expense of the spiral population.

The morphological evolution depends strongly on galaxy stellar mass both in clusters and in the field (Vulcani et al. 2011; Oesch et al. 2010) and it is stronger in low-mass than in massive clusters (Poggianti et al. 2009; Wilman et al. 2009; Just et al. 2010).

Measuring the evolution of galaxy morphologies as a function of environment represents an important step towards a better understanding of the observed morphological mix, and for disentangling betIen the role of environment and the role of galaxy intrinsic effects. Galaxy structure is strongly correlated with galaxy stellar mass (Kauffmann et al. (2003)); on the other hand, the distribution of galaxy stellar masses itself depends on local density (Baldry et al. 2006; Bolzonella et al. 2010; Vulcani et al. 2012). Therefore it is hard to assess the relative roles played by the galaxy mass and by the physical processes linked to the environments that the galaxy experienced during its life-time.

To this aim, in the last decade, a great effort has been made to obtain large catalogues of morphologically classified galaxies. For example, detailed morphological classifications have been obtained by (Fasano et al. (2006)) for cluster galaxies at low redshift in the WIde-field Nearby Galaxy-cluster Survey (WINGS), and several catalogues with visual classifications have been produced for SDSS field galaxies (Nair & Abraham 2010; Baillard et al. 2011; Lintott et al. 2008; Fukugita et al. 2007).

Recently, using a local, visually classified sample from the Galaxy Zoo project, have analysed the relationship betIen galaxy morphology, colour, environment and stellar mass characterising the environment by local galaxy density and by distance from the nearest group/cluster with $M = 10^{13} - 10^{15}\, h^{-1}\, M_{\odot}$ (Bamford et al. (2009)), showing that "only a small part of both the morphology-density and colour-density relations can be attributed to the variation in the stellar-mass function with environment."

In spite of the recent observational progress, what drives the observed trends of the different morphological types remains still a controversial topic not fully explored. For example, to date, there has not been any large statistical study on the morphological distribution of galaxies with *global*, as opposed to local, environment. By galaxy "global environment" I mean the structure to which the galaxy belongs, from massive clusters, to groups, to haloes hosting a single luminous galaxy, over the whole range of galaxy system masses, and corresponding dark matter halo masses.

In the next sections I first analyse how the morphological mix and the relation betIen morphological fractions and galaxy stellar mass change in the local Universe not as a function of local galaxy density, but as a function of global environment.[1] To do this I

[1] See also Wilman & Erwin (2011) submitted, Dave Wilman 2011 private communication.

use two galaxy datasets representative of the whole range of cosmic structures: the Padova-Millennium Galaxy and Group Catalogue (PM2GC) of groups, binary systems and isolated galaxies (Calvi, Poggianti & Vulcani, 2011) built from the Millennium Galaxy Catalogue (MGC)(Liske et al. 2003) and the cluster sample from the WINGS survey (Fasano et al. 2006).

3.1 Data for morphological analysis

The higher quality imaging of the MGC and WINGS surveys compared to the Sloan survey and the combination of multiwavelength photometry and spectroscopy for both our samples allow us to give a clear representation of the morphological distribution of galaxies in different environments as a function of galaxy stellar mass.

For the analysis on the morphology I prune the PM2GC catalogues of isolated, binary system and general field galaxies to the same redshift range of groups, thus $0.04 \leq z \leq 0.1$.

In addition, I use a sample of galaxies belonging to 21 clusters taken from WIde-Field Nearby Galaxy-cluster Survey (WINGS) (see Table3.1) [2]. WINGS (Fasano et al. 2006) is a multiwavelength survey of clusters at $0.04 < z < 0.07$ whose main goal is to characterize the photometric and spectroscopic properties of galaxies in nearby clusters and to describe the changes of these properties depending on galaxy mass and environment. Clusters were selected in the X-ray from the ROSAT Brightest Cluster Sample and its extension (Ebeling et al. 1998, 2000) and the X-ray Brightest Abell-type Cluster sample (Ebeling et al. 1996). WINGS clusters cover a wide range of velocity dispersion $\sigma_{\rm clus}$ (typically $500 - 1100 {\rm km\,s^{-1}}$) and a wide range of X-ray luminosity L_X (typically $0.2 - 5 \times 10^{44} erg\, s^{-1}$). The survey is mainly based on optical B, V imaging of 78 galaxy clusters (Varela et al. 2009), that has been complemented by a spectroscopic survey of a subsample of 48 clusters, obtainedwith the spectrographs WYFFOS@WHT and 2dF@AAT (Cava et al. 2009), by a near-infrared (IR) (J, K) survey of a subsample of 28 clusters obtained with WFCAM@UKIRT (Valentinuzzi et al. 2009), and by U broad-band and H_α narrow-band imaging of a subset of WINGS clusters, obtained with wide-field cameras at different telescopes (INT, LBT, Bok) (Omizzolo et al., in preparation). The

[2] http://Ib.oapd.inaf.it/wings

spectroscopic target selection was based on the WINGS B, V photometry. The aim of the target selection strategy was to maximize the chances of observing galaxies at the cluster redshift without biasing the cluster sample.We selected galaxies with a total $\mathrm{V} \leq 20$ mag and a V mag within the fibre aperture of $\mathrm{V} < 21.5$ and with a colour within a 5-kpc aperture of $(\mathrm{B}-\mathrm{V})_{5\mathrm{kpc}} \leq 1.4$, to reject background galaxies, much redder than the cluster red sequence. The exact cut in colour was varied slightly from cluster to cluster in order to account for the redshift variation and to optimize the observational setup. These very loose selection limits were applied so as to avoid any bias in the colours of selected galaxies. In this paper, we only consider spectroscopically confirmed members of 21 of the 48 clusters with spectroscopy. This is the subset of clusters that have a spectroscopic completeness (the ratio of the number of spectra yielding a redshift to the total number of galaxies in the photometric catalogue) larger than 50 per cent. The completeness is determined using V-band magnitudes and turns out to be rather flat with magnitude for most clusters, for the reasons discussed in Cava et al. (2009). Moreover, completeness is essentially independent from the distance to the centre of the cluster for most clusters. Our imaging covers a $34 \times 34\mathrm{arcmin}^2$ field, that corresponds to about $0.6\mathrm{R}_{200}$, for all the 21 clusters considered, except for A1644 and A3266 where the $rm \sim 0.5R_{200}$ is covered. R_{200} is defined as the radius delimiting a sphere with interior mean density 200 times the critical density of the Universe at that redshift, and is commonly used as an approximation for the cluster virial radius. The R_{200} values for our structures are computed from the velocity dispersions by Cava et al. (2009). Galaxies are considered members of a cluster if their spectroscopic redshift lies within $\pm 3\sigma$ from the cluster mean redshift, where σ is the cluster velocity dispersion (Cava et al. 2009).

Although reliable estimates of individual halo masses are available only for WINGS structures based on cluster velocity dispersions and X-ray luminosity, by combining PM2GC and WINGS certainly I are statistically investigating a very broad range of global environments, and corresponding dark matter halo masses, from $\sim 10^{15} M_{\odot}$ for WINGS, to the order of $\sim 10^{12} M_{\odot}$ or lowerr for single galaxies.

For all galaxies in PM2GC and WINGS, stellar masses have been estimated using the Bell & de Jong relation [170] which correlates the stellar mass-to-light ratio (M/L) with the optical colors of the integrated stellar populations (see §2.7).

cluster name	z	σ $(km\,s^{-1})$
A1069	0.0653	690± 68
A119	0.0444	862± 52
A151	0.0532	760±55
A1631a	0.0461	640±33
A1644	0.0467	1080± 54
A2382	0.0641	888± 54
A2399	0.0578	712± 41
A2415	0.0575	696± 51
A3128	0.06	883± 41
A3158	0.0593	1086± 48
A3266	0.0593	1368± 60
A3376	0.0461	779± 49
A3395	0.05	790± 42
A3490	0.0688	694± 52
A3556	0.0479	558± 37
A3560	0.0489	710± 41
A3809	0.0627	563± 40
A500	0.0678	658±48
A754	0.0547	1000± 48
A957	0.0451	710± 53
A970	0.0591	764± 47

Table 3.1: List of WINGS clusters analyzed in this paper, their redshifts z and velocity dispersions σ.

Envir.	**N. of gal.**	**Galaxy type**			
		Ellipticals	S0s	Late-type	Early-type
WINGS	690 (1056.12)	33.8±1.5%	50.7±1.5%	15.4±1.0%	84.5±1.0%
PM2-GF	1188	27.0±1.3%	28.7±1.3%	44.3±1.5%	55.7±1.5%
PM2-G	583	29.7±1.9%	32.4±2.0%	37.9±2.1%	62.1±2.5%
PM2-FB	174	25.3±3.5%	25.8±3.6%	48.8±4.0%	51.1±4.0%
PM2-FS	334	21.5±2.3%	24.2±2.5%	54.2±2.8%	45.7±3.0%

Table 3.2: Number of galaxies and fractions of each morphological type in the PM2GC and WINGS mass-limited samples with $M_\star$=$10^{10.25} M_\odot$. Early-type galaxies comprise ellipticals and S0s. Errors are binomial. The WINGS number of galaxies betIen brackets is the Iighted total number of galaxies above our completeness limit.

In order to properly investigate the relation betIen morphology, galaxy mass and environment, without being affected by the different distributions of star formation histories (hence colors) in different environments, it is important to restrict the analysis to a galaxy sample that is complete in mass. The PM2GC galaxy stellar mass completeness limit was computed as the mass of the reddest M_B=-18,7 galaxy ($B-V$=0.9) at our redshift upper limit (z=0.1), and it is equal to $M_\star$=$10^{10.25} M_\odot$. The WINGS sample is complete in mass down to $M_\star$=$10^{9.8} M_\odot$, but for the purposes of this work, I have adopted for WINGS the same galaxy mass limit as for the PM2GC.

Hence, all the results presented in this paper are based on galaxy stellar mass limited samples ($M_\star \geq 10^{10.25} M_\odot$), for a [170] IMF. The total numbers of galaxies in each environment above our mass limit are listed in Table 4.3.

3.2 Morphological classification: MORPHOT

To morphologically classify galaxies in both samples I used MORPHOT, an automatic tool purposely designed (Fasano et al 2012), which used B-band images for PM2GC galaxies and V-band images for WINGS. Today the most frequently used classification scheme for statistical studies is the numerical code associated to the so called Revised Hubble Type ($\mathrm{T_{RH}}$ hereafter), first introduced by de Vaucouleurs (1974), subsequently improved in the Third Reference Catalog of Bright Galaxies (de Vaucouleurs et al. 1991, RC3 hereafter). The MORPHOT tool uses a slightly modified version of the $\mathrm{T_{RH}}$ code. The visual estimates $\mathrm{T_V}$ are obtained for two samples, each one including ~ 1000 galaxies, extracted with the same random criteria from the WINGS imaging. The first one will be used as a calibration sample for the tool, while the second one has been used as a test sample in order to assess the performances of MORPHOT. For each galaxy in the calibration sample, (i) the global quantities: size (R), signal-to-noise ratio (S=N) and ellipticity (ε) are recorded; (ii) 20 image-based, numerical diagnostics of morphology ($\mathrm{D_i}$, i=1,...,20) are defined and their values are evaluated. The calibration sample is used to gauge how the diagnostics $\mathrm{D_i}$ depend on $\mathrm{T_V}$ and on the global quantities. This allows to produce a semi-analytical estimator which combines the most effective diagnostics through a Maximum Likelihood technique (ML). The same sample is also used as a training set for a Neural Network

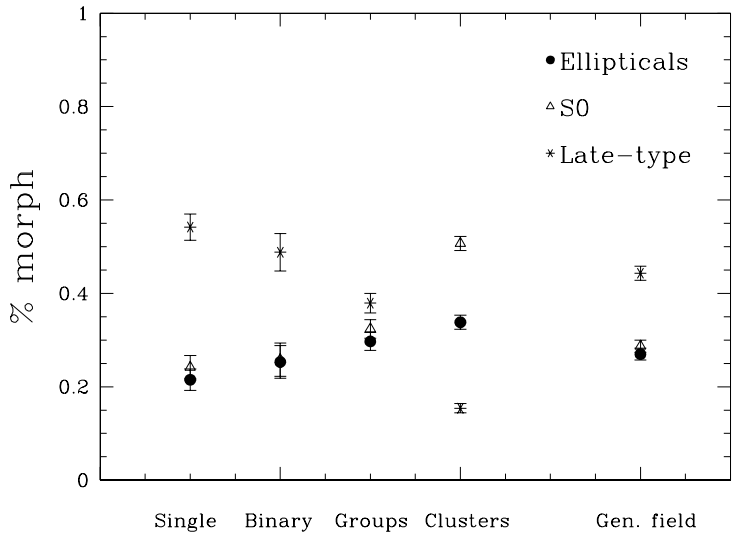

Figure 3.1: Morphological fractions in different global environments for our mass-limited samples (for $log_{10}M_{\star}/M_{\odot} \geq 10.25$), as in Table 4.1. Errors are binomial.

machine (NN) in which the global quantities (R, S=N and ε) and the diagnostics $\mathrm{D_i}$ are the input quantities and the visual codes $\mathrm{T_V}$ are the targets. Finally, the NN and the ML estimators are combined to produce the final MORPHOT estimator $\mathrm{T_M}$.

The MORPHOT estimators produced by the two techniques ($\mathrm{T_{ML}}$ and $\mathrm{T_{NN}}$) should be independent on each other and the *r*ms of their difference should roughly be the square root of the sum of their variances with respect to $\mathrm{T_V}$ (*r*ms[$\mathrm{T_{ML}} - \mathrm{T_{NN}}$]$\sim$2.55). Once the mutual independence of the two estimators has been checked, the last step of the MORPHOT flowchart is the evaluation of the final morphological type estimator $\mathrm{T_M}$, which is simply defined as the average value of the two independent estimators: $\mathrm{T_M} = (\mathrm{T_{ML}} + \mathrm{T_{NN}})/2$. Similarly, the lower and upper limits of the confidence interval of $\mathrm{T_M}$ are obtained by averaging the lower and upper confidence limits of $\mathrm{T_{ML}}$ and T_{NN}, respectively. Visual inspection of a random subset of 300 galaxies shown no significant systematic shift in broad morphological classification (E, S0 or late-type) and a typical scatter

(ΔT=1.2) betIen the V and B WINGS images. By adding to the classical CAS (Concentration/Asimmetry/clumpinesS) parameters a set of 20 additional indicators derived from digital imaging of galaxies, this tool mimics the visual classifications. The MORPHOT morphological classifications have been proved to be as effective as the eyeball estimates, as shown by the comparison with visual classifications of WINGS and SDSS images yielding an average difference in Hubble type ΔT ($\leq$ 0.4) and scatter ($\leq$ 1.7) comparable to those among visual classifications of different experienced classifiers. In particular, MORPHOT has been shown to be able to distinguish betIen ellipticals and S0 galaxies with unprecedented accuracy.

3.3 Result 1: The Hubble type fractions

In Table 4.3 and Figure3.1 I show the morphological fractions for the PM2GC and WINGS mass-limited samples for galaxies with $log_{10}M_{\star}/M_{\odot} \geq 10.25$.

The fractions of ellipticals, S0s and early-type galaxies (E's + S0's) progressively increase in more massive environments, from single galaxies to binary systems, to groups and clusters. Late-type galaxies follow the opposite trend with global environment.

I note that elliptical galaxies have the smallest fractional variation with environment. Their fraction in clusters ($\sim$34%) is not very dissimilar from that in the general field ($\sim$27%) . For isolated galaxies, binary systems and groups, although the trend is slowly increasing as I move towards more massive environments, the fraction of ellipticals is always betIen $\sim$22-30%.

The fraction of S0s is very similar to the elliptical fraction in all environments ($\sim$1:1 number ratio) except in clusters (1.5). The S0 fraction ranges from 24% among single galaxies, to 32% in groups, with a jump to 50% in clusters. S0's in clusters are almost twice more common than in the general field.

As a consequence, the early-type fraction ranges from 46% among single galaxies to 85% in clusters. It is striking that even in the least massive environments I consider, (those of single galaxies), almost half of the total galaxy population above our mass limit is composed of early-type galaxies.

Correspondingly, the fraction of late-type galaxies changes strongly with environment.

For PM2-FS and PM2-FB this fraction is about $\sim$50%, it decreases for group galaxies to $\sim$38%, and then it declines sharply in clusters (mirroring the S0 cluster enhancement) reaching a fraction of $\sim$15%, a third with respect to the general field ($\sim$44%).

In clusters ($\sigma > 500\,\mathrm{km\,s^{-1}}$) [173] [3] it has been found that there is no correlation betIen the fractions of late-types, S0s and ellipticals and cluster velocity dispersion or X-ray luminosity (both of which are cluster mass proxies), except for a Iak anticorrelation of the late-type fraction with X-ray luminosity.

Together with the results previuous described, this suggests that the morphological trends I observe going from less massive (single galaxies) to more and more massive environments (groups and clusters) must flatten out for the most massive haloes.

In summary, there is a smooth increase/decline in the fraction of Es-S0s/late type galaxies going to more and more massive environments. On top of that, the cluster environment is characterized by a sharp enhancement/dearth of the S0/late-type fractions compared to other environments. For clusters above $500\,\mathrm{km\,s^{-1}}$ the morphological fractions do not depend on halo mass anymore. Overall, the fraction of elliptical galaxies represents always at least 20% of the galaxy population even in the least massive environments, and at most 34% in clusters.

3.4 Result 2: The Morphology-Mass relation in different environments

In this section I investigate the dependence of the distribution of morphological types on galaxy stellar mass, and whether this changes with global environment. Table **??** lists the fractions of each morphological type at masses $10.25 \leq \log_{10}M_{\star}/M_{\odot} < 11.0$ and $\log_{10}M_{\star}/M_{\odot} \geq 11.0$ in different environments and can be used in the following to compare the morphological fractions at low- and high-masses, and in different environments in the same mass range.

[3] In the 2009 work the analysis was carried out for a magnitude-limited sample of galaxies. I have verified that the results do not change for the mass-limited WINGS sample I use in this paper.

% morph.type	WINGS	PM2GC-GF	PM2GC-G	PM2GC-FB	PM2GC-FS
ell $M \geq 10^{11} M_{\odot}$	63.2±4.4%	42.0±4.5%	48.2±4.5%	29.4±13.5%	26.6±9.6%
ell $M < 10^{11} M_{\odot}$	29.3±1.6%	24.8±1.5%	26.6±2.0%	24.8±3.7%	21.0±2.5%
s0 $M \geq 10^{11} M_{\odot}$	26.3±4.0%	20.0±3.5%	21.6±5.0%	29.4±13.5%	13.3±7.8%
s0 $M < 10^{11} M_{\odot}$	54.4±1.7%	30.0±1.5%	34.2±2.0%	25.4±3.8%	25.3±2.6%
lt $M \geq 10^{11} M_{\odot}$	10.4±2.9%	38.0±4.5%	30.1±6.0%	41.1±14.3%	60.0±10.4%
lt $M < 10^{11} M_{\odot}$	16.1±1.2%	45.2±1.5%	39.2±2.5%	49.6±4.3%	53.6±3.0%

Table 3.3: Fractions of each morphological type above and below $M = 10^{11} M_{\odot}$ in different environments. Errors are binomial.

3.4.1 Fixed environment

The morphological fractions at masses below and above $\log_{10} M_{\star}/M_{\odot} = 11.0$ are different (Table 3.3). These differences are statistically significant in clusters, groups and general field, while among binaries and single galaxies numbers are too low to draw conclusions.

Figure 3.2 shows how the fraction of each morphological type varies with stellar mass in the four PM2GC environments and in clusters. I note that, as discussed in detail Chapter 4, in binary and single systems there are no galaxies with masses $\log_{10} M_{\star}/M_{\odot} \geqslant 11.2$ and $\log_{10} M_{\star}/M_{\odot} \geqslant 11.55$, respectively, indicating that the most massive galaxies are only present in the most massive haloes. Up to $\log_{10} M_{\star}/M_{\odot} \sim 11.1$, in the PM2GC there is generally little dependence of the morphological fractions on galaxy mass. Moreover, at these masses late-type galaxies tend to be the most common type of galaxies in all PM2GC environments, being matched by S0s only in groups.

In contrast, at masses $\log_{10} M_{\star}/M_{\odot} > 11.1$, there is a noticeable dependence of the morphological mix on galaxy mass in those environments hosting galaxies this massive. In the PM2-FS the late-type galaxy fraction rises towards higher masses, while in groups it declines, as the most massive group galaxies are mostly ellipticals.

In clusters, from [174] the trends partly resemble those in the PM2GC groups, except that in clusters the dominance of ellipticals at high masses is even more pronounced and for $\log_{10} M_{\star}/M_{\odot} > 10.8$ there is a clear declining trend of S0s with galaxy mass that is absent in groups. This behaviour of the S0 fraction-galaxy mass relation in clusters is different from all other environments, where the S0 fraction remains rather constant at all galaxy masses.

Though it is commonly believed that the morphological mix depends on galaxy mass, our results highlight that such a dependence is generally Iak at masses in the range $\log_{10}M_{\star}/M_{\odot} = 10.25 - 11$, while it becomes strong at higher masses, where the dominant galaxy type changes with global environment (elliptical in clusters and groups, late-type among single galaxies).

3.4.2 Fixed morphological type

Figure 3.3 comprises all environments, and directly shows the strong environmental variation of the morphology-mass relation for each galaxy type. The upper panels present the differential fractions, and the loIr panels the cumulative distributions showing the fractions for galaxies more massive than a mass M. Comparing our general field with results obtained using the Nair & Abraham [175] catalogue at the same redshifts of mine, I find qualitatively similar morphological trends with mass, though even steeper high-mass slopes for ellipticals and late-types.

The top panels in the figure highlight that the variation of the morphology-mass relation *with environment* is pronounced (1) above all at high galaxy masses ($\log_{10}M_{\star}/M_{\odot} > 11$), but also (2) at low galaxy masses for S0 and late-type galaxies in clusters compared to the other environments.

(1) In non-cluster environments, the fraction of each morphological type at masses $10.25 < log_{10}M_{\star}/M_{\odot} < 11$ changes relatively little from one environment to the other, while it varies much more strongly with environment for $log_{10}M_{\star}/M_{\odot} > 11$ (also Table **??**). The environmental variation at high masses is especially outstanding for ellipticals and for late-types.

(2) The peculiarity of the behaviour of the S0 and late-type fractions in clusters suggests cluster-specific effects on these two types of galaxies. It also suggests that a significant number of S0 galaxies in clusters has a different origin with respect to S0s in other environments. The S0 fraction-galaxy mass relation in clusters resembles more closely the late-type fraction-mass relation in the general field and groups than the S0-mass relation in non-cluster environments, in agreement with a scenario in which clusters are very efficient in transforming spiral galaxies into (some of today's) S0s [176,177]. I speculate that while a large number of cluster S0s have a "late-type origin", a large number of non-cluster S0s

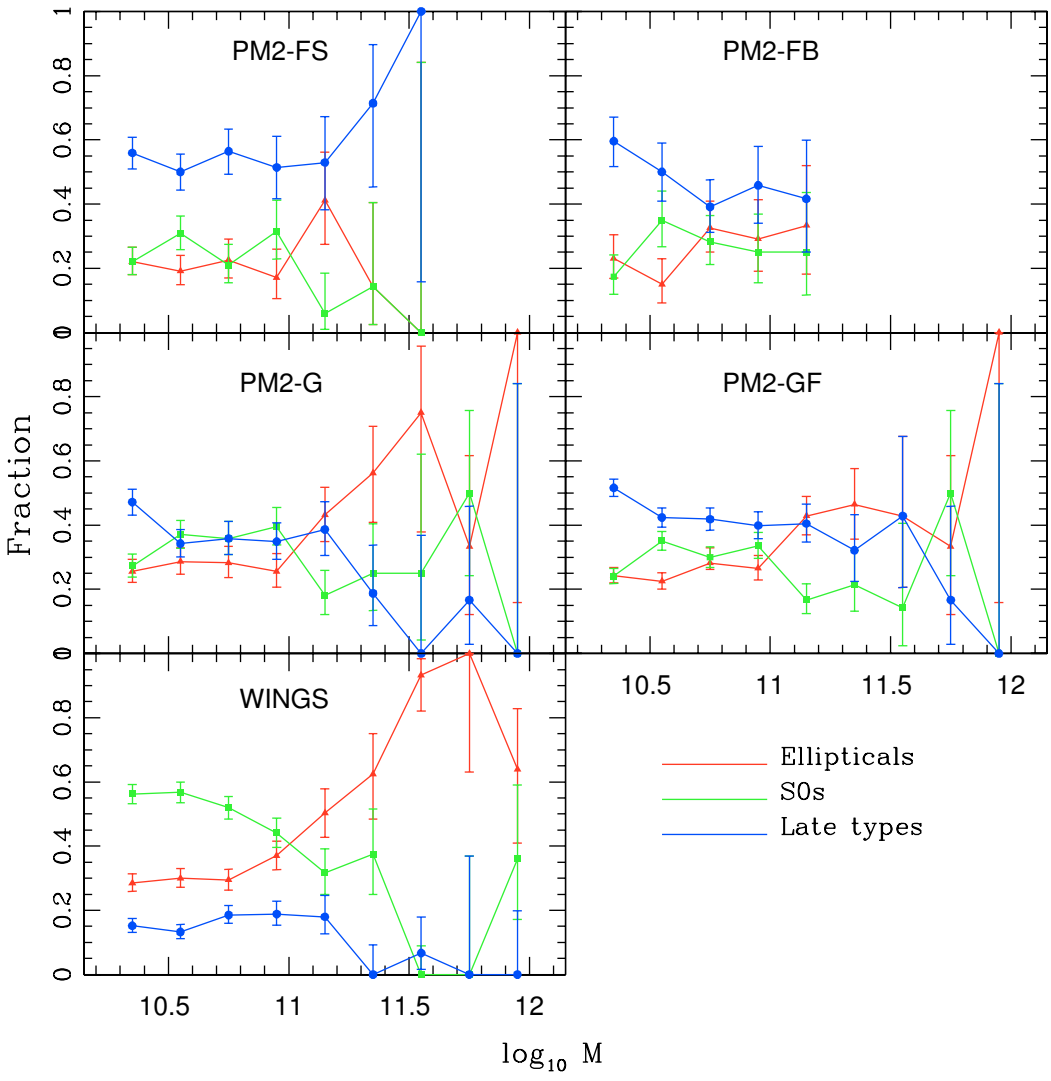

Figure 3.2: The fraction of each morphological type as a function of stellar mass in different environments: PM2 single-field (top left), PM2 binary-field (top right), PM2 galaxy groups (middle left), PM2 general field (middle right), WINGS (bottom left, reproduced from Fig.10 of Vulcani et al. 2011). The WINGS number of galaxies is Iighted on the total number of galaxies above our completeness limit. Errors are binomial.

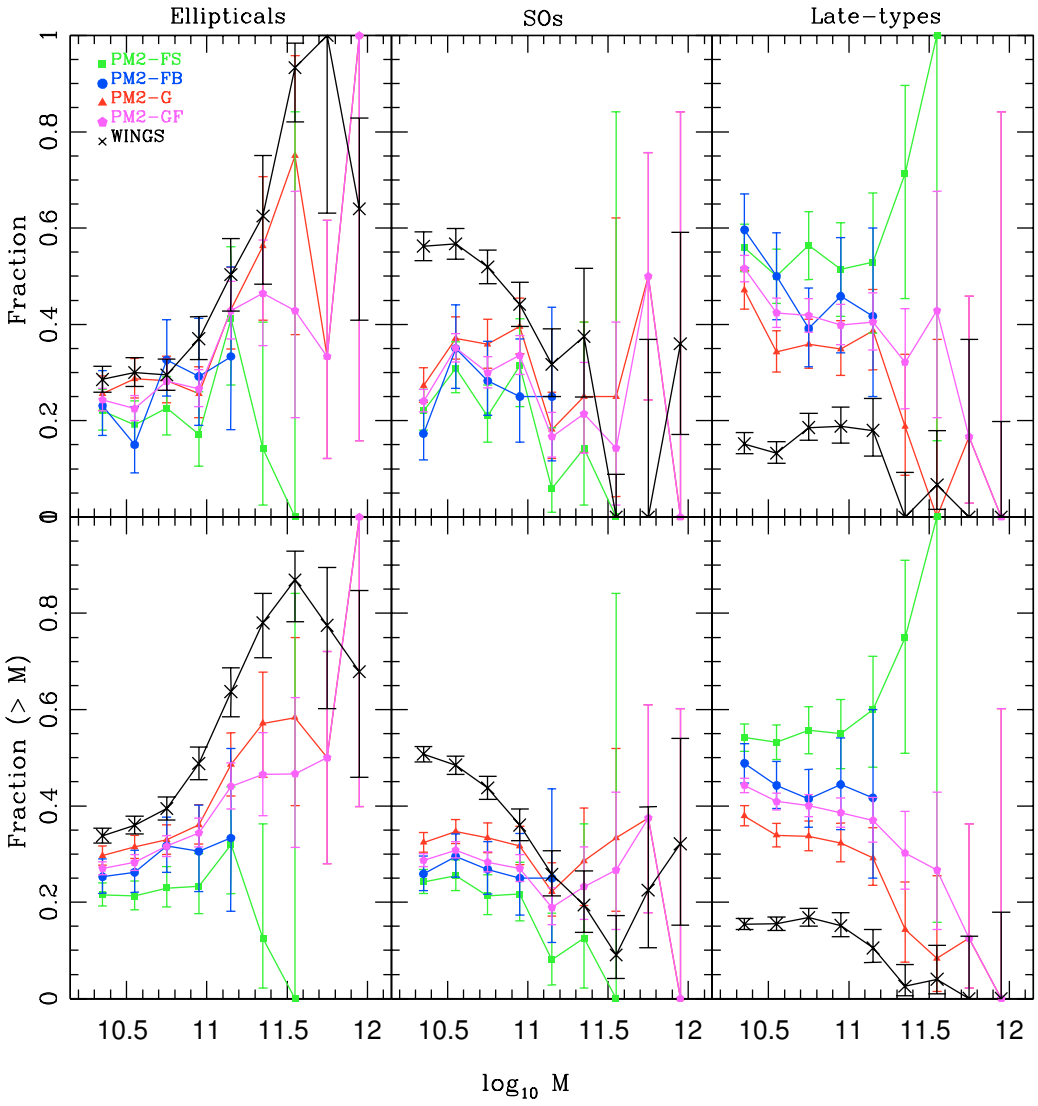

Figure 3.3: **Top.** The fractions of elliptical (left panel), SO (central panel) and late-type (right panel) galaxies in different environments as a function of stellar mass. **Bottom.** Cumulative distributions of ellipticals, S0s and late-type galaxies: fractions of each type among galaxies more massive than $\log_{10}$M on the X axis. This plot can used to infer the global morphological fractions in mass-limited samples for any mass limit higher than ours. Errors are binomial. (The WINGS galaxies are lighted on the total number of galaxies above our completeness limit.)

have a truly "early-type origin" (a dominant spheroidal component that forms a very small disk, an "intermediate type" betIen disky ellipticals and Sa's).

The fact that the morphology-mass relation changes significantly with environment demonstrates that galaxy mass is not the only parameter driving the morphological distribution of galaxies.

Thus, the change of morphological mix with global environment cannot be solely due to an eventual change in the galaxy mass function with halo mass (see Chapter 4 for a description of the galaxy mass function as a function of global environment).

3.5 Summary

I use group, binary and isolated field galaxies from the PM2GC sample and cluster galaxies from the WINGS survey to study the morphological fractions and morphology-mass relation in different environments for mass-limited galaxy samples with $log_{10}M_{\star}/M_{\odot} \geq 10.25$. Morphologies Ire derived from B-band and V-band images in PM2GC and WINGS, respectively, with our tests showing no systematic shift in broad morphological classification betIen B and V.

- I observe a smooth increase/decline in the fraction of Es-S0s/late type galaxies going from single galaxies, to binaries, to groups. Considering all environments, the fractional variation is more conspicuous for S0s and late-types than for ellipticals, due to a sharp enhancement/dearth of S0s/late-types in clusters compared to other environments. Poggianti et al. (2009) found that above $500\,\mathrm{km\,s^{-1}}$ the morphological fractions do not depend on halo mass anymore.

- In all environments the morphological fractions strongly depend on galaxy stellar mass *only* for masses above $\log_{10}M_{\star}/M_{\odot} \sim 11$ (10.8 in clusters), while they are Iakly dependent of mass at $10.25 < log_{10}M_{\star}/M_{\odot} < 11$. At high galaxy masses, the dominant type changes with global environment (elliptical in clusters and groups, late-type in single galaxies).

- Also the variation of the morphology-mass relation with environment is much more pronounced at $\log_{10}M_{\star}/M_{\odot} > 11$, especially for ellipticals and late-types, while at

loIr masses there is relatively little change from one environment to the other, except for clusters.

- The morphology-mass relations for cluster S0s and late-types remarkably differ from the corresponding relations in all other environments.

  These findings strongly suggest that cluster-specific effects act on these two types of galaxies, and that a significant number of S0s in clusters has a different origin with respect to S0s in other environments.

  These results show that the morphology-mass relation changes with global environment and that galaxy stellar mass cannot be the only parameter driving the morphological distribution of galaxies.

Chapter 4

The impact of global environment on galaxy mass functions at low z and variations with morphological type

4.1 Nature or Nurture?

In the hierachical scenario of ΛCDM models, the big picture of the formation of large-scale structure of the universe is well in place and in agreement with observations. Nevertheless, how to interpret in a coherent picture the significant differences that emerge between galaxy formation and evolution models and the observed galaxy trends still remains a topic of controversy. One of the major difficulties in reproducing observations is quantify to what extent the galaxy initial conditions and the surronding environment that a galaxy experience during its lifetime are the driving mechanism in shaping galaxy properties. On the one hand it is natural takes into account that the formation place of the dark matter halo should have an effect on the galaxy that forms in the centre and part of the evolution could be imprinted to the initial conditions (”nature” scenario). Observations have shown that on average more massive dark haloes host more massive galaxies. Thus, the mass is generally assumed as the fundamental parameter that determines the galaxy structure and drives the internal processes. On the other hand it has been noted that the dark matter haloes and galaxies are not alone in the Universe and remain not static throughout the cosmic evolu-

tion. Both observations (e.g. van Dokkum 2005, Bell et al. 2006a,b; Lin et al. 2008, Bundy et al. 2009, Kormendy et al. 2009) and simulations (e.g. Hausman& Ostriker 1978, Hernquist& Mihos 1995, Springel& Hernquist 2005, Naab et al. 2006, Bournaud et al. 2007, Stewart et al. 2009) have shown that galaxies and dark matter haloes merge in dense environments. Therefore, the "global" environmnet, the structure to which a galaxy belongs (from clusters, to groups, to haloes hosting a single luminous galaxy and corresponding dark matter halo masses), drives the external physical processes inducted by gravitational interactions ("nurture" scenario).

In the last years the advent of large spectroscopic and photometric surveys have made possible to explore large galaxy populations, at different cosmic epochs, and to compare their properties across different environments focusing the attention on a major understanding of the physical processes in action as a galaxy becomes part of a more massive systems. The most popular way to measure the environment is based on local galaxy density which can be parametrized following different techniques, for example by the number density of objects within some distance or measuring the distance of a galaxy to the $\mathrm{N_{th}}$ nearest neighbour (tipically between 5-10). Analyzing a wide range of regions of different local density, i.e. from the sparse field to the dense cluster cores, numerous studies have shown that all properties associated with star formation (i.e. colour, morphology) correlate with local density with galaxies in higher density environments that are more massive, form their stars earlier and faster and assume an early-type like morphology (Kauffmann et al., 2004; van der Wel, 2008; Bamford et al., 2009; Lewis et al., 2002; Gó mez et al., 2003). However, it is also well established that the environmental dependence of the epoch when star formation ends is much more pronounced in low mass than in massive galaxies (Peng et al., 2010) and the strong dependence of galaxy global properties with local density is connected with the existence of an ubiquitous bimodality (Kauffmann et al., 2003a,b; Baldry et al., 2004; Hogg et al., 2003; Brinchmann et al., 2004) at a characteristic mass ($\mathrm{M} \sim 3 \times 10^{10} \mathrm{M_{\odot}}$), bimodality that reflects the natural division of the galaxy population in the "red" and "blue" sequence (Hogg et al., 2002; Ellis et al., 2005; Ball et al., 2006). These findings show that mass and environment are correlated but for both observations and simulations it is difficult to disentangle between their relative effects. Hence, the debate over the roles of nature and nurture and their physical mechanisms continues.

4.2 A diagnostic tool: the galaxy mass function

An important question about galaxy formation and evolution is the following: can the variations of the galaxy properties be explained by the dependence of the galaxy mass itself on environment? The galaxy mass function (MF), that describes the distribution of galaxy masses, is a powerful tool for addressing this topic because it constrains the baryonic content of galaxies and takes into account of both the hierarchical mass assembly by dark matter halos and the transformation processes that galaxies experience during their lifetimes and that change the path of their evolution (Brinchmann & Ellis, 2000).

Until a few years ago there were not direct estimates of the MF and astronomers usually substituted the luminosity function in place of the mass function because luminosity required only a single photometric measurement and a redshift and was easier to observe. Combining spectroscopic catalogs with large infrared surveys (2dF, SDSS, 2MASS), the latest particular useful to obtain mass-to-light ratios less sensitive to both stellar population and extintion, has been possible to explore the distribution of galaxy stellar masses in the local universe over the mass range $\mathrm{M}_\star = 10^7 - 10^{12}\mathrm{M}_\odot$. In general, also considering the bimodal distribution of galaxies, the field low-redshift MF shows an upturn with early-type galaxies that dominate at the highest masses and are more luminous while the faint end slope is dominated by late-type galaxies, reflecting the low stellar M/L ratios characteristic of low-mass galaxies (Cole et al., 2001; Bell et al., 2003; Panter et al., 2004; Baldry et al., 2006, 2008). Recently Baldry et al. (2012), using data from GAMA survey, have better characterized the MF for the field population. They found that the double Schechter function provides a good fit to the data for the red population at masses $\mathrm{M} > 10^8\mathrm{M}_\odot$ while the blue population is well described by a single Schechter function. Studying the impact of the environment on the evolution of galaxies in the zCOSMOS field between $0.1 \leq \mathrm{z} \leq 1.0$, Bolzonella et al. (2010) have shown that the MF, and consequently all galaxy properties depending on mass, vary with local environment at $\mathrm{z} \lesssim 1$. They also observed that the bimodality in the total MF up to $\mathrm{z} \sim 0.5$ is more pronounced in high density environments. At higher redshift many works emphasized the evolution of galaxies of mass $\log\mathrm{M}/\mathrm{M}_\odot \gtrsim 10$ with the result that the MF has been strongest and that half of today's stellar mass was still to be assembled in massive systems at $z \simeq 2$ while at $z < 1$ the evolution is moderate and mainly due to star-forming galaxies with intermediate-to-low

masses (Drory et al., 2004; Fontana et al., 2004, 2006; Pozzetti et al., 2007; Bundy et al., 2006). The variation of the MF has also been observated in a quite wide range of densities too. In particular, in Vulcani et al. (2012) has been investigated the importance of the local density in regulating the mass distribution in different environments both at low and intermediate redshift. The authors found that at least at $z \leq 0.8$ local density is more important than global environment in determining the galaxy stellar mass distribution, suggesting that *galaxy properties are not much dependent of halo mass, but do depend on local scale processes.*

Recently, the MF has been also studied separately in clusters and groups. In Vulcani et al. (2011) for the first time the MF in clusters and its evolution from $z \sim 0.8$ to $z \sim 0$ have been analyzed comparing cluster galaxy samples limited in mass at different redshift taken from WINGS (Fasano et al., 2006) and EDisCS (White et al., 2005) surveys. They find that the MF evolves with redshift and clusters at high-z show proportionally more massive galaxies than clusters at low-z. This evolutionary trend is observed both for the total galaxy population, and for ellipticals, lenticulars (S0) and late-type galaxies separately. The authors argued that the observed evolution of the mass functions is probably a consequence of the mass growth of galaxies due to star formation in both cluster galaxies and, most of all, in galaxies infalling from the cluster surrounding areas. However, a further comparison with the field mass functions taken from literature do not find evidence for an environmental mass segregation. This preliminary work has been completed performing an additional study on homogeneous data from ICBS (Lilly et al., 2007, 2009) and EDisCS between $0.3 \leq z \leq 0.8$ (Vulcani et al., 2012) and shows that the mass distribution at these redshifts does not show a dependence on "global environment", being the "global" environment defined as clusters. groups or general field.

At similar redshifts Giodini et al. (2012) analysing a sample of X-ray galaxy groups selected in the COSMOS survey found that the MF of passive galaxies shows a difference from groups to field while the star-forming one is similar in all environments. These systems are crucial to understand the mass assembly because they represent the most common structure in the universe and are considered the place inwhich some pre-process occurs before a galaxy becomes part of a more massive system.

I analyzed the MF of galaxies at low redshift $(0.04 - 0.1)$ as a function of "global"

	Galaxy type			
Envir.	Ellipticals	S0s	Late-type	Early-type
WINGS	33.8±1.5%	50.7±1.5%	15.4±1.0%	84.5±1.0%
PM2-GF	27.0±1.3%	28.7±1.3%	44.3±1.5%	55.7±1.5%
PM2-G	29.7±1.9%	32.4±2.0%	37.9±2.1%	62.1±2.5%
PM2-FB	25.3±3.5%	25.8±3.6%	48.8±4.0%	51.1±4.0%
PM2-FS	21.5±2.3%	24.2±2.5%	54.2±2.8%	45.7±3.0%

Table 4.1: Fractions of each morphological type in the PM2GC and WINGS mass-limited samples with $M_\star$=$10^{10.25} M_\odot$. Early-type galaxies comprise ellipticals and S0s. Errors are binomial. Data taken from Calvi et al. (2012)

environment. I study both the general field MF, and for the first time its variation in progressively less massive "haloes", from clusters, to groups, to binary systems and single galaxies, covering a range of system masses from $10^{15} M_\odot$ to systems that are expected to be of the order of a few times $10^{12} M_\odot$. The aim is to understand if and how the MF varies with the global environment in the local Universe. At intermediate redshifts, as mentioned above, no significant variation has been found by Vulcani et al. (2012) between clusters, groups and general field. Now I want to investigate whether it is possible to detect a variation of the MF with environment at low-z, where I am able to perform a more detailed analysis isolating also lower mass environments.

In addition, I study the MF of different morphological types, ellipticals, lenticulars and later-type galaxies. My aim here is twofold: to characterize the differences in MF between a morphological type and the other, in each given environment, and to investigate whether the MF of a given type changes with environment.

4.3 Datasets at low z and the method

In order to present a complete overview of how galaxies properties vary in different environments I used several galaxy samples in the local universe: samples of group, binary, single and general field galaxies selected from the Padova Millennium Galaxy and Group Catalog (PM2GC) (Calvi, Poggianti & Vulcani, 2011) (Chapter 2) and the sample of cluster galaxies selected from the WIde-field Nearby Galaxy-cluster Survey (WINGS) and described in Chapter 3.

Red. range	***Environment***	***Num. of galaxies***
$0.04< z<0.07$	WINGS	690 (1056)
$0.04\lesssim z \lesssim 0.1$	PM2-GF	1188
”	PM2-G	583
”	PM2-FB	174
”	PM2-FS	334

Table 4.2: Number of galaxies in the PM2GC and WINGS mass-limited samples with $M_\star \geq 10^{10.25} M_\odot$. WINGS = clusters; GF = general field; G = groups; FB = binary systems; FS = single galaxies. The WINGS number of galaxies is given not corrected for spectroscopic incompleteness and the number between brackets is the weighed total number of galaxies above our completeness limit.

The morphological classification process has been performed using the MORPHOT tool (§3.2). The number of elliptical (Ell), S0, early-type and late-type galaxies above our mass limit $M_\star$=$10^{10.25} M_\odot$ in the different samples is indicated in the plots and in Table 4.1 I list again the morphological fractions of each morphological type in each sample with $\log_{10} M_\star/M_\odot \geq 10.25$.

Since I want to perform a detailed analysis of the galaxy properties, I restricted to a galaxy sample complete in mass so that all types of galaxies are potentially observable above this mass. The galaxy stellar mass completeness limit was computed as the mass of the reddest galaxy at the upper redshift limit. See §3.1 for the description. For PM2GC the mass limit is equal to $M_\star = 10^{10.25} M_\odot$. The mass limit for WINGS is lower and corresponds to $M_\star = 10^{9.8} M_\odot$, but for homogeneity we adopted the same galaxy mass limit as for the PM2GC.

The various samples of galaxies above our mass limit are listed in Table 4.2.

The analysis of the galaxy mass function is based both on a visual ispection of the shape of the data's distribution, on the application of the Kolmogorov-Smirnov (K-S) test, and on the analysis of the parameters of Schechter function fits. We built the histograms of the mass distributions of galaxies setting the bin width at 0.2 dex while the number density of galaxies is obtained first summing all galaxies in each bin and then dividing this value by the bin width. The errors along the x direction represent the bin size while in the y direction are computed as poissonian error as in Gehrels (1986).

In combination with these graphs a ”low probability” (typically $P_{K-S} < 5\%$) of the

Kolmogorov-Smirnov (K-S) test is a statistically significant result to discriminate if two samples are different; on the contrary a "high probability" does not prove that they are drawn from the same distribution but only that the test is not able to find differences. In addition, we also perform Schechter et al. (1976) fit of the mass functions using the least square fitting method. The galaxy stellar mass function can be described as

$$\Phi(M) = (\ln 10) \times \Phi^* \times [10^{(M-M^*)(1+\alpha)}] \times exp[-10^{(M-M^*)}] \quad (4.1)$$

where $M = \log(M_*/M_\odot)$, α is the low-mass-end slope, $M^* = \log(M_*^*/M_\odot)$ is the characteristic stellar mass at which the mass function exhibits a rapid change in the slope, and Φ^* is the normalization.

4.4 Comparison with previous works

First of all we compare our MF with previous results of the literature to check if they are in agreement. Figure 4.1 shows the comparison between PM2GC general field MF and the 2dFGRS-2MASS (Table 4 in Cole et al. (2001)), the SDSS-2MASS (Table 5 in Bell et al. (2003)) and the recent GAMA result from Baldry et al. (2008). Only for this plot all MFs are given in units of number per $h^{-3}\,\mathrm{Mpc}^3$ per decade of mass (dex^{-1}, and masses in $M_\odot$ all converted to a Kroupa IMF.

The shape of our MF is in very good agreement with all previous estimates. As for the absolute normalization, the only MF that tends to be slightly lower is the one from Baldry et al. (2008)

The agreement is confirmed by the Schechter fit parameter (see also Table4.3). Our $\log_{10}\mathrm{M}_\star/\mathrm{M}_\odot = 10.96\pm0.06$, $\alpha = -1.12\pm0.12$ and $\phi_\star = 0.060\pm0.011$ are fully consistent with Cole's $\log_{10}\mathrm{M}_\star/\mathrm{M}_\odot = 10.97 \pm 0.01$, $\alpha = -1.18 \pm 0.03$ and $\phi_\star = 0.009 \pm 0.0014$ and Bell's $\log_{10}\mathrm{M}_\star/\mathrm{M}_\odot = 11.02 \pm 0.02$, $\alpha = -1.10 \pm 0.02$ and $\phi_\star = 0.0102 \pm 0.0005$ when they are all converted to our units. Baldry et al. fit their data with a double Schechter therefore parameters cannot be compared.

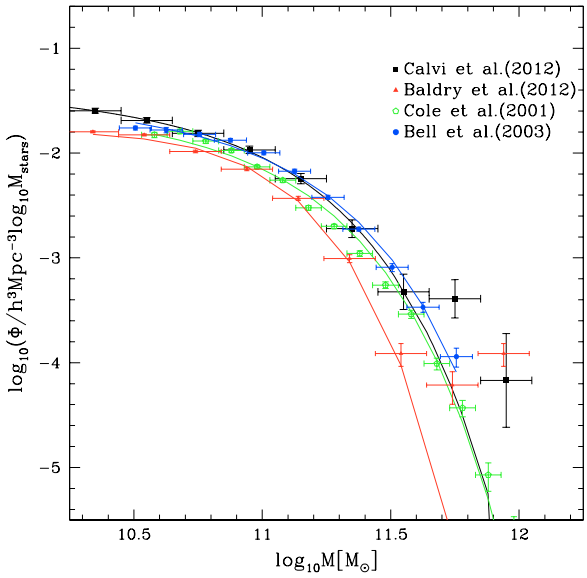

Figure 4.1: Comparison between our general field MF (PM2-GF) and literature results. Masses are in units of $M_\odot$ for a Kroupa IMF. Φ values are in units of number per $h^{-3}\,\mathrm{Mpc}^3$ per decade of mass (dex^{-1}).

4.5 The impact of environment on MF

In the following I focus my attention on how the galaxy mass functions change with galaxy "global environment" in the local Universe comparing PM2GC samples and WINGS above the completeness limit of $M_\star = 10^{10.25} M_\odot$. An analysis of the WINGS's MF up to $M_\star = 10^{9.8} M_\odot$ is in Vulcani et al. (2011)

As the presence of BCG galaxies in WINGS, defined as the brightest galaxies that inhabit the cores of rich galaxy clusters, could alter the total mass distribution I investigated the mass funtions also excluding the BGCs in the WINGS sample.

Finally, for a better comparison between the different combination of galaxy samples, since I are interested mainly in the shape of the mass distributions and not in the counts, I normalized the total mass function of one environment for the number of galaxies in the other in the mass bin between 10.65-11.05 in logarithmic scale. Moreover, unlike the PM2GC samples that are complete, in the case of WINGS each galaxy is weighed by its correction for spectroscopic incompleteness.

4.5.1 General field versus clusters

Figure 4.2 shows the comparison between the mass distribution of galaxies in the general field (PM2-GF, black filled circles) and the mass distribution of all WINGS cluster galaxies (blue filled squares), the latter weighed for incompleteness and normalized to the PM2-GF.

Looking at the plot we can observe that the slope of the mass functions of clusters and general field do not differ. For galaxies with masses up to $\log_{10}\mathrm{M}_{\star}/\mathrm{M}_{\odot} \sim 11.5$ there is a good overlap, while the WINGS sample exhibits an excess of galaxies in three of the four most massive bins at $M_{\star} > 10^{11.5} M_{\odot}$. This excess is due to the presence of BCG galaxies. Removing the BCGs, the mass functions of PM2-GF and WINGS (green crosses) are very similar within the errors. The K-S test also finds no difference both when we include the BGCs ($P_{K-S} \sim 69\%$) or not ($P_{K-S}^{exBCG} \sim 72\%$).

The similarity of the cluster and general field mass functions is also confirmed by visual ispection of the Schechter function and by the analysis of the fit parameters, that are similar within the errors (Table4.3). For PM2GC samples we computed the $\Phi^{\star}$ in units of number per $h^{-3}\,\mathrm{Mpc}^3$ per decade of mass (dex^{-1} while for WINGS we can't obtain a similar estimate because the survey is an all-sky survey. As seen in previous works, the Schechter function is unable to fit the very massive end, and in fact the WINGS Schecter parameters α and $\mathrm{M}^{\star}$, with and without BCGs, are very similar.

The PM2-GF sample is the sum of group galaxies, (which dominate the general field), binary system galaxies, isolated galaxies and galaxies that, although located in a trial group, did not make it into the final group sample. In the following section our aim is to understand if differences in the galaxy mass function become appreciable when considering these finer division of environments.

4.5.2 The MF in groups, binaries, singles and clusters

Figure 4.3 shows the mass distribution of galaxies comparing different pairs of environments. Also in this case we use the WINGS sample both with and without BCGs. In the top panels galaxies in clusters, binary and single galaxies are normalized to groups to have the same total number of galaxies. In the bottom panels binary and single galaxies are normalized to clusters galaxies while binary to single galaxies. The fact that we consider as

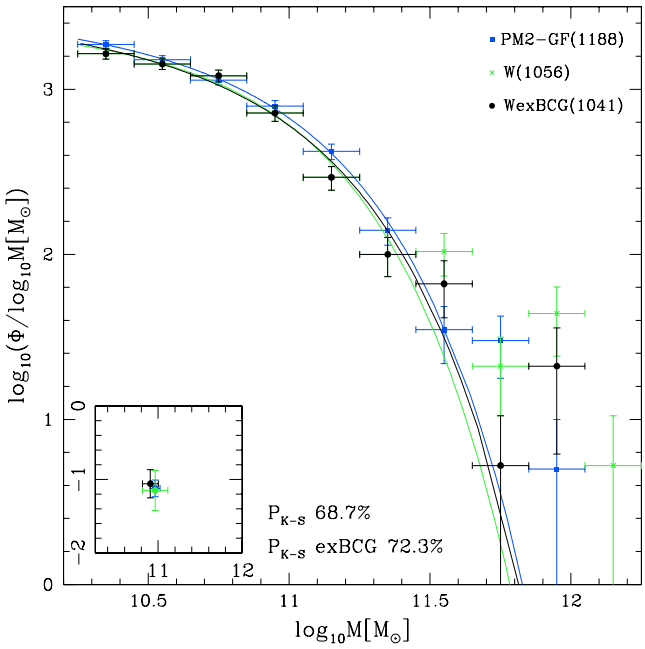

Figure 4.2: Comparison between the mass distribution of galaxies of all morphological types in PM2-GF (blue filled squares) and in WINGS with (green crosses) and without (black filled circles) the BCG galaxies. The mass distributions are normalized to have the same total number of objects. Numbers in the brackets are the total number of galaxies in each sample observed above the completeness limit. The relative K-S probabilities are also shown. Errors are poissonian. Within the plots are shown the α an $\log_{10}\mathrm{M}^{\star}$ of each sample.

	Schechter parameters			
Environments	α	$\log_{10}\mathrm{M}^{\star}$	$\phi^{\star}$	$\phi^{\star}(h^3\,\mathrm{Mpc}^{-3}\log_{10}(\mathrm{M}^{-1})$
WINGS	-0.88 ± 0.31	10.82 ± 0.13	483.23 ± 223.71	...
WINGSexBCG	-0.86 ± 0.23	10.81 ± 0.10	566.10 ± 158.19	...
PM2-GF	-1.12 ± 0.12	10.96 ± 0.06	868.27 ± 160.54	0.060 ± 0.011
PM2-G	-1.16 ± 0.14	11.05 ± 0.08	249.48 ± 64.68	0.017 ± 0.004
PM2-FS	-1.30 ± 0.08	10.94 ± 0.04	225.60 ± 33.75	0.015 ± 0.002
PM2-FB	-0.60 ± 0.56	10.75 ± 0.23	228.08 ± 96.96	0.015 ± 0.006

Table 4.3: Schechter parameters for PM2-GF and WINGS samples.

group galaxies only those galaxies which are in groups with a velocity dispersion less than 500 $\mathrm{km\,s^{-1}}$ make us confident that our findings for groups are not influenced by galaxies in clusters as massive as WINGS's, therefore the group and WINGS distributions sample truly different environments.

If we consider the shapes of the mass functions of groups and clusters we find that they show a similar trend. At masses $\log_{10}\mathrm{M}_\star/\mathrm{M}_\odot < 11.2$ the distributions overlap while at high masses the distribution in groups tends to be steadily higher than the cluster one without BCGs (top left panel). The K-S test is not able to reveal difference being $P_{K-S} \sim 34\%$ and $P_{K-S}^{exBCG} \sim 16\%$ with and without BCGs, respectively, and the compatibility of cluster and group mass functions is also confirmed by the Schecter fit parameters (Table4.3). In addition, we note that both in clusters and groups very massive galaxies ($\log_{10}\mathrm{M}_\star/\mathrm{M}_\odot > 11.5$) are formed.

Looking at the mass function of the PM2-FS, that is the extreme "low-mass halo" environment, hence the most different from clusters, we note that the slope of the PM2-FS MF in Figure4.3 appears steeper at low masses than any other environment (groups, binaries and clusters).

The K-S test is able to conclude that the mass functions of group and isolated galaxies are statistically different ($P_{K-S} < 1\%$). Quite low KS probabilities (of the order of 7-8$\%$) are also suggesting the differences between the MF of single galaxies and that of clusters and binaries might be different.

Indeed, single galaxies have the steepest value of α in the Schecter fit, although the differences with the other environments are not statistically robust given the errorbars.

For PM2-FB it is difficult quantify the differences between different mass functions given the low number statistics and the fact that the upper mass of PM2-FB is lower than the others, as discussed in the next section. Thus, from the slope of PM2-FB mass function we can't draw conclusions, except that there may be a hint that the PM2-FB MF is flatter than others at low masses. No statistically robust difference can be found based on the KS test, and the Schecter α is unconstrained for binaries, while $M_\star$ is compatible with all other environments.

To conclude, the galaxy mass function in groups and clusters is similar, while a variation with global environment starts to be appreciable only when considering single galax-

environment	$M_\star \geq 10^{11.2} M_\odot$	$M_\star < 10^{11.2} M_\odot$	$M_{(\geq 11.2)}/M_{(<11.2)}$
WINGS(exBCGs)	46(34)	644	$7.1 \pm 1.1\% (5.2 \pm 0.9\%)$
PM2-GF	52	1136	$4.6 \pm 0.6\%$
PM2-G	23	386	$6.0 \pm 1.2\%$
PM2-FB	0	174	$0.0 \pm ..\%$
PM2-FS	12	322	$3.7 \pm 1.1\%$

Table 4.4: Number of galaxies in the PM2GC and WINGS mass-limited samples with mass $M_\star \geq 10^{11.2} M_\odot$ and $M_\star < 10^{11.2} M_\odot$ and their ratio as a percentage. Errors are poissonian.

ies, that show a steeper MF, therefore are proportionally richer in lower-mass galaxies, than other environments. It is worth noting that single galaxies represent less than a third (28%) of the general field population above our mass limit, as can be inferred from Table4.2.

4.5.3 Cut-off in mass

In addition to the similarities and differences described above, it is interesting to observe that in binary and single systems there are no galaxies with masses $M_\star \geq 10^{11.2} M_\odot$ and $M_\star \geq 10^{11.55} M_\odot$, respectively, while in groups and clusters there are galaxies up to $M_\star \sim 10^{11.75} M_\odot$ and $M_\star \sim 10^{12} M_\odot$ even excluding cluster BCGs. This might suggest that galaxies in different environments could reach different upper masses.

To begin quantifying the differences, in Table 4.4 we show the number of galaxies in each environment above and below $M_\star = 10^{11.2} M_\odot$, the upper limit of masses for binary sistem galaxies, and their ratio with relative poissonian errors. The ratio varies with environment being higher in clusters, then groups, than among single and binary galaxies.

In order to assess the significance of the variation of the upper mass limit we performed a Montecarlo simulation to understand whether this effect could be due to low number statistics in the least massive environments.

Using each time 1000 simulations, we evaluated the upper mass obtained extracting from the group sample the same number of galaxies once as in the single sample and once as in the binary sample, and then extracting from the single sample the same number of galaxies as in binary systems.

In Table4.5 are shown the median upper masses for the different simulations and the fractions of simulations that reach an upper mass at least as low as the observed mass +

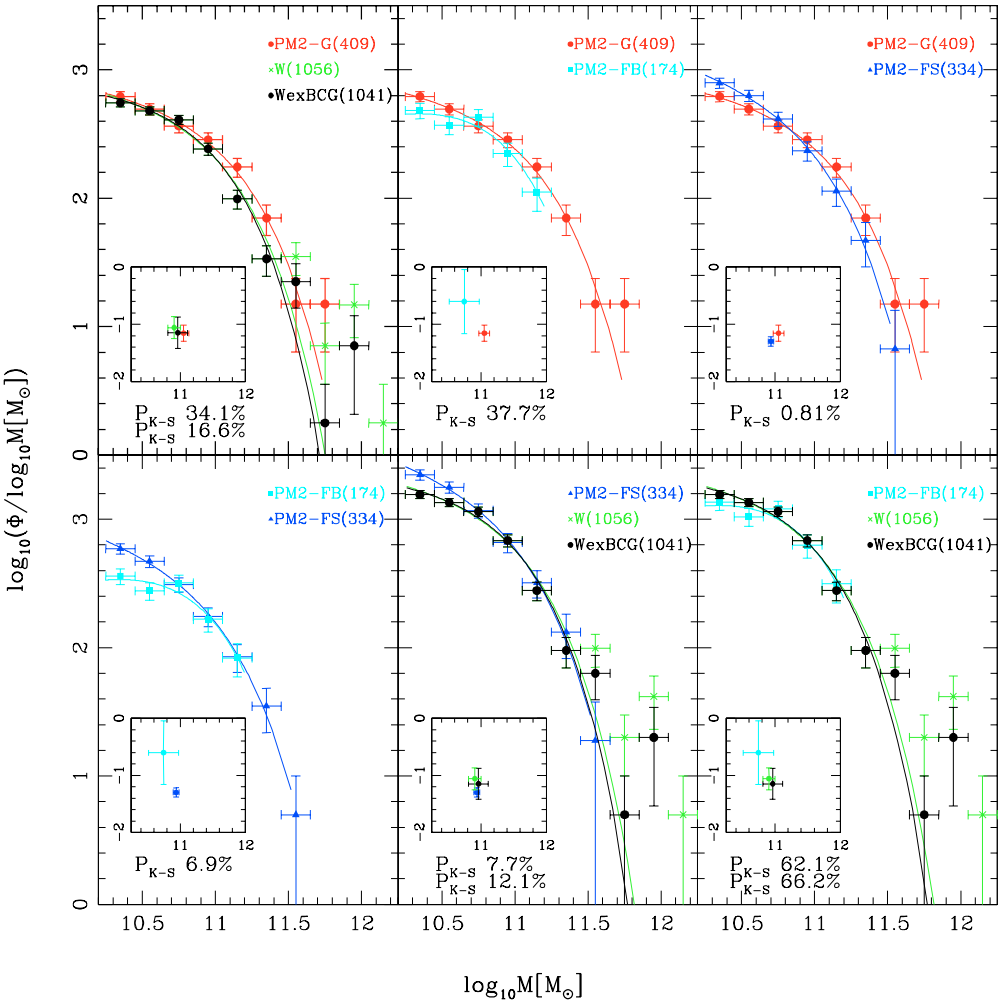

Figure 4.3: Comparison of the mass distributions of galaxies of all morphological types, for the mass limited samples, for different pairs of environments: PM2-G vs WINGS (top left panel) with (green crosses) and without BCGs (black stars), PM2-G vs PM2-FB (top central panel), PM2-G vs PM2-FS (top right panel), PM2-FS vs PM2-FB (bottom left panel), WINGS, with (green crosses) and without BCGs (black stars) vs PM2-FS (bottom central panel), WINGS, with (green crosses) and without BCGs (black stars) vs PM2-FB (bottom right panel). Mass distributions are normalized to have the same total number of objects. For PM2-G we considered only groups with $\sigma < 500\,\mathrm{kms}^{-1}$. Errors are poissonian in the y direction and equal to the bin size in the x direction. Numbers in the brackets are the total number of galaxies above the completeness limits. In the bottom left side of the panels we shown the relative K-S probability.

	Fraction	**Median upper mass**($M_\star$)
groups-bin	0.003%	$10^{11.7}$
groups-sin	0.015%	$10^{11.8}$
sin-bin	0.016%	$10^{11.4}$

Table 4.5: Fractions of simulations which reach an upper mass at least as low as the observed mass +0.1dex and values of the median upper mass reached in the Montecarlo simulations comparing group and binary, group and single, single and binary samples.

0.1dex. The latter can be seen as the probability that the low cut-off mass observed in binary and single systems is due to the small number of galaxies in the sample. This probability is always very low (e.g. 0.003%, that is 3 out of the 1000 simulations, when extracting from the group sample the same number of galaxies composing the binary sample). This demonstrates that even reducing the number of galaxies, we would expect more massive objects among single and binary galaxies. We thus conclude that effectively the cut-off mass varies with environment, and that massive galaxies can only be found in environments that correspond to more massive dark matter haloes.

To summarize, at low redshift, (1) no difference can be found in the mass functions of groups, clusters and general field by analyzing the parameters of the Schechter fits or the KS test. (2) For binary systems, the KS test is inconclusive and the α Schechter parameter is unconstrained, hence secure conclusions cannot be reached for this type of environment. (3) Differences have been found in the mass function of single galaxies compared to other environments. The mass function of singles appears slightly steeper than the others. According to the KS test, the difference is statistically significant between single and group galaxies, while it is only marginally suggested by the KS values when comparing with the binary and cluster samples. Schechter fit parameters are unable to detect statistically significant differences. (4) Very massive galaxies are only found in the most massive environments, groups and clusters, while they are absent among single and binary galaxies. The presence or absence of such massive galaxies is unable to affect both the Schechter parameters (being $M^\star$ anyway lower than such galaxies) and the KS test (dominated by the most frequent, lower mass galaxies and unaffected by the few very massive ones). Only a separate analysis of the mass cut-off have been able to highlight the dependence of the

cut-off mass on global environment.

4.6 The galaxy mass function by morphological type

In the previus sections we found the somewhat unexpected result that the mass function *doesn't depend* on "global environment", except when carefully analyzing single galaxies separately (KS test) and when studying in detail the cut-off mass beyond the Schechter and KS results.

Now we attempt to examine another question. Given the dependence of the morphological types with environment, does the mass function differ from a galaxy type to the other? And does the mass function of each morphological type vary with environment? To address these question(blue filled squares)s we investigated the mass distributions of elliptical, S0, early (elliptical+S0, hereafter ET) and late-type (LT) galaxies in different environments.

4.6.1 The MF of E,S0,ET,LT in the general field versus clusters

The comparison between the mass distribution of elliptical, S0, early and late-type galaxies of PM2-GF and WINGS is shown in Figure 4.4 where WINGS samples have been normalized to PM2-GF ones .

In all cases, the KS test is unable to detect any significant difference between general field and clusters.

The analysis of the Schechter parameteres and the inspection of the plot, instead, reveal a few differences.

Ellipticals in clusters, even when excluding the BCGs, have a higher $M_\star$ and a lower value of α than ellipticals in the general field. This is due to the excess of ellipticals with masses > 11.5 in clusters compared to the field visible in the top left panel of Figure4.4.

The Schechter parameters for S0s in clusters and general field are instead indistinguishable, as they are those of early-type galaxies alltogether. The only noticeable difference is the lack of S0s galaxies in clusters in the mass range $11.35 < \log_{10}\mathrm{M}_\star/\mathrm{M}_\odot < 11.95$ that can be seen in the top right panel of Figure4.4.

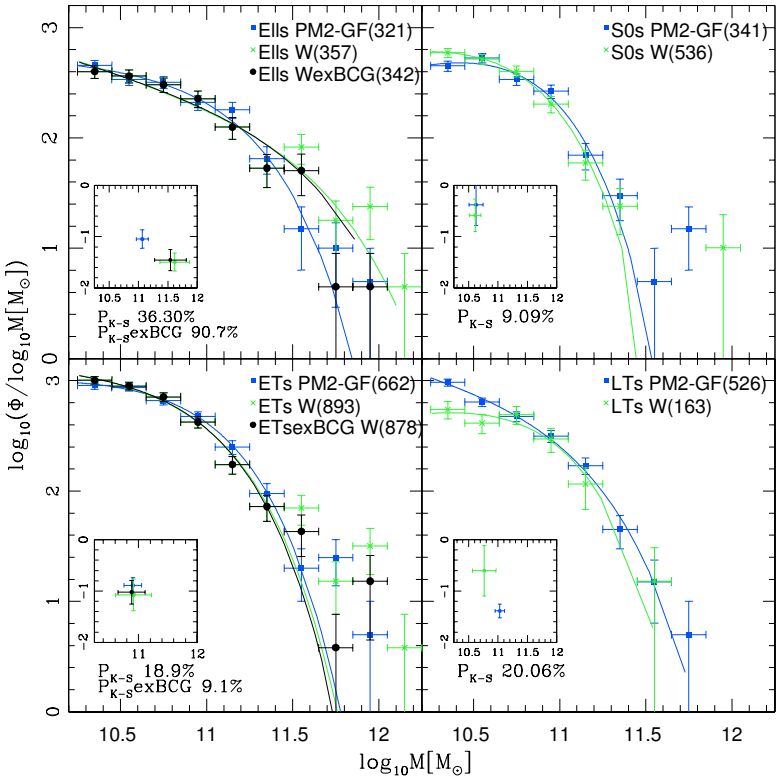

Figure 4.4: Comparison of the mass distribution between PM2-GF and WINGS for elliptical galaxies (top left panel), S0 galaxies (top right panel), early-type galaxies (bottom left panel) and late-type galaxies (bottom right panel). Errors are defined as poissonian errors in the *y* direction and equal to the bin size in the *x* direction. Numbers in the brackets are the number of galaxies of each type above the mass limit (for WINGS the number is wieghed for incompleteness). The K-S probabilities are also shown in the bottom left corner. The WINGS sample has been normalized to PM2-GF one.

Environment	morph. type	*Schecter parameters* α	$\log_{10}M^{\star}$ $M_{\odot}$	$\phi^{\star}$	$\phi^{\star} \pm \delta\phi$ $h^3Mpc^{-3}log_{10}(M^{-1})$
WINGS	ell	-1.495±0.175	11.617± 0.250	53.25 ± 39.38	.....
	ellnoBCG	-1.454± 0.205	11.543 ± 0.270	64.92 ± 51.56	.....
	S0	-0.585 ± 0.314	10.613 ± 0.098	849.80± 154.20	.....
	lt	-0.603 ± 0.490	10.765 ± 0.200	206.58 ± 78.22	.....
	early	-1.076 ± 0.308	10.915 ± 0.159	712.25± 332.78	.....
	earlynoBCG	-1.023 ± 0.231	10.884 ± 0.112	775.09± 248.00	.....
PM2-GF	ell	-1.048 ± 0.179	11.065 ± 0.100	208.88± 61.19	$(14.2 \pm 4.1) \times 10^{-3}$
	S0	-0.379 ± 0.405	10.626 ± 0.122	520.45± 93.06	$(35.3 \pm 6.3) \times 10^{-3}$
	lt	-1.387 ± 0.131	11.030 ± 0.080	271.95± 76.96	$(18.4 \pm 5.2) \times 10^{-3}$
	early	-0.890 ± 0.151	10.904 ± 0.069	612.84± 111.96	$(45.6 \pm 7.6) \times 10^{-3}$
PM2-G	ell	-1.156 ± 0.223	11.256 ± 0.165	57.39± 27.81	$(3.9 \pm 1.9) \times 10^{-3}$
	S0	-0.520 ± 0.268	10.698 ± 0.089	178.05± 29.15	$(12.1 \pm 2.0) \times 10^{-3}$
	lt	-1.428 ± 0.340	11.099 ± 0.261	65.03± 56.68	$(4.41 \pm 3.8) \times 10^{-3}$
	early	-1.089 ± 0.151	11.093 ± 0.092	156.84± 42.08	$(10.4 \pm 2.8) \times 10^{-3}$
PM2-FB	ell	-0.488 ± 1.756	10.853 ± 0.850	48.16± 62.10	$(3.3 \pm 4.2) \times 10^{-3}$
	S0	0.667 ± 0.673	10.412 ± 0.139	64.07 ± 18.33	$(4.3 \pm 1.2) \times 10^{-3}$
	lt	-1.271 ± 0.406	10.997 ± 0.302	53.57± 47.45	$(3.6 \pm 3.2) \times 10^{-3}$
	early	0.073 ± 0.759	10.582 ± 0.214	137.72± 17.36	$(9.3 \pm 1.2) \times 10^{-3}$
PM2-FS	ell	-1.400 ± 0.468	11.002 ± 0.305	38.23± 39.87	$(2.6 \pm 2.7) \times 10^{-3}$
	s0	-0.159 ± 0.890	10.426 ± 0.201	158.21± 27.81	$(10.7 \pm 5.2) \times 10^{-3}$
	lt	-1.491 ± 0.122	11.079 ± 0.087	76.41 ± 23.71	$(5.2 \pm 1.6) \times 10^{-3}$
	early	-1.095 ± 0.208	10.820 ± 0.096	147.71± 42.33	$(10.0 \pm 2.9) \times 10^{-3}$

Table 4.6: Schechter parameters for PM2GC groups, binary systems, single, general field and WINGS clusters.

Looking at the numbers in the plots, one can notice that the PM2-GF consists of a similar number of ellipticals and S0s, while WINGS clusters are preferentially dominated by S0s. A detailed study of the variation of the morphological fractions with environment can be found in Calvi, Poggianti & Vulcani (2011).

Coming to late-type galaxies, at low masses the shape of their mass function in WINGS is flatter than in PM2-GF. As also indicated by the Schechter α parameter, there is a deficit of low-mass late-type galaxies in clusters compared to the general field.

In conclusion, the only variations we detect in the mass function of elliptical, S0 and late-type galaxies is the excess of massive ellipticals and the deficit of low mass late-type galaxies in clusters compared to the general field.

4.6.2 The shape of the galaxy mass function of each morphological type in different environments

As for the total galaxy mass functions, now we investigate the variation of the mass function of elliptical, S0, early and late type galaxies in the more detailed environments. Figures 4.5 to 4.8 show the distributions of each morphological class. Subdiving our samples in both morphological type and detailed environment, the statistics get worse, and in most cases the errors on the Schechter parameters shown in the smaller side by side plots become too large to draw robust conclusions. In particular, the binary sample is always too poor to be compared with the others. Schechter parameters are anyway listed for all environments in Table4.6.

Comparing clusters and groups, which are the two environment with the better statistics, we find a rather similar mass function for ellipticals, as seen in the Fig.4.5, from the KS and the Schechter fits.

Ellipticals in the single sample, instead, show a steeper mass function than those in groups and clusters, as seen in the plot and, marginally, found by the KS for groups.

The mass distribution of S0 galaxies in clusters and groups is indistinguishable on the basis of the KS test and of the Schechter parameters, although the inspection of Fig.4.6 shows a possible flattening at low masses in groups. The S0 mass functions in the other environments are too noisy for any conclusion, although the plot is suggestive of again a steeper function among single galaxies than in groups, and of a decrease in the FB mass function at low masses.

In Figure 4.8 we show the distribution of masses for early-type galaxies. The early-type mass function is simply the combination of the mass functions of E and SO galaxies. Small differences start to be appreciable at high masses between clusters and groups when excluding cluster BCGs: both the KS and the Schechter α show differences at the 1sigma level. Moreover, the differences in the mass function of singles and groups, singles and binaries, binaries and clusters are now statistically significant .

Finally, Figure 4.7 shows the mass distributions of late-type galaxies in all samples. Looking the plots we note that the shape of the mass functions is almost the same in all environments, with only in clusters showing a flattening at masses $\log_{10}\mathrm{M}_{\star}/\mathrm{M}_{\odot} < 10.65$. This may correspond to the small steepening in the mass function of cluster S0s at these

masses, if preferentially low-mass late-types are transformed in S0s by the cluster environment. The K-S test probability in all cases is always greater than 10%, and the errorbar on the low value of α in clusters is too large to allow a statistical discrimination with other environments.

To summarize, the mass functions of ellipticals and S0 galaxies do not differ significantly in clusters and groups, while both distributions appear steeper in the single galaxy sample. The mass distribution of late-type galaxies is strikingly similar in all environments, except for an apparent deficit of low-mass late-types in clusters.

4.7 The galaxy mass function of different morphological types in each environment

We now analyze differences in the mass functions of different morphological types in each given environment (Fig. 9). In this case, we don't apply any normalization to the mass functions, to show which morphological type dominates as a function of mass. To increase the statistics, for the group sample we consider in this analysis also galaxies in groups with $\sigma \geq 500\mathrm{kms}^{-1}$.

Figure 4.9 shows the mass distributions of galaxies in each environment and galaxies of different morphological types are indicated by different colors and symbols with a line that represents the Schechter fit.

In the general field, as well as in the binary sample, the global mass function is dominated by late-type galaxies at low masses ($\lesssim 11$), and by a rather similar mix of all types at higher masses. Moreover, late-type galaxies dominate the global mass function at all masses in the single galaxy sample.

In groups the late-type mass function resemble that of S0 one at masses $\lesssim 11$ except in the first mass bin (< 10.5) where the number of late-type is more numerous. At higher masses dominate the elliptical galaxies. The cluster environment still results peculiar because unlike other stuctures the main population at masses $\lesssim 11$ is that of S0 galaxies but, as mass increases, it sharply decreases and ellipticals dominate. The number of late-type galaxies are steadily lower respect to S0's and elliptical's ones at all masses.

The K-S test for single and binary system galaxies is inconclusive to find difference

between the distributions of each morphological type, even if a difference is found in the comparison between ellipticals versus late-types in binary systems. For groups, general field and clusters the K-S is instead statistically significant to confirm that the distributions of each morphological type are different between each other. In clusters the K-S probability between ellipticals and S0s is ~ 0 while is $\sim 8\%$ for S0s versus late-types thus is more evident the difference ELL-S0 rather than S0-LT.

From the analysis of Schechter parameters we found that the MFs of each morphological type are comparable within 1σ for PM2GC groups, single, binary and general field samples. On the contrary in WINGS clusters is the MF of ellipticals that deviates from the SO's and late-type's ones. In general in each environment the S0's $\mathrm{M}^{\star}$ value is lower than those of ellipticals and late-types and in the single and binary sample reachs the lowest value while in clusters this value resemble that of late-type. In clusters the value of $\mathrm{M}^{\star}$ for the elliptical is higher than the corresponding value of PM2GC environments while the value of $\mathrm{M}^{\star}$ for late-type is lower than the other samples.

All these findings support the fact that cluster environment has a peculiar behavior. The shape of the high mass end is different going from single galaxies, to binaries, to groups and clusters and, as seen in Calvi et al. (2012), this is probably due to a cluster-specific effects that acts on the fraction of Es-S0s and late types.

4.8 Summary

I investigated the galaxy stellar mass functions as a function of "global" environment. I studied the MF variations in the general field and, for the first time, in progressively less massive "haloes", from clusters, to groups, to binary systems and single galaxies, covering a range of system masses from $10^{15} M_{\odot}$ to systems that are expected to be of the order of a few times $10^{12} M_{\odot}$. The analysis is based on (i) a visual ispection of the shape of the data's distribution, (ii) the application of the Kolmogorov-Smirnov (K-S) test, (iii) the analysis of the parameters of Schechter function fits. My findings are:

- The comparison of the MF of PM2GC general field with previous results of the literature shows that the shape of my MF is in very good agreement with all previous estimates. As for the absolute normalization, the only MF that tends to be slightly

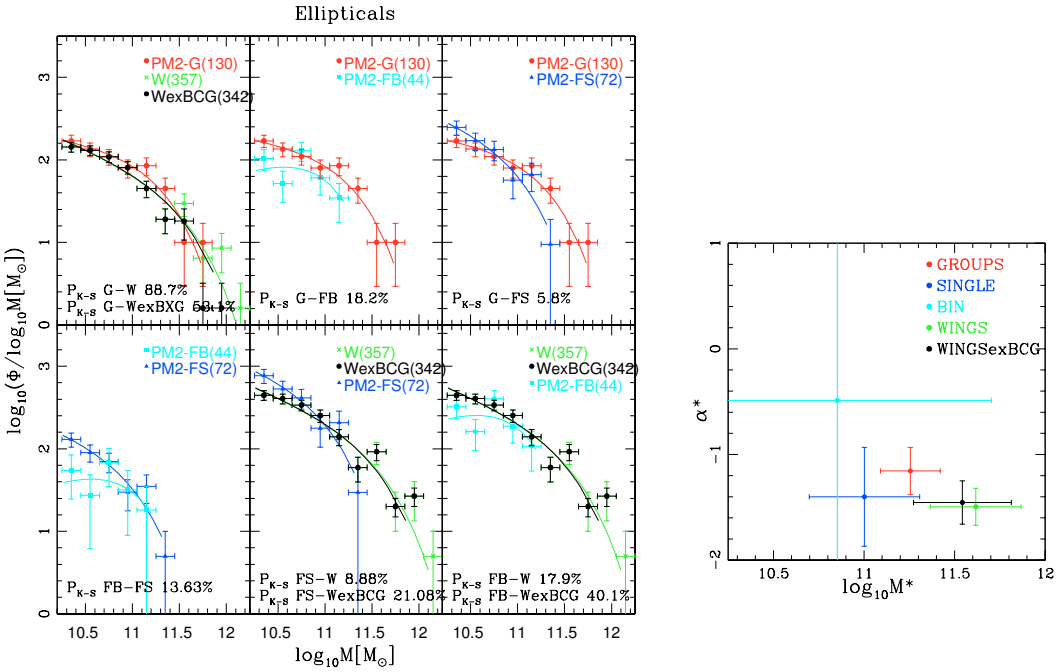

Figure 4.5: **Left** Mass distribution for different pairs of environments for elliptical galaxies. Errors are defined as poissonian errors in y direction and equal to the bin size in x direction. Numbers in the brackets are the number of elliptical galaxies above the mass limit and are weighed for WINGS sample. The K-S probabilities are shown. **Right** Comparison among the Schecter parameters of each environment.

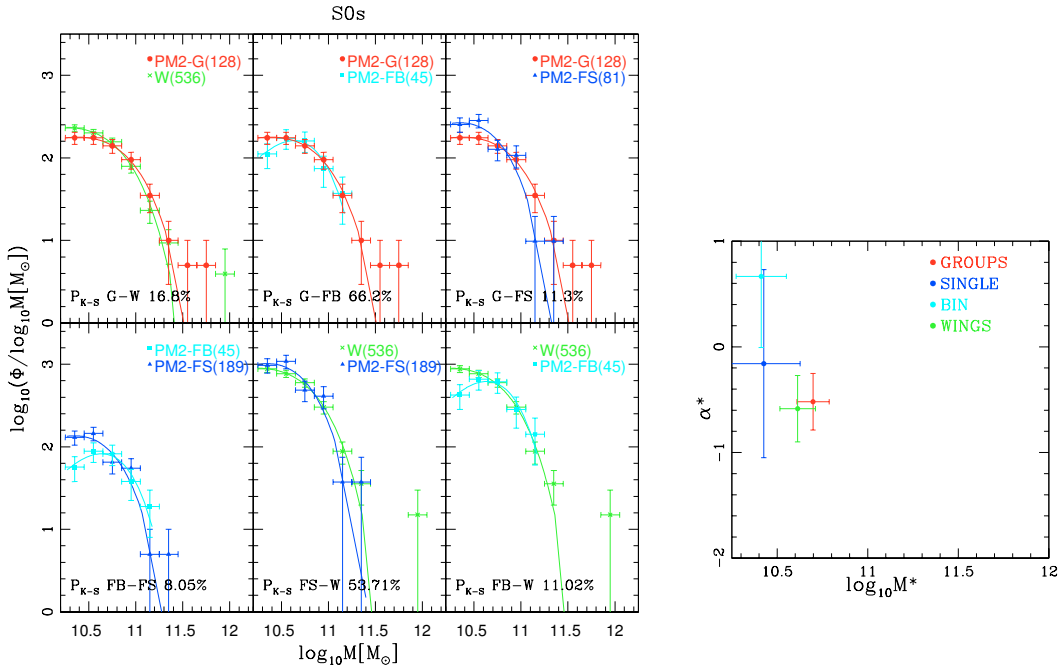

Figure 4.6: **Left** Mass distribution for different pairs of environments for S0 galaxies. Errors are defined as poissonian errors in *y* direction and equal to the bin size in *x* direction. Numbers in the brackets are the number of S0 galaxies above the mass limit and are weighed for WINGS sample.. The K-S probabilities are shown. **Right** Comparison among the Schecter parameters of each environment.

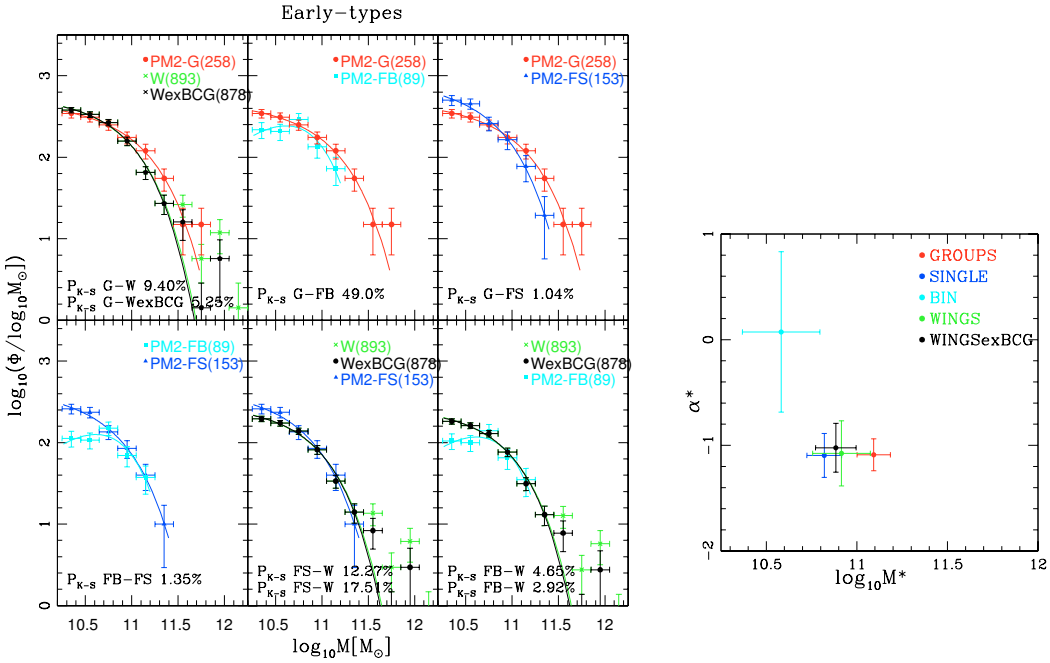

Figure 4.7: **Left** Mass distribution for different pairs of environments for late-type galaxies. Errors are defined as poissonian errors in y direction and equal to the bin size in x direction. Numbers in the brackets are the number of late-type galaxies above the mass limit and are weighed for WINGS sample.. The K-S probabilities are also shown. **Right** Comparison among the Schecter parameters of each environment.

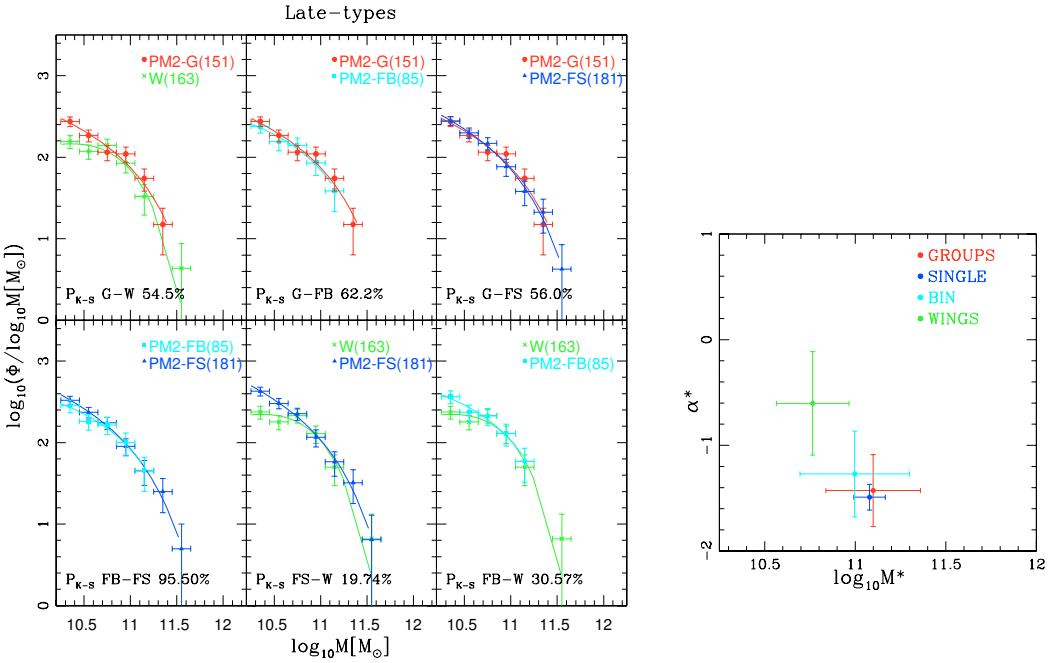

Figure 4.8: **Left** Mass distribution for different pairs of environments for late-type galaxies. Errors are defined as poissonian errors in *y* direction and equal to the bin size in *x* direction. Numbers in the brackets are the number of late-type galaxies above the mass limit and are weighed for WINGS sample.. The K-S probabilities are also shown. **Right** Comparison among the Schecter parameters of each environment.

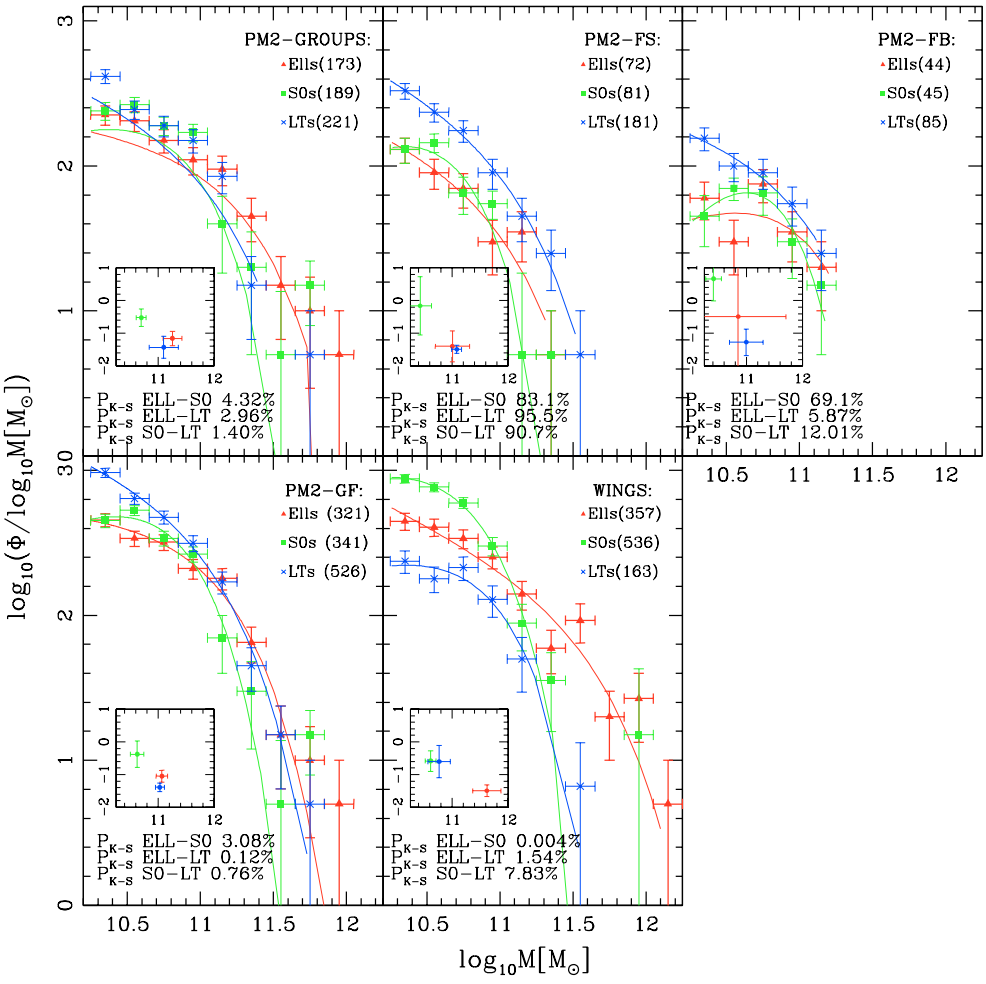

Figure 4.9: Mass distribution of galaxies in the PM2-G (top left panel), PM2-FS (top right panel), PM2-FB (central left panel), PM2-GF (central right panel), WINGS (bottom left panel). The K-S probabilities are shown. Red triangles elliptical galaxies, green square S0s and blue crosses late-type galaxies. Errors are poissonian errors in y direction and equal to the bin size in x direction. Numbers in the brackets are the number of galaxies in each morphological class, above the respective mass limit and are weighed for WINGS sample.

lower is the one from Baldry et al. (2008)

- Contrary to expectations the MF in the general field is indistinguishable from that in clusters in particular whether the BCGs galaxies in WINGS sample, that provide an excess of galaxies in three of the four most massive bins at $M_\star > 10^{11.5} M_\odot$, are removed. The K-S test and the analysis of the fit parameters also finds no difference.

- The variation of the mass function becomes evident only when considering the lowest mass haloes in the PM2GC sample, i.e. single galaxies. However, it has been noted a clear dependence of the upper mass limit on environment, with the most massive galaxies being hosted by the most massive haloes.

- In each given environment I found that the MF of different morphological types (ellipticals, lenticulars and later-type galaxies) are similar in general field and in clusters. The only variations detected is the excess of massive ellipticals and the deficit of low mass late-type galaxies in clusters compared to the general field. The mass functions of ellipticals and S0 galaxies do not differ significantly in clusters and groups, while both distributions appear steeper in the single galaxy sample. The mass distribution of late-type galaxies is strikingly similar in all environments, except for an apparent deficit of low-mass late-types in clusters.

- Investigating whether the MF of a given type changes with environment I found that in the general field, as well as in the binary sample, the global mass function is dominated by late-type galaxies at low masses ($\lesssim 11$), and by mix of all types at higher masses. Late-type galaxies dominate the global mass function at all masses in the single galaxy sample. In groups the late-type mass function resemble that of S0 one at masses $\lesssim 11$ except in the first mass bin (< 10.5) where the number of late-type is more numerous. At higher masses dominate the elliptical galaxies. The cluster environment still results peculiar because unlike other stuctures the main population at masses $\lesssim 11$ is that of S0 galaxies but, as mass increases, it sharply decreases and ellipticals dominate. The number of late-type galaxies are steadily lower respect to S0's and elliptical's ones at all masses.

These findings suggest two important things: (1) the MF not depends on global environment at least at masses $\lesssim 11$. Only considering less massive systems, i.e. single galaxies, it has been noted variations in the MF. Instead the high mass end of the MF varies with environment and morphology; (2) there is a population of low-mass S0 galaxies in clusters that have a different behaviour confirming the hypotesis, already suggested from the morphological analysis, that exist a cluster effect that act on low mass galaxies.

4.9 MF as function of local densities

In this chapter I investigated if and how the distribution of galaxy mass depend from global environment. In this last section I want to show the results obtained by **?** on the analysis of the variations of galaxy mass function with local density. Infact, with the term environment the astronomers describe a wide variety of measures that may or may not correlate with each other and often it is described through the estimates of the local density that generally is not at all equivalent to global environment (Muldrew et al. 2011). As said in §4.1 many studies focusing on local environment have generally agree in finding that the mass distribution is regulated by local density: galaxies in lower- and higher density regions show different mass distributions, in the sense that lower density regions are proportionally more populated by lower mass galaxies. But, all of these studies considered general field data, a quite wide range of densities and moreover they mainly compared the most extreme environments, to maximize the possible differences. Recently the galaxy stellar mass distribution has been investigated as a function of local density in mass-limited samples, in the field and, for the first time, in clusters from low ($z \geq 0.04$) to high ($z \leq 0.8$) redshift (**?**). The aim has been to quantify the importance of the local density in shaping the stellar galaxy mass function of galaxies located in different environments using data from four different surveys: the Padova Millennium Galaxy and Group Catalogue (PM2GC) ($0.039 < z < 0.11$; Calvi, Poggianti & Vulcani 2011), the WIdefield Nearby Galaxy-cluster Survey (WINGS) ($0.04 < z < 0.07$; Fasano et al. 2006), the IMACS (Inamori-Magellan Areal Camera and Spectrograph) Cluster Building Survey (ICBS) ($0.25 < z < 0.45$; Oemler et al., in preparation) and the ESO (European Southern Observatory) Distant Cluster Survey (EDisCS) ($0.4 < z < 0.8$; White et al. 2005). It

has been found that at all redshifts and in all environments, local density plays a role in shaping the mass distribution (see Figure4.10). In the field, it regulates the shape of the mass function at any mass above the mass limits. In clusters, it seems to be important only at low masses ($\log_{10}\mathrm{M}_{\star}/\mathrm{M}_{\odot} \leq 10.1$ in WINGS and $\log_{10}\mathrm{M}_{\star}/\mathrm{M}_{\odot} \leq 10.4$ in EDisCS), otherwise it seems not to influence the mass distribution. It has also been found that not only the shape of the mass function depends on local density, but also the highest mass reached in each density bin: very massive galaxies (having excluded the cluster BCGs) seem to be located only in the highest density bin while they are absent at lower densities (the so-called mass segregation). Putting together this results with those described in this chapter and with those found by Vulcani et al. (2011) for the global environment it can be argued that at least at $\mathrm{z} \leq 0.8$ local density is more important than global environment in determining the galaxy stellar mass distribution, suggesting that galaxy properties are not much dependent on halo mass, but do depend on local scale processes.

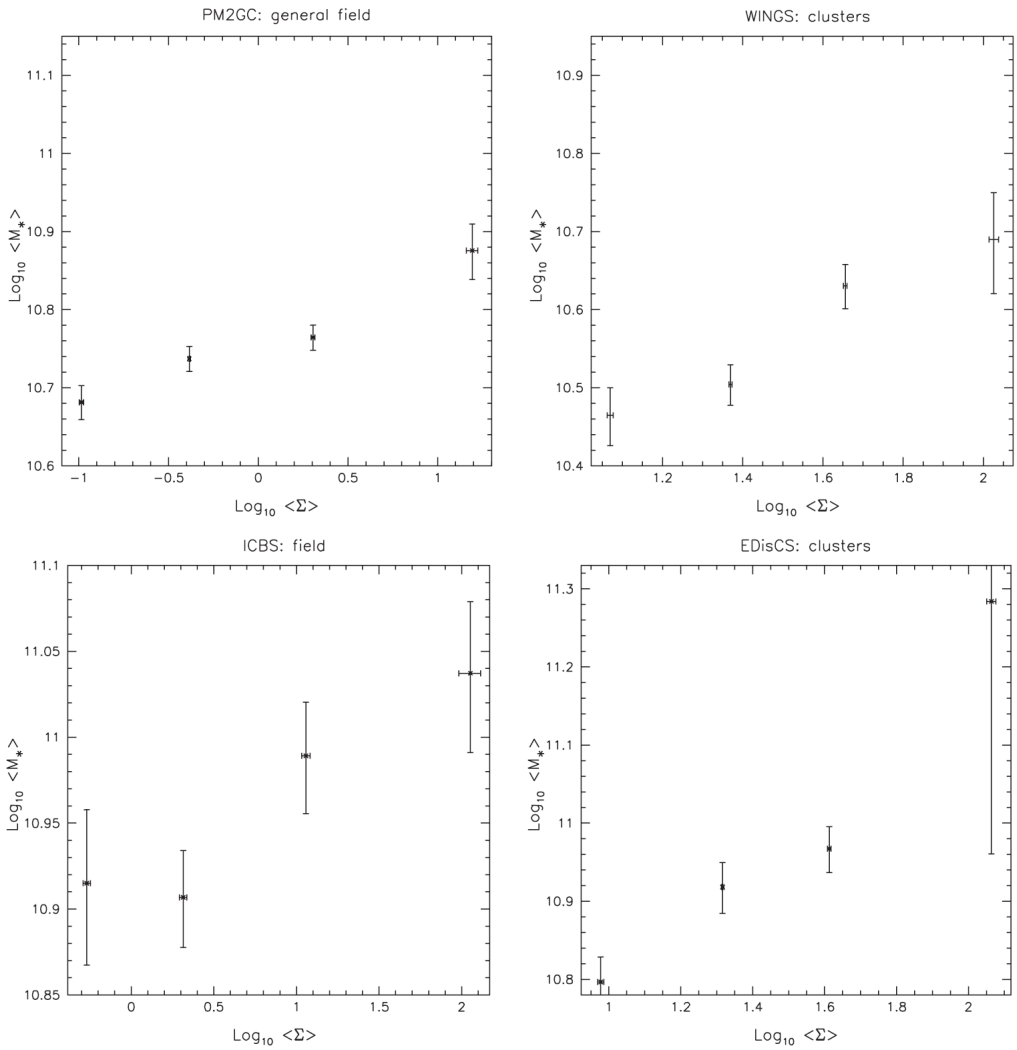

Figure 4.10: Mass-local density relation for the PM2GC (left-hand panel), WINGS (central left panel), ICBS (central right panel) and EDisCS (right-hand panel) surveys. For each sample, above its proper mass completeness limit, the mean mass has been computed separately in the four density bins. Errors are poissonian. For WINGS and ICBS, weighted means are computed. In all samples, the average mass depends on local density: the average mass is higher in higher density bins.

Conclusions

Today one of the most basic areas of investigation in astrophysics concerns the formation and evolution of galaxies. In a ideal Universe galaxies are formed at some characteristic epoch and evolve to their present forms and stellar mix according to the well understood laws governing star formation and evolution. The different distribution of local properties that are obeserved might be explained through the different conditions at birth (”nature” hypotesis) or through the interactions and other local processes that occur since galaxies are not isolated objects (”nurture” hypotesis).

The ”nature vs nurture” scenario is at present still debated. Many observations on the observed properties of S0 galaxies have been used to argue the indipendence between these two hypotesis but, disentangle the role of environment from the role of internal processes is difficult because it is known that the environment where galaxies are located have a decisive influence on several processes that regulate the kinematics and activity of star formation in galaxies.

This thesis attempts to give a valuable contibution in this context. The cluster environment provided a very important window to explore the universe and the properties of clusters can be used to place strong limits on cosmological theories of structure formation and evolution. But, it is now well established that are galaxy groups the key environment to investigate galaxy evolution.

For this purpose I built a new catalog of groups and galaxies representative of the general field population at low redshift, the Padova Millennium Galaxy and Group Catalog (PM2GC). The aim has been to explore in detail the properties of galaxy in groups, for

example the morphology. In addition, I compared the properties of galaxy in groups with those of other samples in PM2GC catalog, the single and binary system samples, and with a sample of cluster galaxies taken from WIde-field Nearby Galaxy cluster Survey (WINGS). The purpose has been to investigate in a consistent manner galaxy properties in the widest range of environments and stellar masses at low redshift.

Many of the results of the thesis confirm a global picture which is becoming quite well established and they can be summarized in two important points:

1. There is a compelling indication that there is a distinct population of low mass S0 galaxies associated only with clusters S0s that probably have a "late-type origin", while a large number of non-cluster S0s have a truly "early-type origin" (a dominant spheroidal component that forms a very small disk, an "intermediate type" between disky ellipticals and Sa's).

2. From the analysis of the distribution of masses in each possible environment I demonstrated how the high mass end of the galaxy stellar mass function varies both with the environment and morphology showing that not only stellar mass but also the environment in which a galaxy resides play a role in galaxy evolution.

Publications

Referred papers

- **Calvi, Rosa**; Poggianti, Bianca M.; Vulcani, Benedetta, "The Padova-Millennium Galaxy and Group Catalogue (PM2GC): the group-finding method and the PM2GC catalogues of group, binary and single field galaxies", 2011, MNRAS, 416, 727.
- **Calvi, Rosa**; Poggianti, Bianca M.; Fasano, Giovanni; Vulcani, Benedetta, "The distribution of galaxy morphological types and the morphology-mass relation in different environments at low redshift", 2012, MNRAS, 419L, 14.
- Vulcani, Benedetta; Poggianti, Bianca M.; Fasano, Giovanni; Desai, Vandana; Dressler, Alan; Oemler, August; **Calvi, Rosa**; D'Onofrio, Mauro; Moretti, Alessia, "The importance of the local density in shaping the galaxy stellar mass functions", 2012, MNRAS, 420, 1481.
- Spavone, M.; Iodice, E.; **Calvi, R.**; Bettoni, D.; Galletta, G.; Longo, G.; Mazzei, P.; Minervini, G., "Revisiting the formation history of the minor-axis dust lane galaxy NGC 1947", 2009, MNRAS, 393, 317.

Other papers

- **Calvi R.**; Poggianti, Bianca M.; Vulcani, Benedetta; Giovanni Fasano, "The impact of environment on galaxy mass function", in preparation

- Poggianti, Bianca M.; **Calvi R.**; Bindoni D.; D'Onofrio M.; Moretti A.; Valentinuzzi T.; Fasano G.; Fritz J.; De Lucia G.; Vulcani, B.; Bettoni D., Gullieuszik M.; Omizzolo A., "Superdense galaxies and the mass-size relation at low redshift", in preparation

Talk at Meeting

- **2011**; *The morphology-mass relation in different environmnets at low redshift* - Meeting GEE2 (Galaxy Evolution and Environment), November 7-9, Milan, Italy.

Conference proceedings

- **Calvi, R.**; Cappellaro, E.; Botticella, M. T.; Riello, M., "Simulation tool of a Supernova search with VST", 2007, 1st Workshop of Astronomy and Astrophysics for Students, Naples (ITALY) on April 19-20, 2006. Published by INFN-Naples, eds. N.R. Napolitano & M. Paolillo, p.159.

Bibliography

Arp H., ApJS, 14, 1

Balogh M.L., Bower R.G., 2003, MxAC, 17, 220

Balogh M.L., Morris S.L., Yee H.K.C., Carlberg R.G., Ellingson E.; 1999, ApJ, 527, 54

Balogh M. et al., 2004, MNRAS, 348, 1355

Barnes J.E., Hernquist L., 1996, ApJ, 471, 115

Baugh C.M., Cole S., Frenk C.S., Lacey C.G., 1998, ApJ, 498, 504

Baugh C. M., 2006, RPPh, 69, 3101

Beers T.C., Flynn K., Gebhardt K., 1990, AJ, 100, 32

Bell E.F., de Jong R.S., 2001, ApJ, 550, 212

Berlind A.A. et al., 2006, ApJ, 167, 1

Berrier J.C., Stewart K.R., Bullock J.S., Purcell C.W., Barton E.J., Wechsler, R.H., 2009, ApJ, 690, 1292

Bertin E., Arnouts S., 1996, A& AS, 117, 39

Blanton M.R., Roweis S., 2007, AJ, 133, 734

Bond J.R., Cole S., Efstathiou G., Kaiser N., 1991, ApJ, 379, 440

Botzler C.S., Snigula J., Bender R., Hopp U., 2004, MNRAS, 349, 425

Buat, V.; Deharveng, J. M.; Donas, J., A& A, 223, 42

Butcher H., Oemler A.Jr., 1984, ApJ, 285, 426

Byrd G., Valtonen M., 1990, ApJ, 350, 89

Caldwell N., Kennicutt R., Phillips A.C., Schommer R.A., 1991, ApJ, 370, 526

Carlberg R.G., Yee H.K.C., Morris S.L., Lin H., Hall P.B., Patton D.R., Sawicki M., Shepherd C.W., 2001, ApJ, 552, 427

Cimatti A. et al., 2008, A& A, 482, 21

Cole S., ApJ, 367, 45

Cox T.J., Jonsson P., Somerville R.S., Primack J.R., Dekel A., 2008, MNRAS, 384, 386

Cross N.J.G. et al., 2004, MNRAS, 349, 576

Croton D.J., 2006, MNRAS, 367, 864

Davies R.L., Efstathiou G., Fall S.M., Illingworth G., Schechter P.L., ApJ, 266, 41

Deharveng, J.-M.; Sasseen, T. P.; Buat, V.; Bowyer, S.; Lampton, M.; Wu, X., 1994, A& A, 289, 715

De Lucia G& Blaizot JÃ©rÃ©my, 2007, MNRAS, 375, 2

Devereux, Nicholas A.; Hameed, Salman, 1997, AJ, 113, 599

Donas, J.; Deharveng, J. M.; Laget, M.; Milliard, B.; Huguenin, D., 1987, A& A, 180, 12

Dressler A., 1980, ApJ, 236, 351

Dressler A. et al., 1997, ApJ, 490, 577

Driver S.P., Liske J., Cross N.J.G., De Propris R., Allen P.D., 2005, MNRAS, 360, 81

Driver S.P. et al., 2006, MNRAS, 368, 414

Eke V.R. et al., 2004, MNRAS, 348, 866

Fasano G. et al., 2006, A& A, 445, 805

Ferguson H.C.& Binggeli B., 1994, A& A Rv, 6, 67

Finn R.A. et al., 2005, ApJ, 630, 206

Font A.S. et al., 2008, MNRAS, 389, 1619

Fritz J. et al., 2007, A& A, 470, 137

Fritz J. et al., 2011, A& A, 526, 45

Gallagher J.S. III, Hunter D.A., Tutukov A.V., ApJ, 284, 544

Gavazzi, G.& Scodeggio, M., 1996, A& A, 312, 29

Gavazzi, G.; Pierini, D.; Baffa, C.; Lisi, F.; Hunt, L. K.; Randone, I.; Boselli, A., 1996, A& AS, 120, 521

Geller M.J., Huchra J.P., 1983, ApJS, 52, 61

Gerke, B.F. et al., 2005, ApJ, 625, 6

Guo Q. et al., 2011, MNRAS, in press

Gunn J.E., Gott J.R., 1972, ApJ, 176, 1

Halliday C. et al., 2004, A& A, 427, 397

Hashimoto Y., Oemler A.Jr. Lin H., Tucker D.L., 1998, ApJ, 499, 589

Henry J.P. et al., 1995, ApJ, 449, 422

Hickson P., Kindl E., Auman J.R., 1989, ApJS, 70, 687

Hopkins A.M., 2004, ApJ, 615, 209

Hubble E.P., 1926, ApJ, 64, 321

Huchra J.P., Geller M.J., 1982, ApJ, 257, 4

Irwin M., Lewis J., 2001, NewAR, 45, 105

Kang X., Jing Y.P., Mo H.J., B*ö*rner G., 2005, ApJ, 631, 21

Kennicutt R.C.Jr., ApJ, 272, 54

Kennicutt, R. C., Jr.& Kent, S. M., AJ, 88, 1094

Kennicutt R.C.Jr., Tamblyn P., Congdon C.E., ApJ, 435, 22

Komatsu E. et al., 2009, Astro2010: The Astronomy and Astrophysics Decadal Survey, Science White Papers, no. 158

Kormendy J.& Djorgovski S., ARA& A, 1989, 27, 235

Kroupa P., 2001, MNRAS, 322, 231

Lacey C. & Cole S., 1993, MNRAS, 262, 627

Lacey C. & Silk J., 1991, ApJ, 381, 14

Larson, R. B.& Tinsley, B. M., 1978, ApJ, 219, 46

Lewis I. et al., 2002, MNRAS, 334, 673L

Lilly S.J., Le Fevre O., Hammer F., Crampton D., 1996, ApJ, 460L, 1L

Lin, H.; Yee, H. K. C.; Carlberg, R. G.; Ellingson, E., AAS, 18910304

Liske J., Lemon D.J., Driver S.P., Cross N.J.G., Couch W.J., 2003, MNRAS, 344, 307

Liu H.B., Hsieh B.C., Ho P.T.P., Lin L., Yan R., 2008, ApJ, 681, 1046L

Madau P., della Valle M., Panagia N., 1998, MNRAS, 297L, 17

Mandelbaum R., McDonald P., Seljak U., Cen R., 2003, MNRAS, 344, 776

Marinoni C., Davis M., Newman J.A., Coil A.L., 2002, ApJ, 580, 122

Martínez H.J., Zandivarez A., Merchán M.E., Domínguez M.J.L., 2002, MNRAS, 337, 1441

McGee S.L. et al., 2008, MNRAS, 387, 1605

Mihos J.C., 2004, Clusters of galaxies: probes of cosmological structure and galaxy evolution, p.278, eds. J.S. Mulchaey, A.Dressler, A. Oemler, Cambridge University press

Miller C.J. et al., 2005, AJ, 130, 968

Milvang-Jensen B. et al., 2008, A& A, 482, 419

Moore B., Frenk C.S., White S.D.M., 1993, MNRAS, 261, 827

Moore B., Katz N., Lake G., Dressler A., Oemler A., 1996, Nature, 379, 613

Mulchaey J.S., Davis D.S., Mushotzky R.F., Burstein D., 2003, ApJS, 145, 39

Murante G. et al., 2007, MNRAS, 377, 2

Oemler, Augustus, Jr., 1974, ApJ, 194, 1

Perlmutter S. et al., 1999, ApJ, 517, 565

Percival W. J. et al., 2007, ApJ, 657, 645

Poggianti B.M., 1997, A& AS, 1997, 122, 399P

Poggianti B.M. et al., 1999, ApJ, 518, 576P

Poggianti B.M. et al., 2006, ApJ, 642, 188P

Press W. H. & Schechter P., 1974, ApJ, 187, 425

Ramella M., Geller M.J., Huchra J.P., 1989, ApJ, 344, 57

Ramella M., Pisani A., Geller M.J., 1997, AJ, 113, 483

Ramella M. et al., 1999, A& A, 342, 1

Ricciardelli E.& Franceschini A., 2010, A& A, 518, 14

Romanishin, W., 1990, AJ, 100, 373

Salpeter E.E., 1955, ApJ, 121, 161

Sauvage, Marc; Thuan, Trinh X., 1992, ApJ, 396, 69

Somerville R.S. et al., 2008, MNRAS, 391, 481

Springel V., White S.D.M., Tormen G., Kauffmann G., 2001, MNRAS, 328, 726

Toomre A., Toomre J., 1972, ApJ, 178, 623

Tomita, Akihiko; Tomita, Yoshio; Saito, Mamoru, PASJ, 48, 285

Tucker D.L. et al., 2000, ApJS, 130, 237

van Breukelen C. et al., 2006, MNRAS, 373, 26

Vulcani B. et al., 2011, MNRAS, 412, 426

Young J.S., Allen L., Kenney J.D.P., Lesser A., Rownd B., 1996, AJ, 112, 1903

Walterbos, Rene A. M.; Greenawalt, Bruce, ApJ, 460, 696

Wang L.L.C., Kauffmann G., De Lucia G., 2007, MNRAS, 377, 1419

Wilman D.J., Balogh M.L., Bower R.G., Mulchaey J.S., Oemler A.Jr., Carlberg R.G., 2005, arXiv:astro-ph/0510077

Weinmann S.M., Kauffmann, G., von der Linden A., De Lucia G., 2010, MNRAS, 406, 2249

White S.D.M. et al., 2005, A& A, 444, 365

White S. D. M. & Frenk C. S., 1991, ApJ, 379, 52

Yang X., Mo H.J., van den Bosch F.C., Weinmann S.M., Li C., Jing Y.P., 2005, MNRAS, 362, 711

Zabludoff A.I., Mulchaey J.S., 1998, ApJ, 496, 39

Baillard et al., 2011, preprint (astro-ph/arXiv:1103.5734)

Baldry I. K., et al., 2006, MNRAS, 373, 469

Bamford S. P., 2009, MNRAS, 393, 132

Bell E.F., de Jong R.S., 2001, ApJ, 550, 212

Bolzonella M. et al., 2010, 524, 76

Cava, A. et al., 2009, A& A, 495, 707

Dressler A., 1980, ApJ, 236, 351

Dressler A., 1980, ApJ, 42, 565

Dressler A. et al., 1997, ApJ, 490, 577

Driver S.P., Liske J., Cross N.J.G., De Propris R., Allen P.D., 2005, MNRAS, 360, 81

Fasano G. et al., 2000, ApJ, 541, 673

Fasano G. et al. 2006, A& A, 445, 805

Fasano G. et al. 2010, MNRAS, 404, 1490

Fasano G. et al. 2011, MNRAS, in press

Fritz et al. 2011, A&A, 526, 45

Fukugita M. et al., 2007, AJ, 134, 579

Goto T., Yamauchi C., Fujita Y., Okamura S., Sekiguchi M., Smail I., Bernardi M., Gomez P. L., 2003, MNRAS, 346, 601

Kauffmann G., White S. D. M., Heckman T. M., Menard B., Brinchmann J., Charlot S., Tremonti C., Brinkmann J., 2004, MNRAS, 353, 713

Kauffmann G. et al., 2003, MNRAS, 341, 54

Kroupa P., 2001, 322, 231

Just D. W., Zaritsky D., Sand D. J., Desai V., Rudnick G., 2010, ApJ, 711, 192

Liske J., Lemon D. J., Driver S. P., Cross N. J. G., Couch W. J., 2003, MNRAS, 344, 307

Lintott C. J. et al., 2008, MNRAS, 389, 1179

Nair P. B., Abraham R. G., 2010, ApJ, 186, 427

Oesch P. A. et al., 2010, ApJ, 714, 47

Poggianti B. M. et al., 2009, 697L, 637

Postman, M., Geller, M. J., 1984, ApJ, 281, 95

Postman M. et al., 2005, ApJ, 623, 721

Kim-Vy H., Simard L., Zabludoff A.I., Mulchaey J. S., 2001, ApJ, 549, 172

Vulcani B. et al., 2011, MNRAS, 412, 246

Vulcani B. et al., 2011, MNRAS, submitted

Wilman D. J., Oemler A. Jr., Mulchaey J. S., McGee S. L., Balogh M. L., Bower R. G., 2009, ApJ, 692, 298

Wilman D. J., Erwin, P., 2011, submitted

Baldry I. K., Glazebrook K., Brinkmann J., Ivezić $\check{Z}$., Lupton R. H., Nichol R. C., Szalay A. S., 2004, ApJ, 600, 681

Baldry I. K., Balogh M. L., Bower R. G., Glazebrook K., Nichol R. C., Bamford S. P., Budavari T., 2006, MNRAS, 373, 469

Baldry, I. K., Glazebrook, K., Driver, S. P. B., 2008, MNRS, 388, 945

Baldry, I. K. et al., 2012, MNRAS, 412, 621

Ball N. M., Loveday J., Brunner R. J., Baldry I. K., Brinkmann J., 2006, MNRAS, 373, 845

Balogh M. L., Morris S. L., Yee H. K. C., Carlberg R. G., Ellingson E., ApJ, 488, 75

Bamford R. et al., 2009, MNRAS, 393, 1324

Bell E. F., McIntosh D. H., Katz N., Weinberg M. D., 2003, ApJS, 149, 289

Bolzonella M. et al., 2010, A& A, 524, 76

Brinchmann J., Charlot S., White S. D. M., Tremonti C., Kauffmann G., Heckman T., Brinkmann J., 2004, MNRAS, 351, 1151

Bell E.F., de Jong R.S., 2001, ApJ, 550, 212

Brinchmann J.& Ellis R. S., 2000, ApJ, 536L, 77

Bundy K. et al., 2006, ApJ, 651, 120

Calvi R., Poggianti B. M. & Vulcani B., 2011, MNRAS, 416, 727

Calvi R., Poggianti B. M., Fasano G., Vulcani B., 2012, MNRAS, 419, 14

Cole S. et al., 2001, MNRAS, 326, 255

Couch W. J., Ellis R. S., Sharples R. M., Smail I., 1994, ApJ, 430, 121

Katz, Neal& Gunn, James E., 1991, ApJ, 377, 365

Kroupa P., 2001, MNRAS, 322, 231

Salpeter E.E., 1955, ApJ, 121, 161

Vulcani B. et al., 2011, MNRAS, 412, 426

Butcher Harvey. & Oemler Augustus., Jr.; 1984, ApJ, 285, 426

Cava A. et al., A& A, 495, 707

Cross N. J. G., Driver S. P., Liske J., Lemon D. J., Peacock J. A., Cole S., Norberg P., Sutherland W. J., 2004, MNRAS, 349, 576

Dressler Alan.; 1980, ApJ, 236, 351

Dressler A., Gunn J. E., Schneider D. P., 1985, ApJ, 294, 70

Dressler A., Smail I., Poggianti B. M., Butcher H., Couch W. J., Ellis R. S., Oemler A. Jr., 1999, ApJS, 122, 51

Driver S.P., Liske J., Cross N.J.G., De Propris R., Allen P.D., 2005, MNRAS, 360, 81

Drory N., Bender R., Feulner G., Hopp U., Maraston C., Snigula J., Hill G. J., 2004, ApJ, 608, 742

Fasano G. et al., 2006, A& A, 445, 805

Fasano G. et al., accepted for publication on MNRAS

Fontana A. et al., 2004, A& A, 424, 23

Fontana A. et al., 2006, A& A, 459, 745

Ebeling H., Voges W., Bohringer H., Edge A. C., Huchra J. P., Briel U. G., 1996, MNRAS, 281, 799

Ebeling H., Edge A. C., Bohringer H., Allen S. W., Crawford C. S., Fabian A. C., Voges W., Huchra J. P., 1998, MNRAS, 301, 881

Ebeling H., Edge A. C., Allen S. W., Crawford C. S., Fabian A. C., Huchra J. P., 2000, MNRAS, 318, 333

Ellis S. C., Driver S. P., Allen P. D., Liske J., Bland-Hawthorn J, De Propris R., MNRAS, 363, 1257

Finn et al., 2005, ApJ, 630, 206

Fritz J. et al., 2011, A& A, 526, 45

Gehrels N., 1986, ApJ, 303, 336

Giodini et al., 2012, A& A, 538, 104

Gómez et al., 2003, ApJ, 584, 210

Hogg D. W. et al., 2002, AJ, 124, 646

Hogg D. W. et al., 2003, ApJ, 585, 5

Kauffmann G. et al., 2003, 341, 33

Kauffmann G. et al., 2003, 341, 54

Kauffmann G., White S. D. M., Heckman T. M., MÃ©nard B.,

Kennicutt, Robert C., Jr., ApJ, 498, 541

Iovino A. et al., 2010, A& A, 509, 40

Lewis et al., 2002, MNRAS, 344, 673

Lilly et al., 2007, ApJS, 172, 70

Lilly et al., 2007, ApJS, 184, 218

Liske J., Lemon D. J., Driver S. P., Cross N. J. G., Couch W. J., 2003, MNRAS, 344, 307

Panter, B., Heavens, A. F., Jimenez, R., 2004, MNRAS, 355, 764

Peng Ying-Jie et al., 2010, ApJ, 721, 193

Poggianti B. M., Bridges T. J., Komiyama Y., Yagi M., Carter D., Mobasher B., Okamura S., Kashikawa N., 2004, ApJ, 601, 197

Pozzetti L. et al., 2007, A& A, 474, 443

Pozzetti L. et al., 2010, A& A, 523, 13

Schechter P., 1976, ApJ, 203, 297

Scodeggio M., 2009, A& A, 501, 21

Thomas D., 2011, efgt.book

Valentinuzzi T. et al., 2009, A& A, 501, 851

van den Bosch F. C., Pasquali A., Yang X., Mo H. J., Weinmann S., McIntosh D. H., Aquino D., 2008, preprint, arXiv:0805.0002

van der Wel A., 2008, ApJ, 675, 13

Vulcani B. et al., 2011, MNRAS, 412, 246

Vulcani B. et al., 2012, arXiv:1111.0830v1

Vulcani B. et al., 2012, MNRAS, 420, 1481

White et al., A& A, 444, 365